UNIVERSITY OF LIVERPOOL

Copper biogeochemical cycle and the organic complexation of dissolved copper in the North Atlantic

Thesis submitted in accordance with the requirements of the University of Liverpool for the degree of Doctor of Philosophy

by

Arthur Corentin Georges Gourain

January 2020

in the

Faculty of Science and Engineering

School of Environmental Sciences

Department of Earth, Ocean and Ecological Sciences

In memory of Xavier Grall

Abstract

The copper biogeochemical cycle has been investigated in the open ocean with a focus on the North Atlantic. Two GEOTRACES sections have been used in order to study the distribution of dissolved copper (DCu) and its organic speciation in the North Atlantic. The GEOTRACES GA01 section was used as a natural laboratory in order to reveal the processes shaping the DCu distribution in the open ocean. Indeed, two contrasting regions were crossed: the east part of the section with increasing DCu concentrations with depth and the Arctic basins (Labrador and Irminger) in the west with homogeneous DCu concentrations with depth. The variability of distribution was driven by the organic speciation, elevated ligand concentrations in the east basin were stabilising copper in the dissolved form, allowing it to accumulate at depth. Moreover, elevated ligands concentrations were associated with an enrichment of copper compared to phosphorus in particles (> 0.45 μm). This enrichment was triggered by an increasing contribution of authigenic particulate copper over the particulate copper (PCu) cycle. Authigenic PCu was predominant at depth of every basin but the highest contributions were observed in the east Atlantic basin. Elevated authigenic PCu at depth demonstrated an intense reversible scavenging thus leading to elevated DCu concentrations. This shows for the first time the impact of reversible scavenging on natural copper samples.

The GEOTRACES GA13 section occurred over the Mid-Atlantic Ridge to study the impact of hydrothermalism on trace metal biogeochemical cycle. Along the cruise, multiple known hydrothermal sites were sampled with a focus on the deep ocean. Within the hydrothermal plumes identified using dissolved manganese (DMn), no variation in the DCu distribution and organic speciation was observable. The absence of DCu signal within the plumes resulted from a combination of dilution with surrounding water masses and removal by coprecipitation with sulphide. The lack of signal of copper complexation is more complex due to the combination of dilution, production of ligands and degradation of organic matter in the close vicinity of the vents. An inter-comparison between two GA13 stations and two GEOTRACES section (GA01 and GA03) showed the comparability of DCu and ligand profiles. The small variability observed between profiles was explained by local and seasonal processes affecting the (sub-)surface layer.

Copper profiles from a global dataset have been studied in order to constrain the DCu distribution in all the world's ocean. The dataset combines previously published datasets with the GEOTRACES IDP 2017 and covers all oceans basins. The distribution of DCu is linear with depth in most of the ocean with a Spearman's rank correlation coefficient higher than 0.8 for 72% of the stations. But the slope of profiles varies between basins; the Atlantic Ocean being characterised by low slope while the Pacific Ocean shows elevated slopes. The variability of slope is driven by the deep DCu concentrations, elevated DCu concentrations in the deep Pacific are leading to an increase of the slope. A diagnostic framework was applied to study the components affecting the copper distribution: the regenerated, preformed and reversible scavenged pools. The regenerated copper pool has the same behaviour as the macronutrients, like phosphate; regenerated copper represents less than 100 % of the total DCu pool. Analysis of the scavenged component demonstrates the transition of scavenging from a sink of copper in surface waters to a source of copper at depth. The switch between a net sink to a net source of DCu occurs at around 2250 m depth in the open ocean. Reversible scavenging is an important source of DCu at depth, shaping its unique linear distribution with depth.

Glossary

%DCu_Regenerated	Percentage of regenerated dissolved copper
%PCu_Auth	Percentage of authigenic particulate copper
%PCu_Bio	Percentage of biogenic particulate copper
%PCu_Litho	Percentage of lithogenic particulate copper
%PO4_Regenerated	Percentage of regenerated phosphate
AOU	Apparent oxygen utilisation
BNL	Benthic nepheloid layer
CLE-AdCSV	Competitive ligands exchange-Adsorptive cathodic stripping voltammetry
CSV	Cathodic stripping voltammetry
CuS	Copper-sulphide complex
DCo	Dissolved cobalt
DCu	Dissolved copper
DCu_Background	Background dissolved copper concentration in hydrothermal environment
DCu_Benthic_Processes	Dissolved copper component from benthic processes
DCu_Fluid	Dissolved manganese concentration within the hydrothermal fluid
DCu_Free	Free dissolved copper
DCu_Plume	Expected dissolved manganese concentration within the hydrothermal plume
DCu_Preformed	Preformed component of dissolved copper
DCu_Regenerated	Regenerated component of dissolved copper

DCu_Scavenged	Scavenged component of dissolved copper
DFe	Dissolved iron
DMn	Dissolved manganese
DMn_Background	Background dissolved manganese concentration in hydrothermal environment
DMn_Fluid	Dissolved manganese concentration within the hydrothermal fluid
DMn_Plume	Dissolved manganese concentration within the hydrothermal plume
DOC	Dissolved organic carbon
DPb	Dissolved lead
DP-CSV	Differential pulse-Cathodic stripping voltammetry
DSOW	Denmark Strait Overflow Water
DZn	Dissolved zinc
EAB	East Atlantic Basin
GEOTRACES IDP	Intermediate data product of the GEOTRACES program
GS	Greenland shelf
HS	Humic substances
IcB	Iceland Basin
ICP-MS	Inductively coupled plasma-Mass spectroscopy
IPCC	Intergovernmental panel on climate change
IrB	Irminger Basin
ISOW	Iceland-Scotland Overflow Water
L	Ligand

L_Excess	Excess of ligand compared to dissolved copper
LB	Labrador Basin
LC-ICP-MS	Liquid chromatography-Inductively coupled plasma-Mass spectroscopy
log K	Conditional stability constant
LSW	Labrador Sea Water
MAR	Mid-Atlantic ridge
MOW	Mediterranean Overflow Water
NACW	North Atlantic Central Water
NEADW	North East Atlantic Deep Water
PAl	Particulate aluminium
pCO2	Partial pressure of carbon dioxide
PCu	Particulate copper
PCu_Authigenic	Particulate copper from authigenic origin
PCu_Biogenic	Particulate copper from biogenic origin
PCu_Lithogenic	Particulate copper from lithogenic origin
PO4_Regenerated	Regenerated phosphate
PP	Particulate phosphorus
PTFE	Polytetrafluoroethylene
RR	Reykjanes ridge
SA	Salicylaldoxime acid
SF-ICP-MS	Sector Field- Inductively coupled plasma-Mass spectroscopy
TChla	Total Chlorophyl a

UCC	Upper continental crust
WEB	West European Basin

Contents

List of Figures and Tables

Chapter 2

Chapter 3

Chapter 4

Acknowledgment

I would like to thank my supervisors Pascal Salaün and Alessandro Tagliabue for their support during this PhD. The last four years and a half were highly enriching both on a personal and professional level. The elevated independence and control over my PhD project, they let me have was appreciable. It has with no doubt prepared me for my future professional life.

My time in Liverpool has been highlighted by many people I met through the years. I was lucky enough to cross path with two of the most wonderful women I‘ve ever met: Jenny and Yael. IN A WAY, the last two years were some of the best of my life and it is mainly resulting from their incredible joy of life, kindness and friendship. Thanks Jenny for all these days out, either running up or climbing up mountains. Thanks Yael for all these memories mainly based around Belgian beer and for showing me all the beauties of the Netherland.

Liverpool will always be associated in my mind with the 96 Allington Street which I considered like a home with the help of my 3 amazing housemates. Joe, your passions for Frozen, Taylor Swift and whiskey were always a source of enjoyment. I will truly miss our bro-date. Stephan, your offensive dark (Dutch?) humour was always here to cheer me up even in the worst day. Alice, thanks for the mix of nights out and talks about the Tour de France. Hopefully 2020 will be successful for Thibault Pinot.

Comme dirait Guenièvre : « Méfiez-vous des cons, y en a qui vont beaucoup plus loin qu’on ne pense », merci Anthony pour m’avoir accueilli dans cet antre qui te sers de logis. Tes remarques sur ma virilité au petit-déj sont irremplaçables.

How not to mention Alice and Clare (and their respective pet: snaky and Oscar) who provided an undoubtful friendship through the years. Our time in the allotment and at the pub (mainly the pub) will stay as some of the best memories in Liverpool. I promise you more Crepes night in the future. Thanks to the donuts team for these several expeditions to find the best donuts in Liverpool, Alice and Clare previously mentioned plus Tom, Laura and Hannah.

Thanks to my officemates of the office 206 and 205 (yes I spend enough time in the office 205 to call you officemates). Many people passed through these offices, so quickly thanks to few of them for

enduring my incredible neediness for hugs: Shaun, Lewis, Ciara and of course Kat and the lovely Jenny. Thanks to Joe and John for making me discover the wonder of Liverpool nightlife.

The last year has been a milestone in my life as a climber, I learnt so much about myself and about climbing as a way of life. That would not have been possible without some amazing persons and climbers: Catherine, Will, Laura, Andreas, Owain (ohhh wiiinnne), Heather, Conor, Phil, Nico, Paul and the incredible Pamela (aka crimp queen).

I would like to thank the people who welcomed me on my first week in Liverpool: Olivia, Hannah and Maddie. This first stressful week in a foreign country when barely speaking English was amazing, exceeding my expectation by far. I also need to thanks everybody I crossed path during my 4 and half years in Liverpool who in a way or another led me to be the person I am now.

To finish this incredible long list, I want to thank my family. Et plus particulièrement ma mère pour son soutien inconditionnel depuis toujours. Je ne serais jamais devenu l'homme que je suis aujourd'hui sans elle.

1. Chapter 1: Introduction

1.1. Motivation

The planet Earth is covered by 70 % of oceans and seas giving it one of its names: The Blue Planet. The presence of liquid water makes our planet unique in our solar system (to our current knowledge). These vast expanses of water are important in controlling the world's climate creating some of the most powerful natural event on Earth such as El Nino, the monsoon or cyclones and various storms. Oceans are also the source of 50 % of the dioxygen (O_2) present in the atmosphere allowing life to prosper over the globe. Microscopic algae flourishing in the incredibly dynamic and diverse aquatic ecosystems are consuming carbon dioxide (CO_2) and releasing O_2. With increasing concentration of CO_2 in the atmosphere, over 412 ppm in December 2019 at the Mauna Loa observatory (Hawaii, https://www.esrl.noaa.gov/gmd/ccgg/trends/, last access: 10/01/2020), the crucial role of the ocean in biologically pumping CO_2 is intensifying. The efficiency of CO_2 consumption by primary production is function of the phytoplankton biomass and health. Primary productivity is regulated by the availability of light and nutrients. Nutrients are classified in two categories: macronutrients with micromolar concentrations such as phosphate, nitrate and silicate; and micronutrients with nanomolar concentrations such as iron, cobalt, zinc and copper. Despite, their really low concentrations, micronutrients are playing an essential role for biological physiology. The study of trace elements as micronutrients is required to better constrain their impact on biological production in the ocean. In this chapter, I will discuss the essential role of copper in aquatic systems as a nutrient and a toxic element. Then, the distribution of copper in the open ocean is described with the main external and internal processes shaping it. The influence of speciation on copper biogeochemical cycle is discussed in the last section.

1.2. Copper biological influence

1.2.1. An essential nutrient

Copper (Cu) is an essential micronutrient for marine organisms, being a core in several enzymes. Cu is involved in the nitrogen cycle along every four steps of denitrification (Amin et al., 2013; Moffett et al., 2012; Philippot, 2002) through nitrate reductase, nitrite reductase, nitric oxide

reductase and nitrous oxide reductase (Casciotti and Ward, 2001; Merchant et al., 2006; Philippot, 2002). Moreover, it is essential for nitrification process as a co-factor for ammonium oxidation mediated by archaea (Amin et al., 2013; Francis et al., 2005; Jacquot et al., 2014; Walker et al., 2010). Copper plays an important role during the iron (Fe) uptake by phytoplankton, especially for the high-affinity Fe uptake system (Annett et al., 2008; Maldonado et al., 2006; Robinson et al., 1999; Stearman et al., 1996; Wells et al., 2005) where multi-copper oxidase is used for the iron oxidation and transport inside the cell (La Fontaine et al., 2002; Maldonado et al., 2006; Merchant et al., 2006; Peers et al., 2005; Valentine, 1997). Copper is involved in the photosynthetic process, the Cu-containing plastocyanin enzyme being an important component of the photosystem where it can replace the iron-containing cytochrome C_6 (Merchant et al., 2006; Peers and Price, 2006) to transfer electrons between cytochrome b_6-f and the photosystem I (Barón et al., 1995; Raven et al., 1999). Respiration process also requires copper, the three Cu atoms-containing cytochrome oxidase being essential for mitochondrial electron transport (Amin et al., 2013; Annett et al., 2008; Merchant et al., 2006; Raven et al., 1999; Valentine, 1997). Furthermore, copper is involved in the oxygen radical detoxification throughout the activity of the superoxide dismutase (Chadd, 1996; Rae et al., 1999; Raven et al., 1999; Valentine, 1997).

The important role of copper in all these enzymatic processes entails an imperative requirement for the phytoplankton communities. Typical surface concentrations in the open ocean are adequate to sustain biologic production (Annett et al., 2008; Peers et al., 2005; Peers and Price, 2006). Diatoms and coccolithophores are limited from free copper (Cu^{2+}) concentration below 10^{-15} M (Annett et al., 2008; Guo et al., 2012b; Peers et al., 2005; Semeniuk et al., 2015). But under lower concentration, phytoplankton can be copper-limited (Annett et al., 2008; Guo et al., 2012b; Lelong et al., 2013), especially in environment where iron is also limiting (Annett et al., 2008; Guo et al., 2012b; Lelong et al., 2013; Wells et al., 2005; Zhu et al., 2010). Involvement of Cu in nitrogen cycle can also initiate a possible limitation for ammonia oxidizing archaea (Amin et al., 2013; Jacquot et al., 2014) and denitrifying bacteria (Moffett et al., 2012).

Copper assimilation by phytoplankton is accomplished by two mechanism, a high-affinity uptake system and a low affinity uptake system (Guo et al., 2010, 2015; Quigg et al., 2006; Semeniuk et al., 2009). These two systems, based on a Michaelis-Menten kinetics, reduce copper from Cu^{2+} to Cu^{+} at the surface of membrane cell by copper reductase (Croot et al., 2003; Guo et al., 2010, 2015; Valentine,

1997). For decades, only free copper was believed to be bio-available for aquatic life (Sunda et al., 1987; Sunda and Huntsman, 1983). However, some recent studies demonstrated that organically complexed copper might be available to phytoplankton communities (Annett et al., 2008; Guo et al., 2010; Quigg et al., 2006; Semeniuk et al., 2009, 2015). Some complexes can be reduced at the cell surface followed by transport of the Cu^{+} throughout the membrane using ligand-exchange reaction (Semeniuk et al., 2015). Inside the cell, Cu transporter and Cu chaperone distribute copper for different biological function and maintain homeostasis to avoid limitation or toxicity (Guo et al., 2010, 2015; Merchant et al., 2006; Pufahl et al., 1997; Rae et al., 1999; Valentine, 1997). The optimal metal uptake rate varies according to species, net Cu:C assimilation ratio being between 0.3 and 4 µmol Cu mol C^{-1} (Annett et al., 2008; Guo et al., 2012a; Semeniuk et al., 2009; Tottey et al., 2008).

Copper requirement varies with other metal concentrations (e.g. Mn, Fe …) in the medium (Brand et al., 1986; Mann et al., 2002). For example, under iron-limited conditions, copper demand from phytoplankton increases (Annett et al., 2008; Biswas et al., 2013; Guo et al., 2010, 2012b; Maldonado et al., 2006; Peers et al., 2005; Peers and Price, 2006). Consequently, oceanic phytoplanktonic strains growing in lower [Fe] environment have higher copper requirement than coastal strains (Annett et al., 2008; Guo et al., 2012a, 2010; Peers et al., 2005). The complex interaction between copper and iron is difficult to constrain. An addition experiment in the Bering Sea demonstrated an increase of biomass after copper addition (Peers et al., 2005). Three hypotheses emerged to explain the mechanism involved: the copper addition increased the Fe uptake and subsequently biomass production, the Cu directly stimulated biomass production or the Cu was reducing the grazing pressure by negatively affecting the grazer communities known to be more sensible to copper toxicity than phytoplankton (Coale, 1991; Sunda et al., 1987). Variation in requirement leads to a wide range of Cu quota in phytoplankton cells. Culture studies observed a Cu/C elemental ratio comprised between 0.3 and 9.5 µmol mol^{-1} (Ho et al., 2003; Sunda and Huntsman, 1995b). Variability between species resulting from their requirement is highlighted by the low quota observed in diatoms, while dinoflagellates have a higher quota (Ho et al., 2003). These quotas are measured for culture phytoplankton in an optimised environment; studies in the natural environment were complicated for many years due to the elevated copper blank induced by the use of gold electron microscopy grids with elevated Cu content (Twining et al., 2015). Recently, Twinning and al. have developed a new method to measure cellular quota in natural samples (Twining et al., 2015, 2019; Twining and Baines, 2013). In the open ocean, the geometric median Cu/C ratio is

10.9 µmol mol^{-1} with a ± one standard error of 8.2-16.7 µmol mol^{-1} (B. Twining, personal communication).

1.2.2. Toxic properties of copper

Despite being a nutrient, copper can also be toxic at high concentration for aquatic life (Biswas et al., 2013; Bruland and Lohan, 2003; Sunda et al., 1987). Several studies on copper toxicity for different organisms have been carried out: mammals (Linder and Hazegh-Azam, 1996), polychaetes (Campbell et al., 2014), copepods (Sunda et al., 1987, 1990) and phytoplankton (Brand et al., 1986; Buck and Bruland, 2005; Croot et al., 2000; Mann et al., 2002). These studies agreed on dissolved free copper (Cu^{2+}) being the most toxic speciation for living organisms. But lipid-soluble copper complexes with elevated toxicity to diatoms have also been identified (Florence and Stauber, 1986; Stauber and Florence, 1987). Deleterious effects due to elevated Cu concentrations encompass damage to sperm DNA of polychaete (Campbell et al., 2014), early larval-stage death of polychaetes and copepods (Campbell et al., 2014; Sunda et al., 1987, 1990). Phytoplankton are affected by copper catalysis of hydrogen peroxide formation and other oxygen radicals, which affect DNA (Florence and Stauber, 1986; Mann et al., 2002; Stauber and Florence, 1987). High intracellular copper concentrations can also be detrimental to photosynthesis and cell division rate (Brand et al., 1986; Mann et al., 2002; Stauber and Florence, 1987). Free copper concentration harms phytoplankton physiology from 10 picomolar (Brand et al., 1986; Buck and Bruland, 2005; Gerringa et al., 1995; Mann et al., 2002; Sunda et al., 1987), but a wide range of responses is observed according to phytoplankton strains (Brand et al., 1986; Buck and Bruland, 2005). According to Brand et al. (1986), diatoms are the most resistant with 50 % of the reproduction rate inhibited in presence of 92 pM Cu^{2+}. Similar inhibition is obtained for coccolithophores and dinoflagellates from 37 pM and 40 pM, respectively. Cyanobacteria are highly sensitive to Cu^{2+} concentration; approximately 13 pM reduces the reproduction rate by a factor of two. Variability in copper sensitivity could be a reflect of the evolutionary age of the phytoplankton species; cyanobacteria are an ancient strain which appeared when the ocean was anaerobic (Brand et al., 1986; Dupont et al., 2010; Rasmussen et al., 2008; Saito et al., 2003). In the sulfidic ocean (Scott et al., 2008), DCu concentrations were low due to the formation of extremely insoluble Cu-S complexes. Cyanobacteria grew and developed under scarce Cu concentrations; after the oxygenation of the world

ocean, DCu concentration increased to present day concentrations. Insufficient adaptation by cyanobacteria to the new environment could explain their weak resistance to copper exposure.

Within the climate change perspective, the acidification of the world's ocean will lead to an increase in the copper toxicity for marine organisms (Campbell et al., 2014; Lewis et al., 2016). The increasing pCO_2 in the atmosphere is leading to an increase in the surface pCO_2 in the ocean driven by gas-exchange equilibrium. Higher aqueous pCO_2 lowers the pH following the carbon cycle in the ocean (Doney et al., 2009; IPCC, 2019). Dissolved copper chemical speciation is a function of many parameters including the pH; at low pH, the fraction of toxic Cu^{2+} increases due to the shift of the thermodynamic equilibrium (Gledhill et al., 2015; Millero et al., 2009; Richards et al., 2011).

1.2.3. Protective mechanisms from biology

As previously described, copper speciation is driving its toxicity in the ocean. Free and lipid-complexed copper are the most toxic form for aquatic organisms, while, organic complexes are less detrimental (Florence and Stauber, 1986; Stauber and Florence, 1987; Sunda, 1975). In consequence, phytoplankton have developed a protective mechanism against Cu^{2+} noxiousness; each species produces specific intracellular organic ligands and exudes them to the surrounding medium (Croot et al., 2000, 2003; Dupont and Ahner, 2005; Gerringa et al., 1995; Mcknight and Morel, 1979; Quigg et al., 2006; Wei and Ahner, 2005). According to Croot et al. (2000), conditional stability constants (log K) of the copper-ligand complexes are higher when ligands are produced by cyanobacteria than by diatoms which is in agreement with the suggestion that species more sensitive to copper stress produce ligands with higher copper-affinity (Mcknight and Morel, 1979). The exact composition of produced ligands is not fully known, but some ligands include molecules with organo-sulphur group. The coccolithophore *Emiliania huxleyi* produces thiol compounds in response to high copper concentration (Leal et al., 1999), including arginine-cysteine and glutamine-cysteine (Dupont et al., 2004; Dupont and Ahner, 2005). The copper-thiol complexes are formed intracellularly and then exudate into the medium (Dupont et al., 2004). Diatoms produce phytochelatin compounds, these polypeptides with thiol structure are enzymatically synthetized after exposure to high Cu concentration (Abner et al., 1997; Ahner et al., 1995; Ahner and Morel, 1995; Wei and Ahner, 2005). Diatoms also produce domoic acid, especially in iron-limited environments (Lelong et al., 2013; Rue and Bruland, 2001). Rue and Bruland (2001) describe domoic acid production as a mechanism to decrease copper bioavailability and

consequently reduce its toxicity. While, Lelong et al. (2013) hypothesise the production of domoic acid as a response of low iron concentration to increase the copper bioavailability. A higher intracellular copper content could stimulate the activity of the Cu-containing high affinity iron uptake system and reduce the iron-limitation. The imperative requirement and toxicity of copper for marine organism led Bruland and Lohan (2004) to describe copper as a "Goldilocks element", phytoplankton require neither too low nor too high copper concentrations.

1.3. Copper cycle in the ocean

1.3.1. Sources of copper in the ocean

The copper cycle in the ocean is impacted by several external sources adding Cu at the interfaces (e.g. surface waters, margin/benthic sediments). Aerosol deposition is an important input of particulate copper in the surface ocean through dry (Guo et al., 2012a; Jordi et al., 2012; Mackey et al., 2012; Paytan et al., 2009) or wet deposition (Cheize et al., 2012; Helmers and Schrems, 1995; Jickells et al., 1984). Atmospheric deposition provides an average of 450 Tg per year of dust in the ocean (Jickells et al., 2005); they are highly variable events, deposition rates varying according the region, the season, and the occurrence of dust storms (Jickells et al., 2005). Once deposited into the ocean, the fate of these particles is complex, a fraction of them will dissolve in the surrounding water. The solubility rate is varying depending on many parameters including water acidity, particles load and composition (Buck et al., 2010b; Sholkovitz et al., 2010; Spokes and Jickells, 1995). Copper solubility is elevated in anthropogenic particles (10-100 %) while mineral origin aerosols have a lower solubility (1-7 %) (Sholkovitz et al., 2010). According to dust deposition and average solubility, atmospheric inputs of dissolved copper are approximately 9.6 10^8 mol yr^{-1} (Takano et al., 2014).

Inputs of copper from atmospheric deposition can influence the phytoplankton community, addition of toxic Cu^{2+} in surface waters can be toxic for *Prochlorococcus* and *Synechococcus* cyanobacteria (Guo et al., 2012a; Jordi et al., 2012; Paytan et al., 2009). The toxic effect of copper addition could explain the shift in biomass community usually observed after important deposition of dust (Guo et al., 2012a; Paytan et al., 2009).

Rivers are an important source of material within the surface ocean affecting the global biogeochemical cycle of copper. According to Takano et al. (2014) and references therein, average DCu input from riverine discharge are approximately 7.6.10^8 mol yr^{-1}, comparable to the atmospheric

deposition flux. Chemical and physical Cu speciation in rivers and estuaries have been extensively studied over the last decades (Abualhaija et al., 2015; Gledhill et al., 2015; Jacquot et al., 2014; Laglera and van den Berg, 2003; Louis et al., 2009b; Nelson and Mantoura, 1984; Rozan et al., 2000; Waeles et al., 2004, 2005, 2015; Whitby and van den Berg, 2015; Yang and van den Berg, 2009). Riverine runoff is a highly seasonal process (Waeles et al., 2005), mainly driven by water discharge being more important in winter. Copper concentrations in rivers and estuaries vary between 2 nM for pristine rivers up to 40 nM for contaminated systems (Jacquot et al., 2014; Laglera and van den Berg, 2003; Louis et al., 2009b; Waeles et al., 2004, 2005, 2015). Some rivers are highly contaminated by anthropogenic activities, leading to an increase in copper concentrations (Beck and Saudo-wilhelmy, 2007; Cotte-Krief et al., 2000; Louis et al., 2009b; Waeles et al., 2004, 2005, 2015) and complexing matter concentrations (Rozan et al., 2000). During its journey along the river, DCu is affected by several interactions with particles including adsorption and desorption processes. Moreover, according to Waeles et al. (2015), colloids represent a significant fraction of the copper pool in rivers.

Hydrothermal vents are known to be an important source of trace metals in the deep ocean (Hawkes et al., 2014; Tagliabue et al., 2010), including copper (Boyle et al., 1977; Edgcomb et al., 2004; Jacquot and Moffett, 2015; Kleint et al., 2015; Klevenz et al., 2012; Metz and Trefry, 2000; Sander and Koschinsky, 2011; Sarradin et al., 2009; Trefry et al., 1985). Copper concentrations in the plume reach extremely high values within the micromolar range (Edgcomb et al., 2004; Sarradin et al., 2009 and references therein). Inside high-temperature vents (up to 300°C), Cu is mainly present as a highly-soluble chloride complexes (Edgcomb et al., 2004; Leal and Van Den Berg, 1998; Metz and Trefry, 2000; Seewald and Seyfried, 1990). During mixing with surrounding water and cooling, speciation of copper changes, chloride complexes are dissociated while sulphide complexes are formed (Edgcomb et al., 2004; Sander and Koschinsky, 2011). High sulphide concentrations (up to micromolar values) at the vents vicinity strongly bind copper (Edgcomb et al., 2004; Kleint et al., 2016; Klevenz et al., 2012; Metz and Trefry, 2000; Sander and Koschinsky, 2011; Sarradin et al., 2009; Seewald and Seyfried, 1990). Sulphide complexes have a high affinity with particles and are quickly scavenged from the water column to the sediments (Edgcomb et al., 2004). Hence, sediments containing high sulphide concentrations are observed around hydrothermal vents (Kleint et al., 2015). Important sulphide complexation reduces the bioavailability and toxicity of copper for the marine life living around the vents (Edgcomb et al., 2004; Klevenz et al., 2012). Hydrothermal inputs have been estimated to

represent almost 14% of the DCu budget in the deep ocean (Sander and Koschinsky, 2011). It is important to note that hydrothermal activity can be a sink for dissolved copper (Roshan and Wu, 2015). Elevated concentrations of (oxo-)hydroxide particles formed in the close vicinity of the vents increase the scavenging for trace metals including copper (Jacquot and Moffett, 2015; Sander and Koschinsky, 2011; Trefry et al., 1985).

Benthic resuspension of sediments are a source of copper for the continental shelves and the open ocean (Boyle et al., 1977, 1981; Chapman et al., 2009; Cotte-Krief et al., 2000; Croot, 2003; Danielsson et al., 1985; Heggie et al., 1987; Roshan and Wu, 2015). Dissolved copper is released from sediments by diagenetic reactions under reducing conditions (Beck and Saudo-wilhelmy, 2007; Boyle et al., 1981). In the case of continental shelves or margins, copper can be laterally advected to the open ocean by hydrographic currents (Boyle et al., 1981; Heggie et al., 1987; Roshan and Wu, 2015). Benthic Nepheloid Layers (BNLs) contribute to resuspended particulate copper, dissolution of these particles can increase the concentration of dissolved metals (Boyle et al., 1977; Bruland, 1980; Roshan and Wu, 2015). BNLs are a layer of few hundred meters above the seafloor where benthic sediments are resuspended by intense hydrographic stresses as boundary currents, deep eddies and benthic storms (Gardner et al., 2017, 2018). But, elevated particulate concentrations in the BNL increase the scavenging rate of copper; hence, BNL can be a sink of dissolved copper (Roshan and Wu, 2015).

1.3.2. Sinks and internal processes affecting DCu

Scavenging is the main abiotic process removing DCu form the water column through adsorption on the surface of particles (Bruland and Lohan, 2003; Craig, 1974; Ellwood et al., 2008). Scavenging is an important process exporting trace elements from the surface layer to the deep ocean (Honeyman et al., 1988) and ultimately burying them within sediments. The intensity of scavenging is dependent of the particle's concentration in the water column (Craig, 1974; Honeyman et al., 1988). In consequence, maximum scavenging is happening in surface waters where particles load is at its highest while scavenging rate decrease with depth (Craig, 1974; Honeyman et al., 1988). It is a main sink of dissolved trace metals as iron (Johnson et al., 1997; Tagliabue et al., 2014), manganese (Kuss et al., 1999), aluminium (Bruland and Lohan, 2003; Menzel Barraqueta et al., 2018), thorium (Bruland and Lohan, 2003; Clegg and Whitfield, 1991; Trimble et al., 2004) and its influence is non-negligible on copper cycle (Craig, 1974; Ellwood et al., 2008; Little et al., 2013; Richon and Tagliabue, 2019).

Interestingly, in recent years, this process has been described as an equilibrium between dissolved and particulate phase. Hence, scavenging is not only a sink of dissolved elements on particles, it can also by a source by desorbing them from the particles within the surrounding medium. Reversible scavenging has been initially described for thorium (Bacon and Anderson, 1982; Clegg and Whitfield, 1991; Trimble et al., 2004), but more recent studies are showing its influence on other elements such as iron (Abadie et al., 2017; Dutay et al., 2015; Jeandel and Oelkers, 2015; Labatut et al., 2014) and copper (Little et al., 2013; Richon and Tagliabue, 2019). Copper distributions are believed to be mainly driven by reversible scavenging as described in recent modelling studies (Little et al., 2013; Richon and Tagliabue, 2019).

1.3.3. Distribution of copper in the open ocean

The distribution of copper in the open ocean is shaped by the sources, sinks and internal processes affecting it. The dissolved copper profile is unique; it does not match any of classic profiles, i.e. not a nutrient type (e.g. phosphorus, cadmium), nor a hybrid type (e.g. iron), nor a scavenged type (e.g. aluminium, manganese). Profiles of DCu are linear with low concentrations in surface waters followed by a steady increase with depth and maximum concentrations near the seafloor (Bruland and Lohan, 2003; Danielsson, 1980; Heller and Croot, 2014; Roshan and Wu, 2015; Saager et al., 1992, 1997). At first, the main process driving this peculiar profile was believed to be the benthic resuspension of sediments releasing DCu (Boyle et al., 1977, 1981) . It is now known that benthic inputs cannot affect copper profiles over the entire water column. Recent studies demonstrated the driving influence of reversible scavenging in shaping copper profiles (Little et al., 2013; Richon and Tagliabue, 2019). In the open ocean, DCu concentrations in surface waters are around 1 nM in most of the oceanic basins (Danielsson, 1980; Heller and Croot, 2014; Roshan and Wu, 2015, 2018; Saager et al., 1992, 1997). Some regions are characterised by higher concentrations due to strong surface inputs (i.e. atmospheric deposition, riverine input) such as the Mediterranean Sea or the Arabian Sea (Jordi et al., 2012; Saager et al., 1992). At depth, strong inter-basins variability is observed; [DCu] are low in the Atlantic Ocean (around 2.5 nM; Roshan and Wu, 2015; Schlitzer et al., 2018; Yeats and Campbell, 1983) while elevated concentrations are observed in the Pacific Ocean (around 4 nM; GEOTRACES IDP 2017, Mackey et al., 2002; Schlitzer et al., 2018)). The variability between basins is not yet explained and a lot of questions are still arising on copper biogeochemical cycle in the open ocean.

Sources and sinks of copper lead to its long residence time in the ocean; the average residence time varies between studies from 830 to 5000 years (Boyle et al., 1977; Bruland, 1980; Craig, 1974; Takano et al., 2014). A shorter time is observed in surface waters with 10 years within the mixed layer (Boyle et al., 1977; Bruland, 1980; Craig, 1974; Roshan and Wu, 2015; Takano et al., 2014). However, a more recent modelling study using the first global copper biogeochemical model described shorter residence time of 400-500 years over the entire water column and 3 years within the first 100m (Richon and Tagliabue, 2019).

Despite the growing interest on copper cycle over the last decade, there are many uncertainties in the copper biogeochemical cycle. The linear profile of dissolved copper is still not completely understood. Reversible scavenging has been identified in modelling studies as the main driver of Cu distributions, but it has never been demonstrated using natural samples. The main explanation is coming from the current impossibility to identify directly reversible scavenging of copper using current sampling and analytical methods. More studies of this process are necessary in order to tackle this grey area of copper biogeochemical cycle. The qualitative and quantitative identification of reversible scavenging through the water column will help to confirm the finding of modelling studies.

1.4. Ligands cycle in the ocean

1.4.1. Characterisation and method

Copper ligands are any molecules having the potential to chemically bind atoms of copper. Following this definition, ligands are a bulk of organic and inorganic species with various structures and characteristics. Within the marine ecosystem, ligands are a mixture of exported terrestrial ligands, marine ligands produced in-situ and degradations by-products (e.g. cell lysis, grazing, photodegradation) of these compounds. The exact composition of the bulk is not yet fully constrained; a study using liquid chromatography- inductively coupled plasma mass spectrometry (LC-ICP-MS) measurement method demonstrated the highly complex ligands matrix (Boiteau et al., 2016). A complete description the entire ligand matrix is not currently possible due to its complexity. Nevertheless, voltammetric measurements of ligands by class/group have demonstrated the predominance of organo-sulphur compounds (Yang and van den Berg, 2009). Humic substances (HS) and thiols are two main compound classes observed in estuaries and coastal waters (Abualhaija et al., 2015; Simpson et al., 2002; Waeles et al., 2013, 2015; Whitby and van den Berg, 2015; Yang and van

den Berg, 2009). Humic substances are a complex class of molecule including both humic acids and fulvic acids (Waeles et al., 2013). Between 15 and 50 % of the dissolved organic matter in estuaries and coastal waters is believed to be HS (Waeles et al., 2013; Whitby and van den Berg, 2015). They are considered to be weak copper ligands with a conditional constant of complexation log K around 12 (Kogut and Voelker, 2001; Whitby et al., 2018; Whitby and van den Berg, 2015). Thiols are also a complex class of compounds including molecules such as glutathione, phytochelatin and cysteine (Dupont et al., 2006; Leal et al., 1999; Leal and Van Den Berg, 1998; Tang et al., 2000). They strongly bind copper in aquatic medium with a log K around 14 (Chapman et al., 2009; Leal et al., 1999; Whitby et al., 2018; Whitby and van den Berg, 2015). As for HS, the thiol pool is not fully constrained and their roles in the open ocean for copper cycle is still unclear despite few studies (Anderson et al., 1988; Chapman et al., 2009; Dupont et al., 2004, 2006; Laglera and van den Berg, 2003, 2006; Luther et al., 1991; Matrai and Vetter, 1988; Whitby et al., 2018).

Most of the studies on copper speciation in aquatic systems use voltammetric analyses to identify and quantify ligands (van den Berg et al., 1987; Croot, 2003; Donat et al., 1994; Heller and Croot, 2014; Jacquot and Moffett, 2015; Kogut and Voelker, 2001; Lucia et al., 1994; Ružić, 1996; Whitby et al., 2018). The main method of ligands determination is the competitive ligand exchange adsorptive cathodic stripping voltammetry (CLE-AdCSV) using a mercury drop electrode. The method uses a competitive ligand (salicylaldoxime usually), that forms a copper complex that is measured on the mercury electrode. The competitive ligand will be in competition with the natural ligands in order to complex the dissolved copper present in the sample. Variation in the measured signal is indicative of the equilibrium between the DCu, the natural ligands and the competitive ligand. Knowing the concentration of DCu, the competitive ligand concentration and binding strength, the natural ligands parameters are calculated by adding successively free copper to the sample. Every addition modifies the overall equilibrium between ligands and DCu; the study of the overall variations allows the calculation of the initial natural ligand properties (concentration and binding strength). Copper ligands are always present at higher concentration than dissolved copper in seawater. Their concentrations can reach up to 150 nM in coastal systems (Abualhaija et al., 2015; Buck and Bruland, 2005; Croot, 2003; Shank et al., 2004b) while concentrations are constrained to be under 10 nM in the open ocean (Heller and Croot, 2014; Jacquot et al., 2013; Jacquot and Moffett, 2015; Moffett and Dupont, 2007; Thompson et al., 2014). Their binding strength, log K, ranges from 11.5 to 14.5 in both systems. In the open ocean,

HS and thiols are believed to be the main ligands binding copper (Dupont et al., 2006; Heller and Croot, 2014; Jacquot and Moffett, 2015; Whitby et al., 2018). Some studies using CLE-AdCSV found two classes of ligands (with a weak and a strong ligand class, Whitby et al., 2018) while other measured only one unique class (Heller and Croot, 2014; Jacquot and Moffett, 2015; Moffett and Dupont, 2007). To summarise, most of the ligands characteristic of aquatic systems are obtained from an indirect measurement where the actual ligand or copper-ligand complex is never measured. Indirect analysis creates some uncertainties on what is actually measured by the method. Indeed, some compounds (inorganic complexes and/or colloids) could interfere with the competitive ligand and create artefact ligands. In consequence, in some specific situations, the ligands properties might not characterise the actual organic ligands but a mixture of organic/inorganic ligands and colloids (Fitzsimmons et al., 2015b).

1.4.2. Sources, sinks and internal processes in the open ocean

One of the main internal sources of organic ligands is the in-situ biogenic production by phytoplankton. Phytoplanktonic cells produce ligands in order to either increase or decrease copper bioavailability according to the Cu^{2+} concentration in the medium (Croot et al., 2000, 2003; Dupont and Ahner, 2005; Gerringa et al., 1995; Lelong et al., 2013; Mcknight and Morel, 1979; Quigg et al., 2006; Wei and Ahner, 2005). Biological production of ligands happens mainly in surface waters where most of the primary production occurs. The produced compounds are believed to mainly consist of thiols and domoic acid (Dupont et al., 2004; Dupont and Ahner, 2005; Leal et al., 1999; Lelong et al., 2013; Rue and Bruland, 2001). Production of ligands has also been observed in the deep ocean around hydrothermal vents where life must flourish in hard conditions of high pressure, low light and toxic trace elements concentrations. Hydrothermal bacteria produces strong organic ligands such as thiols in order to complex the elevated concentration of Cu^{2+} and reduce its toxicity (Kleint et al., 2015; Klevenz et al., 2012). Organic ligands can also be by-product of biological activity. Biology through grazing by zooplankton and bacterial remineralisation produce ligands within the medium (Buck et al., 2018; Kondo et al., 2008; Sato et al., 2007; Witter et al., 2000). Cell lysis leads to the release of complexing ligands previously present within phytoplankton cells (Boyd et al., 2010; Kondo et al., 2008; Poorvin et al., 2004; Witter et al., 2000).

Rivers and estuaries provide important concentrations of dissolved organic matter within the costal ocean (Abualhaija et al., 2015; Kogut and Voelker, 2001; Shank et al., 2004b; Whitby and van den Berg, 2015). This organic matter contains various molecules including thiols and humic substances which are complexing agents for the DCu (Abualhaija et al., 2015; Croot, 2003; Jacquot et al., 2014; Laglera and van den Berg, 2003; Louis et al., 2009a; Shank et al., 2004b; Whitby and van den Berg, 2015). Some of the organic ligands present in the water column of rivers and estuaries originate from the sediments. Indeed, sediments release copper ligands to the water column (Chapman et al., 2009; Shank et al., 2004a; Skrabal et al., 1997, 2006; Waeles et al., 2015). Benthic inputs of ligands have not yet been observed in the open ocean, but organic-rich sediments might be a source of organic ligands within the deep ocean. The export of ligands from rivers and estuaries have not yet been documented to our knowledge but their potential elevated residence time could lead to their export within the surface layer of the open ocean.

Atmospheric deposition is believed to provide organic ligands to the surface ocean (Baker et al., 2016; Fitzsimmons et al., 2015b; Wozniak et al., 2013, 2015). Most studies have focused on iron-binding ligands (Cheize et al., 2012; Fitzsimmons et al., 2015b; Kieber et al., 2001, 2005; Paris et al., 2011; Paris and Desboeufs, 2013) but a few studies have demonstrated the deposition of copper complexing species (Nimmo and Fones, 1994; Spokes et al., 1996). Atmospheric organic ligands have been identified as improving the dissolution of iron from dust particles by a factor of 6.5 (Paris and Desboeufs, 2013). The identical behaviour is expected for other trace elements including copper. Moreover, wet deposition is a source of ligands into the surface ocean. Indeed, rainwater contains many organic molecules binding trace elements as iron and copper (Cheize et al., 2012; Kieber et al., 2001, 2005; Spokes et al., 1996; Willey et al., 2008). The presence of humic substance has been identified in rainwater (Paris and Desboeufs, 2013) leading to over 99.99 % of complexed copper (Spokes et al., 1996).

The main sink of organic ligands in the ocean is their degradation by biological activity or abiotic chemistry (Buck et al., 2018; Völker and Tagliabue, 2015). Little is known on the residence time of these organic compounds but Hansell et al. (2012) studied the residence of dissolved organic carbon (DOC). They observed a wide range of residence times of DOC from 1.5 years for semi-labile compounds to over 16 000 years for refractory DOC. Direct comparison between DOC and complexing organic compounds is difficult, but it shows the important range of residence time between organic

molecules in the open ocean. Some studies focused on the photodegradation of organic ligands like thiols (Buck et al., 2010c; Laglera and van den Berg, 2006; Powell and Wilson-Finelli, 2003; Shank et al., 2006; Thompson et al., 2014; Völker and Tagliabue, 2015). According to Laglera and van den Berg (2006), after one day of daylight exposure between 2 and 60 % of copper ligands are photodegraded while over 30 to 50 % of thiols are degraded.

1.4.3. Unknow on copper organic ligands biogeochemical cycle

Despite the important effort over the last decades to better understand the copper ligand cycle in the open ocean, many uncertainties remain. A recent copper speciation study in the North Atlantic (Jacquot and Moffett, 2015), showed a really patchy distribution of ligands over the entire water column. The ligand distribution does not reveal any obvious source nor sink. The most plausible explanation is an elevated residence time of organic complexing ligands leading to a homogenisation of ligands distribution over the water column. But specific studies of their residence time in surface and at depth will be necessary in order to understand better copper ligands cycle.

Moreover, some of the uncertainties of ligand distributions is derived from the method mainly used to measure them. The CLE-AdCSV is a powerful method to measure ligand concentration at a nanomolar level. But with this method, ligands are not detected directly; in consequence, some factors like inorganic colloids can produce artefacts, skewing the results obtained (Fitzsimmons et al., 2015a). As an example, Sarradin et al. (2009) discovered that 98 % of the ligands complexing copper within hydrothermal plumes were inorganic. Using CLE-AdCSV, some of these inorganic ligands might be interpreted as organic compounds. The study of organic speciation of copper needs to be done cautiously knowing that some artefacts might exist. Further development of complementary methods such as pseudopolarography (Gibbon-Walsh et al., 2012) and LC-ICP-MS (Boiteau et al., 2016) will be necessary to understand the fate of copper complexing ligands within the ocean.

1.5. Aim of the thesis and structure

In this thesis, I investigate the copper biogeochemical cycle with a highlight on its organic speciation. The aim is to understand the influence of organic complexation on the distribution of copper in the open ocean. A focus has been done on the reversible scavenging process; understanding this key process using speciation is essential to better constrain the copper cycle and distribution. The

implication of complexation on dissolved-particulate exchange is needed to understand how reversible scavenging is driving copper distribution. These processes were studied in open ocean with a focus in the North Atlantic. The effect of hydrothermalism on copper speciation was also be studied to comprehend this potential strong deep copper source.

This thesis structure starts with an introductory chapter where the key concept developed in the following chapters are introduced. Chapter 2 is a case study of the GEOTRACES GA01 section in the North Atlantic. Dissolved copper, its speciation and particulate copper are studied together to describe the overall copper cycle in the North Atlantic. The GA01 section spans over contrasted regions where copper distributions varied from one oceanic basin to another, giving an excellent opportunity to use it as a natural laboratory. Chapter 3 focusses on the GEOTRACES GA13 section along the Mid-Atlantic Ridge. The aim of this cruise was to study of hydrothermal vents and their influence on the trace elements cycle. We investigated on the influence of hydrothermal plumes on the organic ligands and dissolved copper distributions. Chapter 4 is concerned with the global distribution of dissolved copper using a compilation of data. In this chapter, the copper profiles are analysed in order to understand the processes shaping them. By deconstructing copper distributions, the main drivers affecting copper are studied along the water column. Finally, Chapter 5 summarises the main findings and conclusions obtained through this study. The perspectives opened by these new findings are discussed as well as the future work necessary to fully comprehend the copper biogeochemical cycle of copper in the open ocean.

2. Chapter 2: Effect of dissolved organic speciation and reversible scavenging on copper cycle in the North Atlantic (GEOTRACES GA01 section)

Abstract:

The copper biogeochemical cycle has been studied in the North Atlantic along the GEOTRACES cruise GA01. The section crossed two contrasted regions, DCu concentrations increased with depth in the East Atlantic Basin (EAB) while homogeneous DCu concentrations are observed in the Arctic basins: the Labrador and Irminger basins. The speciation of copper showed that a median 98.5 % of copper was complexed by organic ligands. The ligand concentrations ranged from 1.19 to 8.28 nM with a conditional stability constant between 12.1 and 13.9. Along the section, organic ligands were stabilising dissolved copper (DCu) allowing it to accumulate at depth in the EAB. Moreover, elevated [DCu] in the EAB were associated with an increase of particulate copper (PCu) to particulate phosphorus ratio. This increase was due to the elevated authigenic PCu concentration in this basin compared to the other basins. Authigenic PCu dominated the PCu cycle at depth, more than 70 % of PCu was authigenic below 1000 m. Elevated authigenic particles at depth of the EAB indicated a strong reversible scavenging leading to higher DCu concentrations in this basin. This study shows for the first time the effect of reversible scavenging on natural samples.

2.1. Introduction

Copper (Cu), as many other trace elements (e.g. iron, zinc or cobalt), is an essential micronutrient for the phytoplanktonic community. Copper is used as an active core in several enzymes required for the phytoplankton physiology (Twining and Baines, 2013). It is the main element in plastocyanin, a protein strongly involved in photosynthetic processes (Merchant et al., 2006; Peers and Price, 2006; Raven et al., 1999). Copper is the active core in the multi-copper oxidase that is important in the high-affinity Fe uptake system (Annett et al., 2008; Stearman et al., 1996; Wells et al., 2005) where it is essential for iron oxidation and transport inside the cell (La Fontaine et al., 2002; Maldonado et al., 2006; Valentine, 1997). Cu is also key in the production of superoxide dismutase, an antioxidant

protein that controls the intracellular superoxide concentrations (Chadd, 1996; Rae, 1999; Valentine, 1997). It also plays an important role in several denitrification steps (Amin et al., 2013; Moffett et al., 2012; Philippot, 2002). However, copper can also be toxic to the biological community at high concentration (Biswas et al., 2013; Bruland and Lohan, 2003; Sunda et al., 1987) with toxicity thresholds varying according to the species and strain. For instance, in algal culture experiments, small cyanobacteria were found to be significantly more sensitive to free copper (Cu^{2+}) than large diatoms, with a toxic effect from 13 pM of Cu^{2+} compared to 92 pM Cu^{2+} (Brand et al., 1986; Buck and Bruland, 2005). In the natural environment, deleterious copper effects in surface waters have been previously observed in the Mediterranean Sea (Jordi et al., 2012; Paytan et al., 2009).

As an active protective mechanism, some phytoplankton have the ability to produce organic ligands in order to reduce the concentration of Cu^{2+} (Croot et al., 2000; Moffett, 1995; Moffett and Brand, 1996). They produce copper-specific intracellular ligands and exude them in the surrounding medium (Dupont and Ahner, 2005; Gerringa et al., 1995; Wei and Ahner, 2005). Species highly sensitive to copper stress (i.e. cyanobacteria) produce strong ligands while less sensitive species (i.e. diatoms) excrete ligands with a lower copper-affinity (Croot et al., 2000; Mcknight and Morel, 1979). Moreover, some culture studies have also demonstrated the biogenic production of ligands in order to facilitate copper assimilation (Lelong et al., 2013; Semeniuk et al., 2015). The ligands cycle is still largely unknown; mainly due to their broad definition: copper-ligands are any molecules able to chemically bind an atom of copper. Following this definition, ligands represent a various and complex bulk of molecules which have not been yet identified. Nevertheless, some studies (e.g. Laglera and van den Berg, 2003; Leal et al., 1999; Tang et al., 2000; Waeles et al., 2015; Whitby and van den Berg, 2014) have demonstrated the predominance of two main ligand classes: thiols and humics substances. Organic ligands (L) complex more than 99.9 % of the dissolved copper in the open ocean (Jacquot et al., 2013; Jacquot and Moffett, 2015; Moffett, 1995; Moffett et al., 1990) and are believed to stabilise copper in the dissolved phase. Ligands and specifically copper-ligands cycling in the open ocean is highly uncertain. Little is known about the sources, the sinks and especially the internal cycle of these molecules.

In the open ocean, the main sources of DCu are riverine inputs and aerosol deposition, each of them contributing for around $9 * 10^{8}$ mol $year^{-1}$ (Takano et al., 2014). Pure hydrothermal fluids are rich in copper with concentrations reaching micromolar concentrations (Sander et al., 2006; Sarradin et al., 2009) but most of it is trapped within the hydrothermal system and not exported to the water column

(GEOTRACES IDP2017, Schlitzer et al., 2018). The high affinity of Cu with sulphide to form copper sulphide (CuS), a highly insoluble compound, actively removes copper from the hydrothermal fluid as it mixes with the surrounding seawater (Alt et al., 1987; Styrt et al., 1981). Unlike for other metals, continental margins have never been identified as a source of copper within the ocean (GEOTRACES IDP 2017, Schlitzer et al., 2018). These external sources of copper, by their magnitude, input rate and the physical/chemical forms under which copper is entering the marine system, are shaping its distribution in the open ocean. While concentrations in coastal waters have been regularly reported at levels of tens of nanomolar (van den Berg et al., 1987; Waeles et al., 2004, 2015), in most of the surface ocean waters, dissolved copper (DCu) concentrations are around 1 nM. With depth, DCu concentration increases linearly reaching a maximum close to the oceanic seafloor. Maximum concentrations at depth vary according the oceanic basin; in the Atlantic Ocean, [DCu] increases up to 3.7 nM while within the Pacific, it reaches 4.9 nM (GEOTRACES IDP 2017, Schlitzer et al., 2018). As a consequence, the typical copper profiles through the water column do not fit with those of nutrient-like, nor scavenged, nor hybrid elements (Tagliabue, 2019). It is still unclear why the copper distribution is so peculiar, but some modelling studies have suggested the influence of reversible scavenging (Little et al., 2013; Richon and Tagliabue, 2019). Reversible scavenging corresponds to a process where the element is first scavenged onto the surface of sinking particles in the particle rich upper ocean and then released from the particles in the particle poor ocean interior. The processes triggering the desorption from particles is not fully understood but the particle load and the equilibrium between the dissolved and particulate pools play a non-negligible role (Little et al., 2013). As a consequence, scavenging is always a reversible process; the equilibrium between dissolved and particles is leading under specific conditions to an adsorption on particles or to a desorption from particles.

Interaction between DCu and particulate copper (PCu) are key to better understand the biogeochemical cycle of copper in the open ocean. Indeed, particles through their 3 components (lithogenic, biogenic and authigenic) play an essential role in the global biogeochemical cycle of trace elements in the ocean (Jeandel and Oelkers, 2015). Despite representing less than 10 % of the total copper pool (GEOTRACES IDP 2017, Schlitzer et al., 2018), PCu is present in all the main processes affecting DCu distribution. External sources of DCu (i.e. atmospheric, riverine and hydrothermal inputs) release lithogenic PCu into the ocean. While biogenic PCu produced by biological activity dominates the upper ocean particulate copper distribution (Lee et al., 2017). Authigenic particles are particles forming in-

situ the water column, by processes such as passive scavenging, flocculation of colloids (Bergquist et al., 2007) and formation of (oxo)-hydroxide or sulphide compounds. Formation of CuS has been observed in the close vicinity of hydrothermal vents, where sulphur concentration are extremely high compared (mM at the fluid vents) to the open ocean where it is scarce (hundreds of nanomolar, Ksionzek et al., 2016).

This chapter describes the copper biogeochemical cycle in the North Atlantic. Dissolved, particulate and speciation data are combined to constrain all components of the copper cycle. The role of ligands concentrations in shaping copper profiles was studied by using the GEOVIDE section as a natural laboratory. Dissolved-particulate copper exchange will be discussed in light of the organic copper complexation. A combination of these parameters is used in order to reveal the effect of reversible scavenging on copper cycle.

2.2. Material and methods

2.2.1. Overview of the GEOVIDE section

The GEOVIDE cruise occurred between May and June 2014 in the North Atlantic aboard the R/V *Pourquoi pas?*. The section started from Lisbon (Portugal), sampling the Iberian shelf before crossing the West European Basin (WEB) and the Iceland Basin (IcB) up to the Reyjkanes Ridge (RR), the upper section of the mid-Atlantic ridge (Figure 2.1). The cruise then crossed the Irminger Basin (IrB), reaching the southern tip of Greenland before sailing south through the Labrador Basin to St John's (Newfoundland). For clarity, the WEB and IcB have been merged into the East Atlantic Basin (EAB) for future reference along the manuscript.

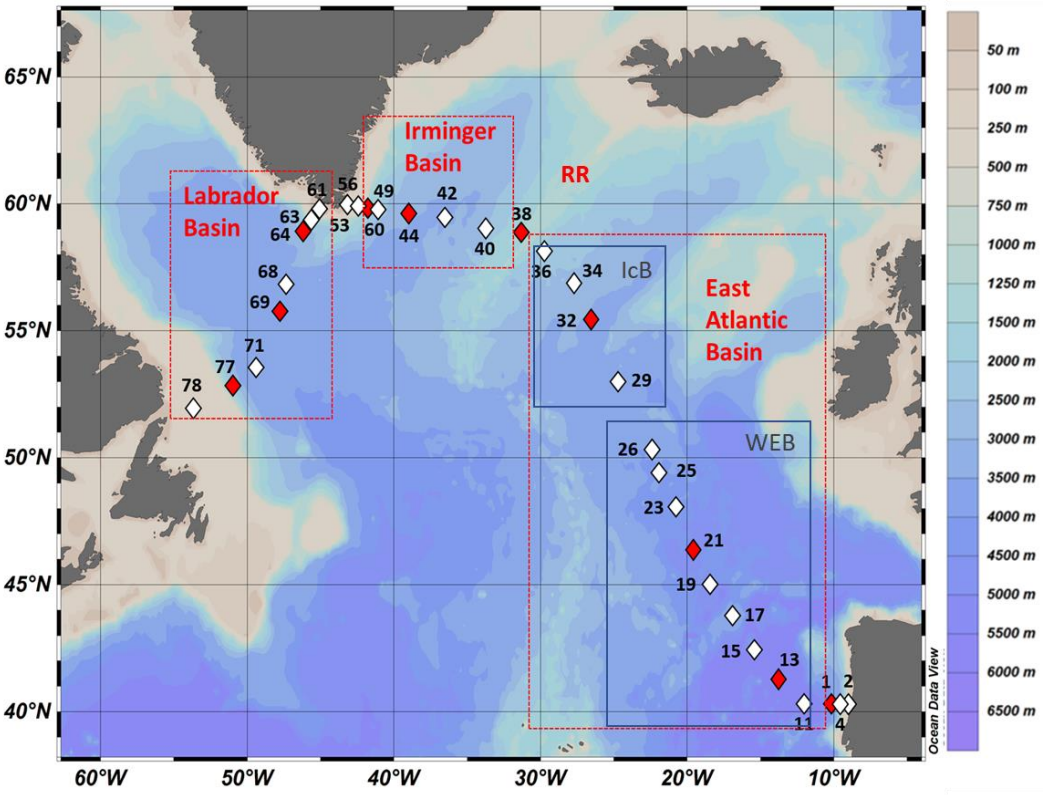

Figure 2.1: Map of the GEOVIDE section with the three biogeochemical area delimited by red squares. Diamonds represent each station with its label, red ones are stations where copper organic speciation samples have been collected. Bathymetry is indicated by the colour scale on the right. This map was generated by Ocean Data View (Schlitzer, R., Ocean Data View, 2017, http://odv.awi.de/, last access: 13/01/2020).

2.2.2. Sampling

Samples were collected during the GEOVIDE cruise using a 22-bottles trace metal clean rosette. The 12 litter bottles had been previously cleaned in the LEMAR laboratory (France) following the GEOTRACES cookbook instruction (Cutter and Bruland, 2012). After recovery, bottles were protected from contamination using plastic bags at both ends. They were then immediately transferred and processed inside a clean container (Class 100). Bottles were shaken 3 times before filtration took place under pressurised conditions using 8 psi filtered (0.2 µm) nitrogen gas. The filtration system (e.g. tubing, filter holder, filters) were acid-cleaned before use following the GEOTRACES protocols (http://www.geotraces.org/images/Cookbook.pdf), rinsed and stored using Milli-Q (18 MΩ cm). Filters were 25 mm diameter to optimise the filter blank to sample signal ratio; except in surface waters where high biological productivity led us to use 47 mm filters to avoid clogging. The dissolved fraction was sampled after filtration on paired filters of 5 µm (Millipore mixed ester cellulose MF) and 0.45 µm (Pall

Gelman Supor™ polyethersulfone). Dissolved copper was collected in 125 mL bottles acidified at pH ~ 1.7 with hydrochloric acid (Merck, Ultrapur®) following the sampling. Samples for the copper organic speciation were collected in 125 mL bottles and stored at -20 °C until analysis. Once all dissolved samples were collected or until clogging, filter holders were disconnected, and the remaining water was drained using a syringe. Filters were removed using acid-clean tweezers and stored as a pair at -20 °C inside polystyrene Petrislide (Millipore).

2.2.3. Analytical measurements

2.2.3.a. Dissolved copper analysis

DCu measurements were performed using a sector field inductively coupled plasma mass spectrometer (SF-ICP-MS Element XR instrument, Thermo Fisher, Bremen, Germany), at Pôle Spectrométrie Océan (IFREMER, France), alongside with DFe, DMn, DZn, DCo and DPb. The spectrometer was coupled to an ESI seaFAST-pico™ introduction system and ran with a method analytically similar to that of Lagerström et al. (2013). A six-point calibration curve was prepared by standard additions of the mixed element standard to our acidified in-house standard and ran at the beginning, the middle and the end of each analytical session. Each analytical session consisted of about sixty samples. Final concentrations of samples and procedural blanks were calculated from indium-normalized data. Accuracy was determined from the analysis of four triplicate consensus materials (SAFe S, SAFe D2, GSC and GSP) during each analytical run to ascertain accuracy and precision.

2.2.3.b. Organic speciation of dissolved copper

Speciation of dissolved copper was determined using competitive ligand-exchange adsorptive cathodic stripping voltammetry (CLE-AdCSV) within a clean laminar flow hood (class 100). The voltammetric system consisted in a μAutolab type III connected to a 663-VA stand (Metrohm) mounted with a hanging mercury drop electrode and a glassy carbon counter electrode. An Ag/AgCl reference electrode was used with a salt bridge filled with 3M potassium chloride (KCl) solution. Voltammetric analyses were done using a home-designed polytetrafluoroethylene (PTFE) voltammetric cell and its specific PTFE steering rod. This cell has been developed to minimise the sample volume required in the cell from 10 mL to a minimum of 3 mL. A volume of 5 mL has been used to analyse all samples.

Salicylaldoxime acid (SA, Acros organics) was used as a competing ligand to measure the natural copper complexing ligands. Solutions at 10^{-2} M SA were prepared by dissolving 13.7 mg of SA powder in 10 mL milli-Q (18.2 mΩ cm^{-1}) acidified with 10 µL hydrochloric acid (HCl, TraceSELECT® ultra, Fluka). To fix the pH, borate buffers were elaborated with 1 M boric acid (salts, analytical grade, Fisher Scientific) and 0.35 M ammonia (TraceMetal grade, Fisher) in a 250 mL bottle. After UV-irradiation to remove any organic contaminants, the solution was cleaned using 100 µM manganese oxide (MnO_2; Van Den Berg, 1982). After vigorous shaking, the solution was left to settle overnight and then filtered through 0.2 µM filters (Cellulose Nitrate Membrane 47 mm diameter, Whatman®). KCl solutions were made from KCl salts dissolved in Milli-Q water and cleaned by co-precipitation with MnO_2 identically to the borate buffer. Copper standard solutions of 100 µM were prepared from a standard 1000 mg L^{-1} solution (SpectrosoL®, BDH) in 20 mL milli-Q water acidified at pH 2 with HCl (TraceSELECT® Ultra, Fluka). From the 100 µM solutions, 1 µM Cu^{2+} standards were prepared by dilution in 20 mL milli-Q at pH 2.

Samples were defrosted at ambient temperature for at least 6 hours before preparation. They were shaken carefully to ensure complete redissolution of all precipitated salts. Then, 75 mL of sample was poured in a 125 mL clean bottle with 2 µM SA and 0.01 M borate buffer. From this bottle, 13 aliquots were collected within individual PTFE cells and spiked with increasing Cu^{2+} concentrations. The first two aliquots were not spiked with copper while the last one was spiked with up to 15 nM copper. The range of copper addition was decided according to the dissolved copper concentration of the sample. High DCu concentrations were associated with a higher range of addition. The leftover sample in the 125 mL bottle was poured inside the analytical voltammetric cell to condition it. Aliquots were left for overnight equilibration until analysis. Voltammetric measurements were done by transferring the aliquot inside the analytical voltammetric cell from the aliquot with no added copper to the aliquot with the highest Cu^{2+} spike. The measurement cell was not rinsed in between aliquots to keep the conditioning intact.

Analyses were conducted using the GPES software (version 4.9, Eco Chemie) to control the voltammetric system. Samples were initially purged for 240 s with N_2 to remove the interference from the oxygen wave. After discarding 5 mercury drops, a deposition was held at -0.15 V for 300 s. Following 5 seconds of equilibration, a differential pulse stripping scan was accomplished from 0 to -0.5 V using the following optimised parameters: a modulation amplitude of 0.05 V, a modulation time

of 0.015 s and an interval time of 0.1 s. The intensity of the Cu-SA peak was measured using the peak derivative calculated using the GPES analysis tool with a curve cursor to delimit the peak extent accurately. A minimum of two scans were always done; in case of discrepancies in peak intensities, a third scan was produced, and the two closest scans were used for analysis.

Treatment of each titration was accomplished using the ProMCC software (Omanović et al., 2015). This software allows the user to compare 3 fitting methods: the Langmuir, the Ruzic/Van den Berg and the Scatchard methods. All samples have been analysed using the Ruzic/Van den Berg method, but a comparison with the other methods was performed. If all methods were giving similar results, the sample was considered as of good quality. If results from these 3 methods were different, the sample was considered as of poor quality and discarded from any future interpretation. ProMCC allows the user to choose the number of ligands class to model on the titration. In our case, a one-ligand model was best suited to fit our titration data, similarly to that recently found for copper speciation in the Atlantic (Jacquot and Moffett, 2015). After data treatment, the concentration of ligands (L) and its conditional binding strength (logK) are obtained as well as the calculated free-copper concentration (Cu^{2+}). The excess of ligands ($L_{\_Excess}$) compared to dissolved copper was calculated by subtracting [DCu] from the ligands' concentration. This proxy indicates the number of additional moles of copper that the ligands could complex. Samples have been measured randomly per station in order to avoid any interpretation bias. All statistical analyses are performed using the software Minitab® 18.

2.2.3.c. Particulate copper and particulate trace element analysis

Particulate copper measurements, as well as particulate aluminium and phosphorus, were realised following the procedure described in Gourain et al. (2019). Briefly, PCu analyses were conducted at the LEMAR laboratory (France, Plouzané) inside a clean room (class 100). Filters were cut in half using a ceramic blade; one half was used for total particulate analysis and the other half for acid-leachable particulate analysis. The half filter for total particulate was then removed from its storage unit (PretiSlide) using acid-clean tweezers and placed inside a PFA vial (Savillex™). A 2 mL mixture of 2.9 mol L^{-1} hydrofluoric acid (HF, suprapur grade, Merck) and 8 mol L^{-1} nitric acid (HNO_3, Ultrapur grade, Merck) was added. After sealing the vials, they were heated on a hot plate at 130 °C for 4 hours to complete the total digestion of the particulate materials. After cooling, filters were removed, and the digest solution was evaporated at 110 °C. The residue was re-dissolved in 3 mL of 0.8 mol L^{-1} HNO_3

(Ultrapure grade, Merck) and stored at 4 °C in a 15 mL polypropylene centrifuge tube (Corning®) until analysis.

Analyses were accomplished on a sector field inductively coupled plasma mass spectrometer (SF-ICP-MS Element 2, Thermo-Fisher Scientific). Samples were diluted 7 times with a 0.8 mol L^{-1} HNO_3 (Ultrapur grade, Merck) spiked with 1 µg L^{-1} of indium (^{115}In) solution to track the instrumental drift. All the data were normalised using the ^{115}In signal and concentrations were calculated from multiple external calibration curves. The data presented in this chapter noted as PCu are the sum of both small (0.45 to 5 µm) and large (> 5 µm) fractions.

2.2.3.d. Biogenic, lithogenic and authigenic particulate copper determination

To investigate the particle composition, elemental ratios are a useful tool (Gourain et al., 2019; Lam and Bishop, 2008). The lithogenic fraction of PCu has been calculated using the copper to aluminium (PAl) Upper Continental Crust ratio of 0.132 mmol.mol^{-1} (Taylor and McLennan, 1995).

$$\%PCu_{Litho} = 100 * \left(\frac{\mathrm{PAl}}{\mathrm{PCu}}\right)_{\mathrm{sample}} * \left(\frac{\mathrm{PCu}}{\mathrm{PAl}}\right)_{\mathrm{UCC.ratio}} \quad (2.1)$$

The biogenic fraction of PCu was calculated using the copper to phosphorus (PP) content in phytoplankton cells (Twining and Baines, 2013). However, trace element ratios within phytoplankton cells are variable according to the species from 0.06 mmol Cu mol^{-1} P (diatom) to 1.36 mmol mol^{-1} (dinoflagellates); and subsequently the community composition (Ho et al., 2003; Twining and Baines, 2013). Moreover, the plasticity of phytoplankton requirement involves a variable ratio according to nutrients availability and health of the community (Guo et al., 2012a). In consequence, a maximum PCu/PP ratio in the North Atlantic of 2 mmol.mol^{-1} (Twining and Baines, 2013) was used in order to provide an upper limit to the biogenic fraction.

$$\%PCu_{Bio} = 100 * \left(\frac{\mathrm{PP}}{\mathrm{PCu}}\right)_{\mathrm{sample}} * \left(\frac{\mathrm{PCu}}{\mathrm{PP}}\right)_{\mathrm{cell.quota}} \quad (2.2)$$

The authigenic fraction was estimated by subtracting the lithogenic and biogenic fraction from the total fraction, 100 %.

$$\%PCu_{Auth} = 100 - \%PCu_{Litho} - \%PCu_{Bio} \quad (2.3)$$

Due to the uncertainty in some ratios (i.e. UCC and cell quotas), some samples were associated with $\%PCu_{\_Litho}$ and $\%PCu_{\_Bio}$ proxies higher than 100 %. To resolve this issue, $\%PCu_{\_Litho}$ was calculated first and values higher than 100 % were set at 100 %. The remaining percentage could only be biogenic

and/or authigenic. Secondly, $\%PCu_{\_Bio}$ was calculated with a maximum value set by $\%PCu_{\_Litho}$ ($\%PCu_{\_Bio} \leq 100 - \%PCu_{\_Litho}$). Finally, the $\%PCu_{\_Auth}$ was calculated using Equation 2.3.

2.3. Results

2.3.1. Hydrography and biological production along GEOVIDE

The GEOVIDE section encountered several water masses of various physical characteristics (Figure 2.2). Starting off the Iberian coast, the warm and salty ($\theta° = 11.7°C$, $S = 36.50$) Mediterranean Overflow Water (MOW) was flowing northward along the Iberian margin between 600 and 1700 meters depth. In surface of the EAB, the warmest water mass of the section was observed, the North Atlantic Central Water (NACW, $\theta° > 12.3°C$, $S > 35.60$). At depth of the EAB, the North East Deep Atlantic Water (NEADW, $\theta° = 2.0°C$, $S = 34.89$) was spreading southward into the east Atlantic. Between 1000 and 2500 meters, an old Labrador Sea Water (LSW) was flowing in the east part of the EAB. The flanks of the Reykjanes Ridge were surrounded by the Iceland-Scotland Overflow Water (ISOW, $\theta° = 2.6°C$, $S = 34.98$), which mixes with artic water masses to form the NEADW.

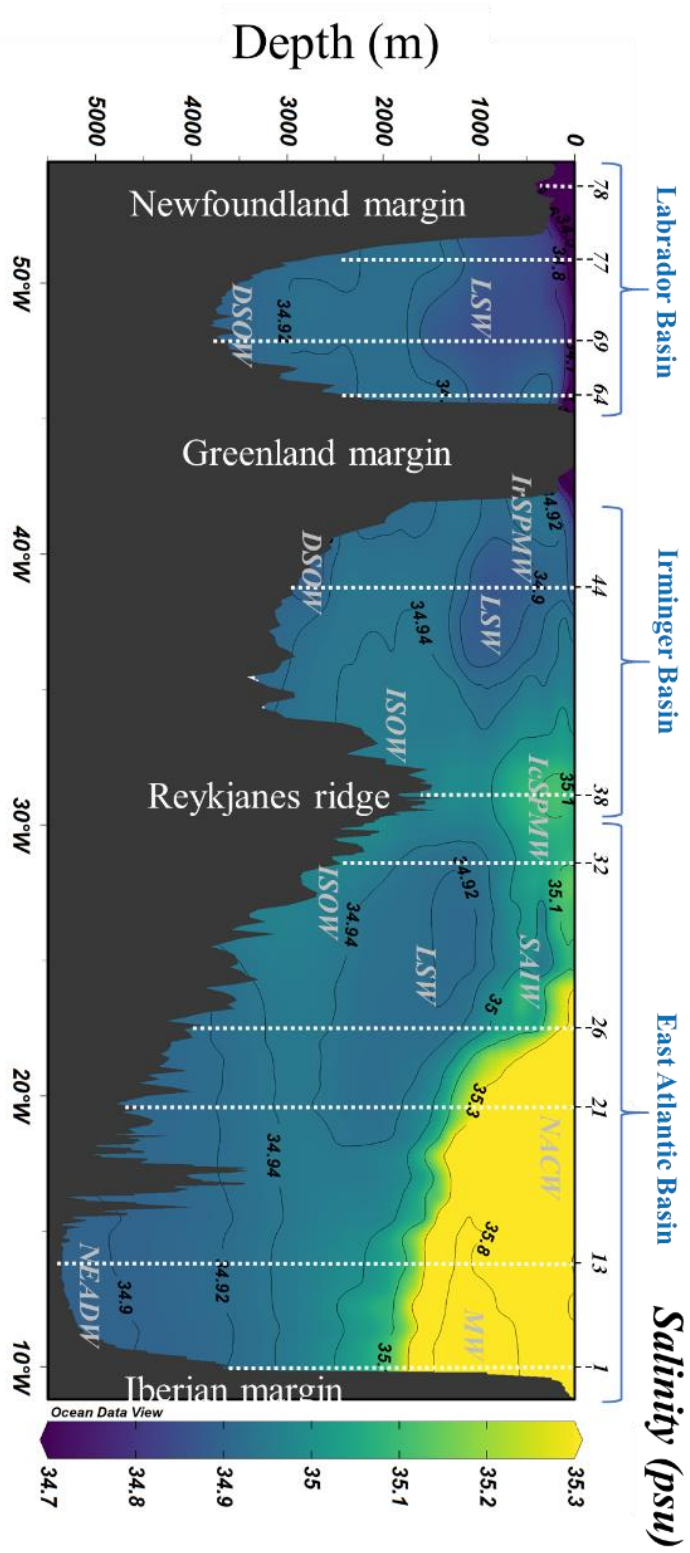

Figure 2.2: Section of salinity along the GEOVIDE section. Biogeochemical provinces are indicated in blue above station labels in order to visualise the position of the map. Important bathymetric feature are signalised in white. Main water masses are indicated in grey. The contour line are indicated by black line. This figure was generated using Ocean Data View (Schlitzer, R., Ocean Data View, http://odv.awi.de/, 2017.

In the Irminger and Labrador basins, the cold and fresh Denmark Strait Overflow Water (DSOW, θ° = 1.3°C, S = 34.91) was spreading along the seafloor. In the LB, a deep convection (> 2000 m) was leading to the formation of the LSW (θ° = 3.0°C, S = 34.9) and its transport through the North Atlantic was observable in the IrB between 500 and 1200 meters.

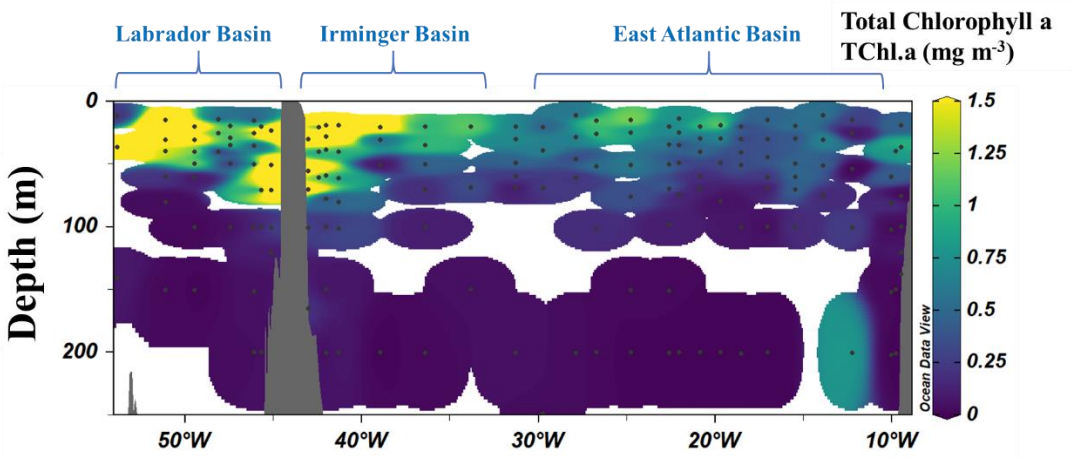

Figure 2.3: Total chlorophyll.a concentration (mg m^{-3}) within the first 250 m along GEOVIDE. This figure was generated using Ocean Data View (Schlitzer, R., Ocean Data View, http://odv.awi.de/, 2017.

The North Atlantic is one of the most productive regions of the world's ocean, playing a key role in biological carbon export at depth (Martin et al., 1993; Sanders et al., 2014). Along the section, total chlorophyll.a (TChl.a) concentrations were between 0.004 and 1.217 mg m^{-3} (Figure 2.3) in the range of previous North Atlantic observations (Andersen et al., 1996; Campbell and Aarup, 1992; MODIS dataset). Elevated [TChl.a] were found within the first 50 meters of each station, with a strong spatial variability. TChl.a was relatively low in the WEB while being elevated within the IrB and LB (Figure 2.3).

2.3.2. Distribution of DCu along GEOVIDE

In surface waters, dissolved copper concentrations were low at almost every station with a median value in the first 50 meters of 1.14 nM (Figure 2.4). The only exception was at station 78, above the Newfoundland shelf where DCu values of up to 2.64 nM were found in surface waters where a low salinity layer was identified. Copper distributions were variable between the basins encountered along the section. Within the East Atlantic basin, DCu concentrations were increasing linearly with depth

along the entire water column. Below 2500 m, [DCu] were always higher than 1.50 nM with a maximum of 4.98 nM at 4500 m of station 21 (Figure 2.4). On the contrary, within the Irminger and Labrador basin, DCu concentrations were homogeneous with depth leading to a low median value of 1.25 nM. Above the Greenland shelf, at station 53 and 61, high concentrations of dissolved copper were observed ranging from 1.77 to 3.56 nM. The eastern Greenland shelf had lower DCu concentration than the western shelf, with a median of 2.06 nM compared to 3.40 nM, respectively.

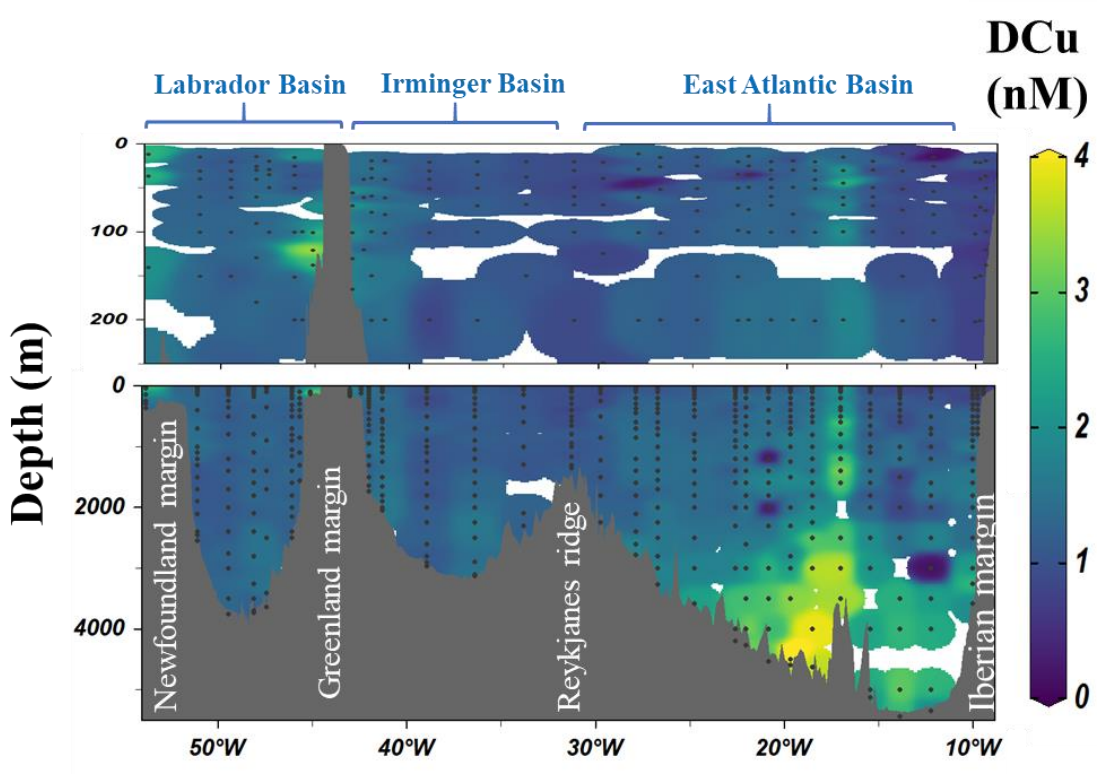

Figure 2.4: Dissolved copper (nM) concentration along the section with a focus on the 250 first meters.

2.3.3. Organic complexation of copper in North Atlantic

Concentrations of Cu Ligands in copper-equivalent units in the North Atlantic ranged from 1.19 to 8.28 nM with a median of 3.14 nM. The global distribution of copper ligands was scattered, not following any smooth profiles nor any obvious trends (Figure 2.5a). The East Atlantic Basin presented a median [L] value of 3.46 nM. At depth, for stations 13 and 21, an increase of concentrations was observed with values reaching 7.47 nM (5000 m at St 13). Station 13 was also characterised by a strong ligand signal from 200 to 1000 meters depth reaching a maximum of 8.28 nM at 500 m. Within the Labrador and Irminger basins, ligand concentrations were lower than in the East Atlantic basin with a

median value of 2.85 nM. Along the east Greenland margin, at station 60, an increase of copper ligands concentration was measured between 350 and 650 m with values reaching more than 4.3 nM.

Along the section, the binding capacities of the copper ligands, log K, ranged from 12.1 and 13.9 (Figure 2.5b). Log K values were relatively homogeneous along the section but 3 areas presented particularly low values (log K < 13.0): above the Reykjanes Ridge (St 38) up to 400 meters depth, in (sub-)surface (up to 600 m) of station 13 and at depth (below 4000 m) of station 13.

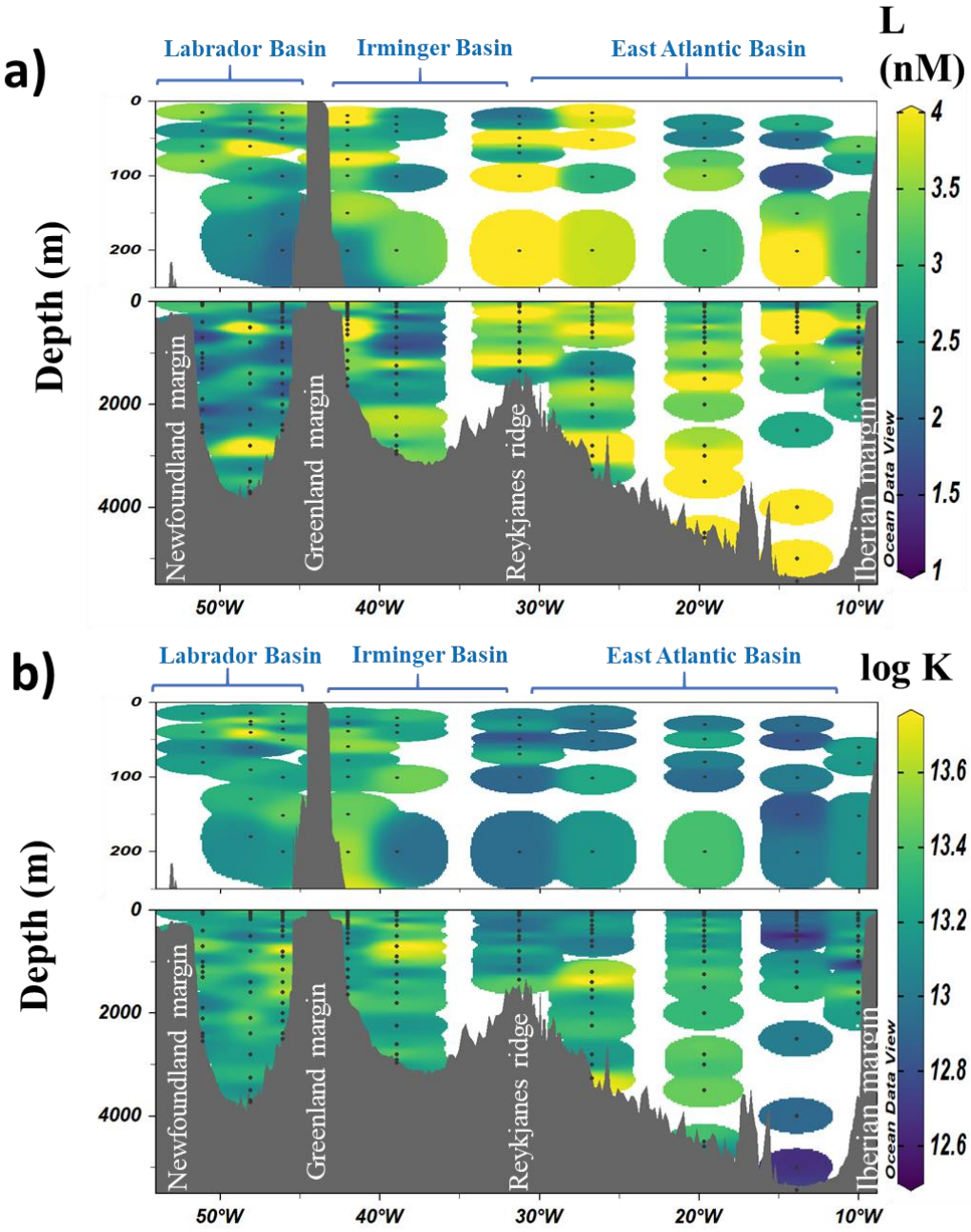

Figure 2.5: Distribution of a) copper-equivalent ligands concentrations and b) binding strenght in the first 250 m and the entire column.

The concentration of excess ligands $L_{\_Excess}$ (Figure 2.6a) displays a similar distribution as the copper-equivalent ligand concentration (Figure 2.5a). High concentrations were observed in the East Atlantic basin where a median of 2.09 nM was measured. The highest concentration observed, 7.38 nM, was at 500 meters depth of station 13. Above the Reykjanes ridge, the excess ligand concentrations were high (median: 2.63 nM) through the water column, except at the deepest sample close to the seafloor, where it only reached 1.20 nM. Within the Irminger basin, $L_{\_Excess}$ concentrations ranged from 0.10 to 3.61 nM; the median $L_{\_Excess}$ was 1.83 nM with the maximum observed at 550 m of station 60. Lower concentrations were measured in the Labrador basin with a median of 1.34 nM.

Along GEOVIDE, surface free copper concentration, $DCu_{\_Free}$ were below the picomolar concentration with a maximum of 100 fM at 15 m of station 69 (Figure 2.6b). Within the East Atlantic basin, $DCu_{\_Free}$ ranged from 17 to 1706 fM with the lowest values being measured within the water column while higher concentrations were measured at interfaces (margin-ocean, air-ocean and sediment-ocean). Along the Iberian margin, several samples, collected below 600 m at station 1, had elevated [$DCu_{\_Free}$] up to 1.7 pM. These elevated concentrations were scattered through the water column with low concentrations observed in between the elevated ones. At stations 13 and 21, high free dissolved copper concentrations (>56 fM) were measured in (sub-)surface up to 150 meters depth. At these same stations, elevated concentrations were observed at depth with a maximum close to the seafloor of 204 fM at station 13 and 123 fM at station 21. The Irminger basin was characterised by a low median $DCu_{\_Free}$ concentrations of 34 fM. In the Labrador basin, free copper values were elevated but scattered, median of 58 fM with a standard deviation of 59 fM (n= 54). Along the west Greenland margin, high [$DCu_{\_Free}$] are measured between 200 and 500 m of station 64. On the other side of the basin, along the Newfoundland margin, concentrations were elevated, > 60 fM, from 400 meters depth to the seafloor at 2560 m.

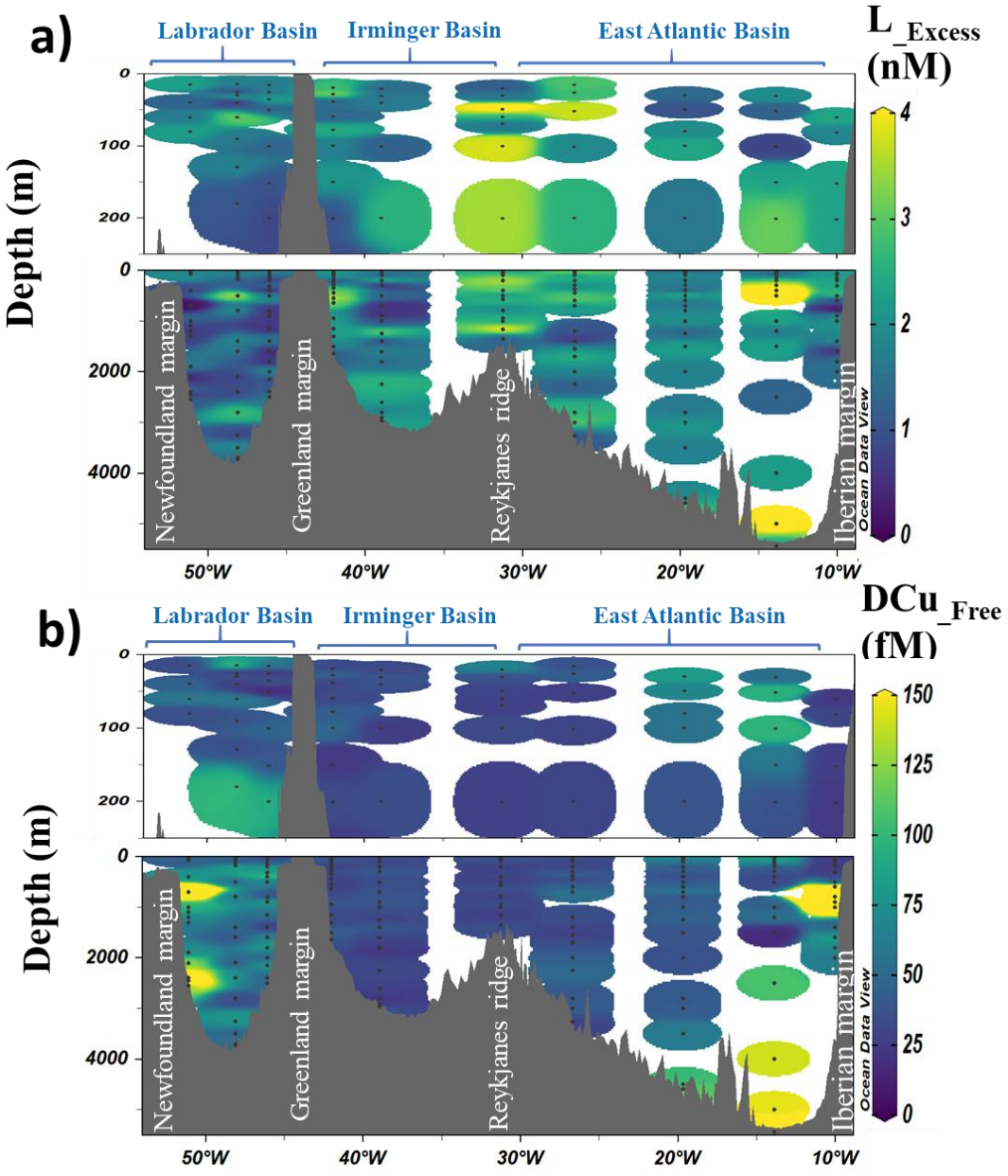

Figure 2.6: Distribution of a) excess ligands concentrations and b) free dissolved copper in the first 250 m and the entire column.

2.3.4. Particulate copper along GEOVIDE

Particulate copper (> 0.45 µm) was present at picomolar concentration along the section, with concentrations ranging from below detection limit to 876 pM (Figure 2.7). In the East Atlantic basin, surface concentrations were low from station 2 to 19 with a median [PCu] of 25 pM within the first 100 m. From station 21, PCu reached higher values with a median of 40 pM and a maximum of 880 pM at station 34. Within the mesopelagic layer, PCu distribution was scattered with high values (up to 190 pM) surrounded by low background concentrations (~ 1 pM). Close to the seafloor, increasing [PCu]

was observed at every station of the basin (Figure 2.7). The Irminger and Labrador basins had similar PCu distribution along the GEOVIDE cruise. In the first 100 m, elevated PCu are observed with a median of 50 pM. In the water column of open ocean stations, concentrations dropped to values less than 18 pM until the vicinity of the seafloor where PCu increase up to 96 pM.

The three shelves encountered along the section track (Iberian, Greenland and Newfoundland) were characterised by high concentrations close to the sedimentary-water interface (Figure 2.7). The Iberian shelf (station 2) had only elevated concentration by the seafloor (up to 220 pM) while the Greenland and Newfoundland shelves showed elevated concentration along the entire column with a median of 55 pM and 64 pM, respectively.

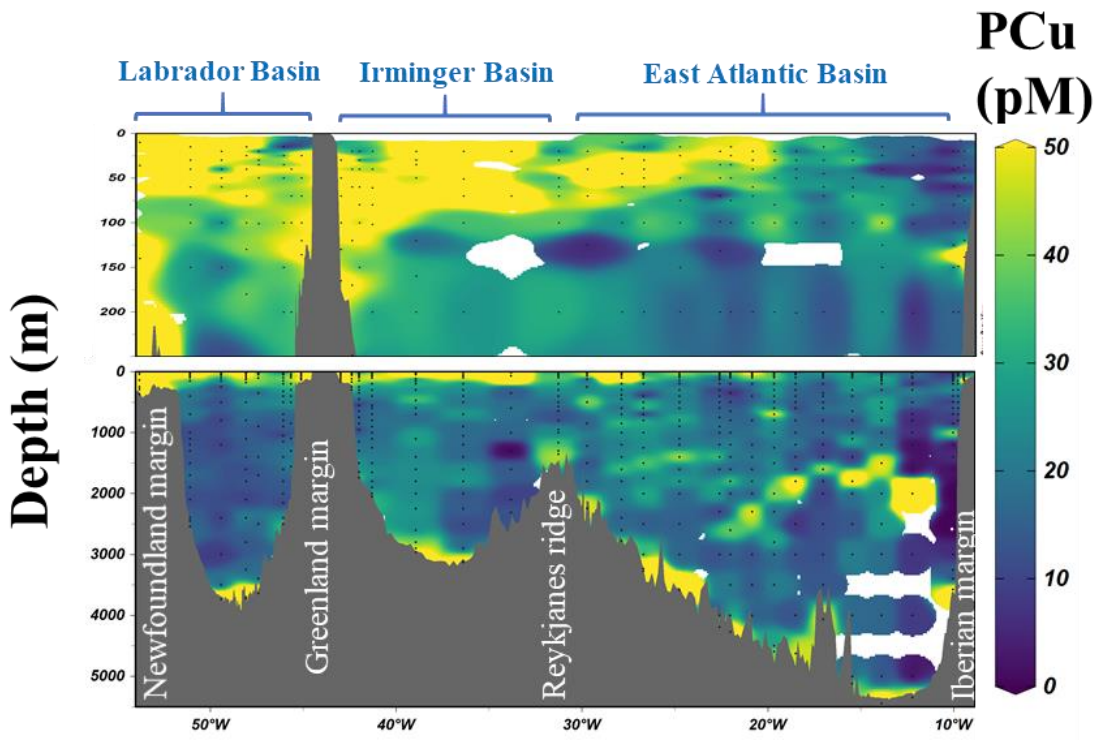

Figure 2.7: Section of the particulate copper along GEOVIDE. Please note that the colorbar has been scaled in order to show the interesting features. In consequence, some extreme values higher than 50 pM have the same color as those at 50 pM concentration.

2.4. Discussion

2.4.1. Dissolved and particulate copper biological transfer in open ocean surface

In the open ocean, two main processes affect the copper cycle in surface: atmospheric deposition and biological uptake. During the GEOVIDE cruise, atmospheric deposition fluxes were low (Shelley et al., 2018) and surface dissolved aluminium concentrations did not show any dust inputs (Menzel

Barraqueta et al., 2018). But a possible previous deposition event was suggested by Gourain et al. (2019) based on the particulate iron to particulate aluminium ratio (in particles > 0.45μm size). Low PFe/PAl ratios were observed in surface waters between stations 11 and 23, similar to the anthropogenic aerosol ratio previously observed in the North Atlantic (Buck et al., 2010a). In consequence, the influence of atmospheric deposition was likely insignificant for surface copper cycle along GEOVIDE and discussion will instead be focused on the impact of biology in surface waters. GEOVIDE section is an ideal natural laboratory to study the influence of biology on copper cycle. The cruise spanned several biological provinces with varying chlorophyll.a concentration (Figure 2.3) including the highly productive Irminger (Sanders et al., 2005) and Labrador basins (Fragoso et al., 2016). During the cruise, the phytoplankton community was constrained to the first 50 meters (Figure 2.3), thus this depth range has been selected to study the influence of biology on the copper cycle (Figure 2.8). Two proxies were used to follow the biological productivity, the chlorophyll a pigment concentration (TChla) and the particulate phosphorus concentration (PP).

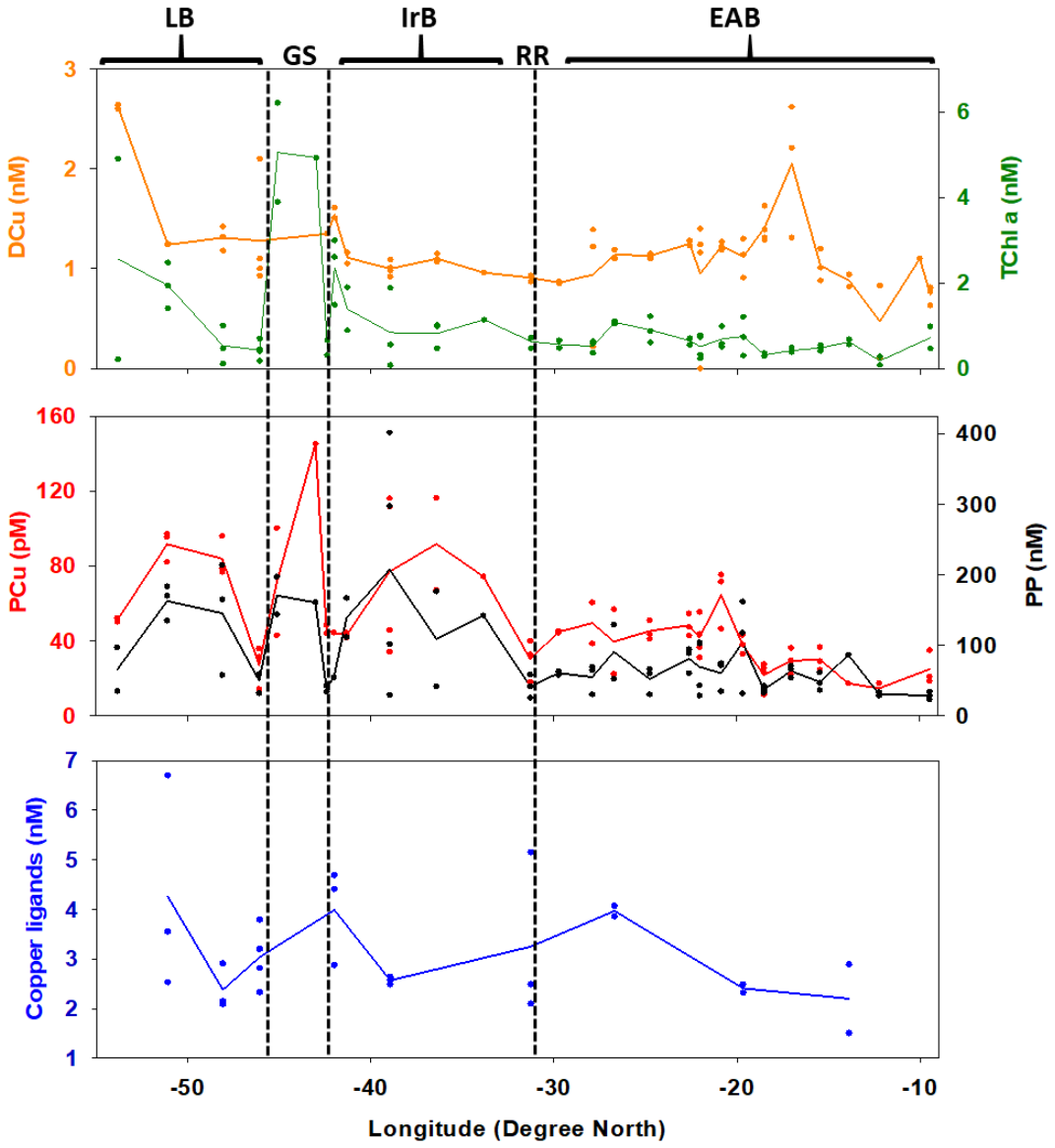

Figure 2.8: Panels of dissolved copper (orange), chlorophyll.a (dark green), particulate copper (red), particulate phosphorus (black) and ligands concentration (blue) in surface. Average within the first 50 meters are represented in function of the section distance, Lisbon being considered as the start (km 0). Location of oceanic basins (EAB, IrB and LB), Keykjanes Ridge (RR) and Greenland shelf (GS) are indicated above the panel.

Along the section, biological uptake was not strong enough to actively draw down the DCu concentrations in surface waters (Figure 2.4). Dissolved copper concentrations were low in surface with a median of 1.14 nM and were relatively constant along the cruise track (sd: 0.42 nM, n: 125). Low surface concentration has been previously documented around the globe, e.g. Heller and Croot (2014), Roshan and Wu (2018). It has been associated with biological uptake depleting bioavailable nutrients in surface waters (Boyle et al., 1977; Jacquot and Moffett, 2015; Sunda and Huntsman, 1995a). During

GEOVIDE, DCu concentrations were not inversely correlated with biological proxies such as chlorophyll.a or particulate phosphorus (PP) (Figure 2.8). The lack of correlation does not indicate the absence of biological uptake; it indicates that the DCu pool was high compared to the copper nutrient requirement of the phytoplankton community. To our current knowledge, copper has never been shown as being a limiting nutrient for primary productivity in open ocean, in contrast to iron (Behrenfeld et al., 1996; Martin and Fitzwater, 1988) or cobalt (Panzeca et al., 2008; Saito et al., 2002).

Despite the lack of correlation between DCu and chlorophyll.a, the production of organic particulate copper by phytoplankton was clear. Figure 2.7 shows maximum [PCu] in surface in every basin along the section; within the first 50 m, the median concentration was 43 pM. The biological uptake was observable due to the lower concentration of PCu compared to DCu. Figure 2.8 displays PCu and PP variations in surface waters (up to 50 m) along the entire section, PP being used here as a biological proxy. There is a strong significant correlation ($p < 0.05$) between PCu and PP along the entire GEOVIDE section clearly indicating that particulate copper is driven by the biology. In the EAB, PP and PCu were low where low biological productivity was observed (Figure 2.3 and 2.8). In the Arctic basins (IrB and LB), concentrations of PCu and PP increased to values up to 876 pM and 402 nM, respectively. The two proxies varied from station to station following the same trends (Figure 2.8). Ligand concentrations and binding strengths along the section were elevated enough to maintain the low DCu_{Free} concentrations and contain any possible toxicity. Indeed, [DCu_{Free}] was maintained under 100 fM in surface waters (Figure 2.6b), while significant toxic effect is observed at picomolar levels; 13 pM for cyanobacteria and 92 pM for large diatoms (Brand et al., 1986). In surface waters, no correlation was found between [L] and biological activity (Figure 2.8), similar to what was recently reported in the North Atlantic by Jacquot and Moffet (2015). It suggests that copper ligands in these surface waters were not of recent biogenic origin. Despite culture experiments demonstrating the biological production of ligands by phytoplankton (Croot et al., 2000; Dupont and Ahner, 2005), such production has not yet been observed in the open ocean. Lack of correlation does not however mean the absence of biological production. Few studies measured the photochemical degradation of copper complexing ligands including thiols within rivers (Laglera and van den Berg, 2006; Moingt et al., 2010). Within a day of sunlight exposure, 2 to 60% of ligands and 30-50 % of thiols were degraded (Laglera and van den Berg, 2006). Interestingly, thiols complexing copper are more stable than free thiols with a half-life increasing from 2 days to almost a decade (Laglera and van den Berg, 2006). Such variability

in residence time could be leading to a buffering of the ligand concentration in surface by the DCu concentration. The excess ligands are quickly degraded while the complexed ligands have a long residence time allowing a homogenisation of L distribution and conceal their sources, including biological one. Along GEOVIDE, the copper cycle in surface waters was driven by the biological activity.

2.4.2. Copper cycle at the sedimentary interfaces

During the GEOVIDE cruise, benthic nepheloid layers (BNLs) were present in most basins: the west part of the EAB, the IrB and the LB (Gourain et al., 2019; Le Roy et al., 2018). BNLs are resuspension of benthic particles triggered by hydrographic stresses in the vicinity of the seafloor as deep eddies, boundary currents and benthic storms (Gardner et al., 2017, 2018). Along the section, the extent of all BNLs were consistently 300 meters above the seafloor (Gourain et al., 2019). In the following discussion, the depth range of 300 meters above seafloor is considered to study the sedimentary interface impact on copper cycle. Moreover, all shelf stations (2, 53, 56, 61 and 78) have been discarded to focus on the deep benthic processes. Particulate aluminium is used as a proxy of BNLs; being the most abundant particulate lithogenic trace element, it can be used to estimate the intensity of resuspension at each station (Gourain et al., 2019).

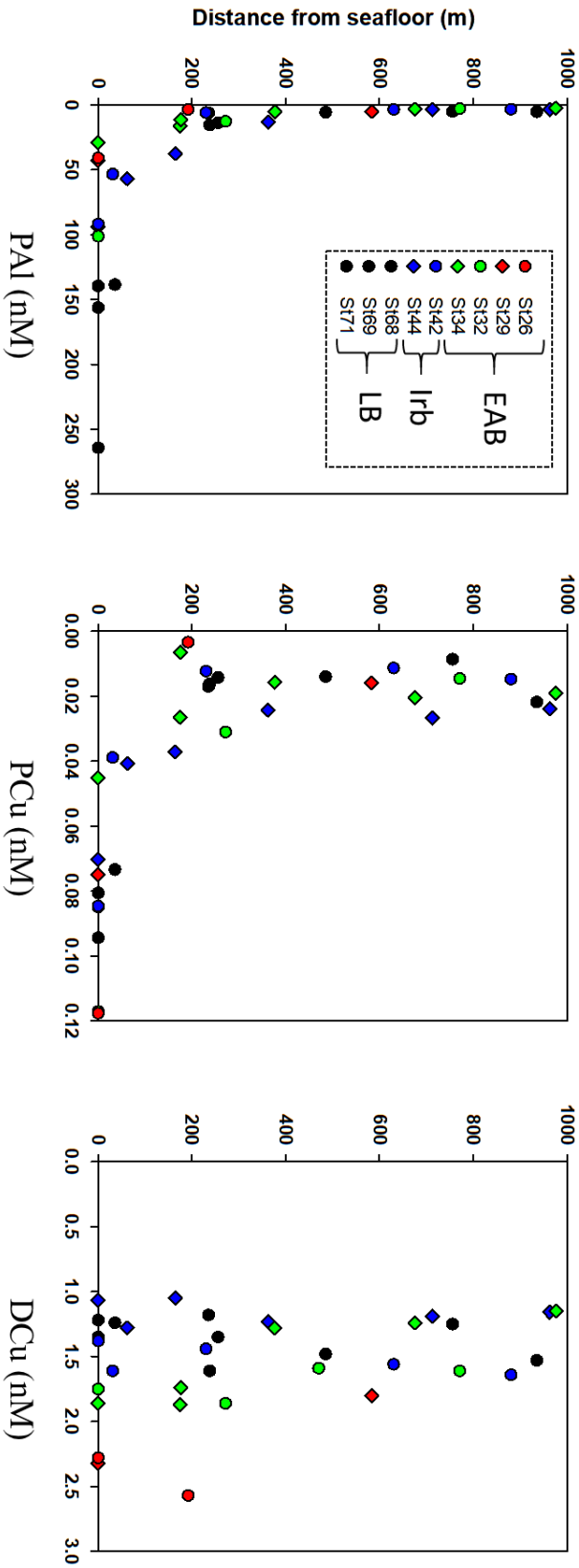

Figure 2.9: Distribution of PAl, PCu and DCu function of the distance from the seafloor at all stations affected by benthic nepheloid layers (BNLs).

Dissolved copper concentrations were not influenced by sediment resuspension in the vicinity of the seafloor as observed on Figure 2.4 and 2.9. Within the LB and IrB, no increases nor decreases of [DCu] were observed within the nepheloid layer (Figure 2.9). While in the EAB, an increase was apparent (Figure 2.10), although it was likely due to the linear vertical distribution of copper rather than any release processes induced by BNLs. The DCu increase with depth started from the upper ocean to depth and no change of that slope is detected within the BNLs (Figure 2.4) suggesting that sediment resuspension was neither a source nor a sink of dissolved copper along the GEOVIDE section. Higher resolution sampling would be needed to confirm this observation.

Within the LB and IrB, benthic resuspension was driving the PCu cycle. In these basins, PCu and PAl were closely correlated ($p < 0.05$, Figure 2.10) demonstrating the inputs of PCu from BNLs. In the eastern EAB, resuspensions of PAl were less important (< 57 nM) but the [PCu] stayed at a high level (> 29 pM), indicating the de-coupling of the two proxies (Figure 2.10). A source of PCu apart from benthic resuspension was impacting the particulate copper pool in this basin. Sediments resuspension were not the main process driving PCu cycle in the EAB. The increase of PCu concentration at depth in the EAB is further discussed in section 4.4.

Resuspension of sediment along GEOVIDE was a source of particulate copper but no influence on the dissolved pool was observed. Newly resuspended PCu did not dissolve to enrich the DCu pool. In consequence, the role of BNLs on the global copper biogeochemical cycle might not be significant. Resuspended particles being contained within 300 meters above the seafloor, BNLs would not be a source of copper in the surface layer.

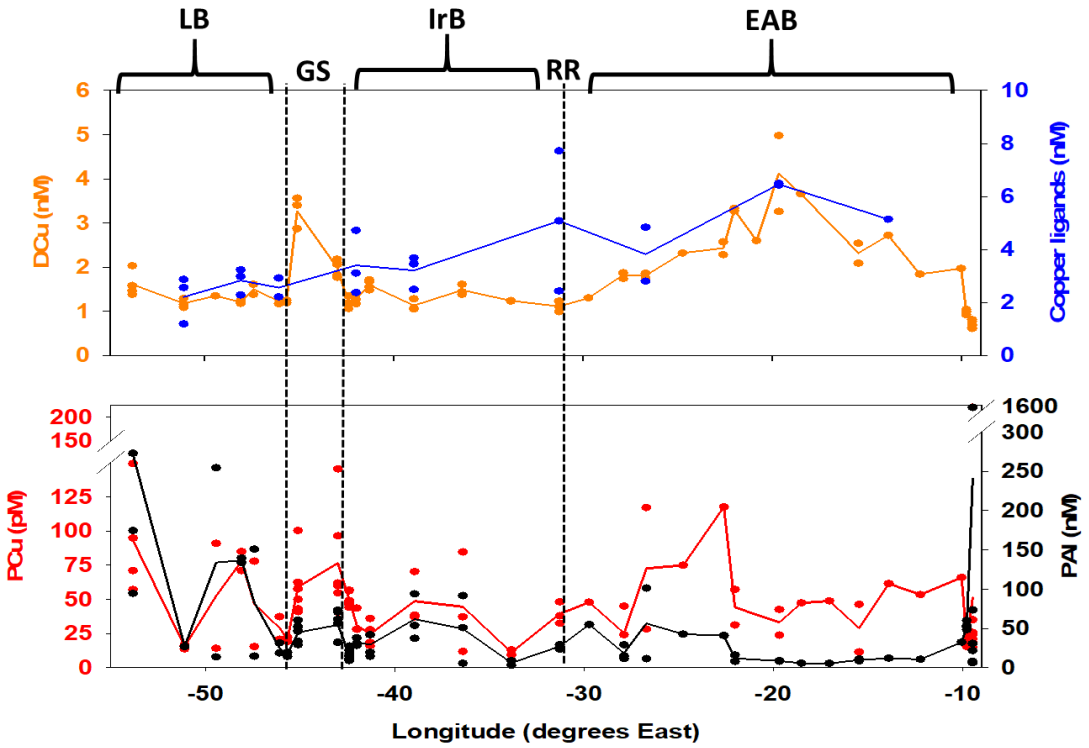

Figure 2.10: Panels of dissolved copper (orange), particulate copper (red), particulate aluminium (black) and ligands concentration (blue) at the sedimentary interface. Average within 300 meters from the seafloor are represented in function of the section distance, Lisbon being considered as the start (km 0). Location of oceanic basins (EAB, IrB and LB), Keykjanes Ridge (RR) and Greenland shelf (GS) are indicated above the panel. Notice the breaks in y-axis for the bottom panel.

Copper-ligands were not influenced by sediments resuspension during GEOVIDE. Ligand concentrations were not correlated with the lithogenic proxy PAl (Figure 2.10). Spatial distributions of ligands followed the same patterns as DCu with low concentrations in the LB and IrB and increasing concentrations when entering in the EAB. The excess ligand concentration was scattered along the section with no clear trend between intense and moderate BNLs (Figure 2.6a). Distribution of $DCu_{\_Free}$ followed the same trend as DCu (Figure 2.6b). Similarly, [DCu_Free] were not influenced by sediment resuspension. Overall, the BNLs had no influence on any dissolved proxy (DCu, L, $L_{\_Excess}$ and $DCu_{\_Free}$) but highly impacted PCu cycle within the LB and IrB.

2.4.3. Stabilisation of DCu by ligands at depth of the EAB

Along GEOVIDE, inter-basins differences in dissolved copper distribution were striking (Figure 2.4). Within the WEB, DCu concentrations were increasing with depth up to 4.98 nM. While in the

Labrador and Irminger Basin, DCu concentration were homogeneous with depth with a median of 1.24 nM (SD: 0.19, n=200). A linear increase with depth is the predominant distribution of DCu in open ocean (Chapter 4). Distribution differences along the section are an opportunity to study the process behind the linear accumulation of DCu with depth and the implication of organic complexation. As previously stated, ligands distribution was relatively homogeneous along the entire GEOVIDE section. But an increase of the copper-equivalent ligand concentration was observed at depth of the East Atlantic Basin (Figure 2.5a) where DCu is also the highest.

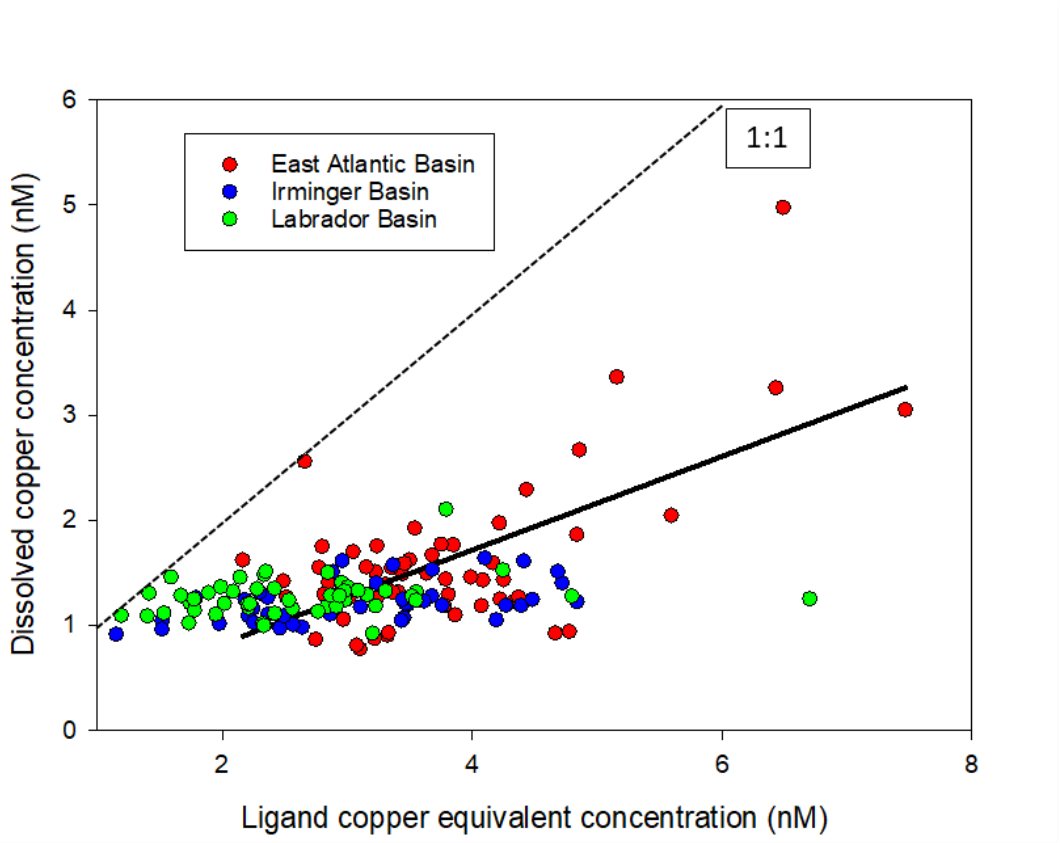

Figure 2.11: Dissolved copper concentration (nM) variation function of ligands concentrations (nM). Each colour represents an oceanic basin: red (EAB), blue (IrB) and green (LB). Linear regression of the EAB plot is shown in black. The 1:1 line is represented by a dashed black line.

Figure 2.11 reveals two different behaviours along the section between DCu and L. In the LB and IrB, increases in ligands concentrations were not associated with an increase of dissolved copper. In contrast, in the EAB, high concentrations of L were correlated with higher DCu values ($p < 0.01$). High concentrations of ligands were stabilising copper under the dissolved fraction, preventing its removal through adsorption onto sinking particles and thus allowing high concentrations of DCu to accumulate at depth. Within the Arctic basins, ligand concentrations were not elevated enough to sustain high DCu

concentrations. Interestingly, the $L_{\_Excess}$ concentrations were relatively homogenous along the section (Figure 2.6a). No increase was observed at depth of the EAB supporting the idea of the buffering of [DCu] by ligands.

The origin of the elevated ligand concentrations is unknown; ligands sources have not yet been constrained (see section 4.1.). Along the section, no obvious source was observed, neither in surface waters nor at depth. Higher concentration of ligands at depth could be due to the age of the deep water-mass (i.e. NEADW) in the EAB compared to the younger DSOW in the LB and IrB. A better understanding of the biogeochemical cycle of ligands and their nature will be necessary to explain their distribution and subsequently their influence on copper distribution.

2.4.4. The fate of particulate copper in the deep ocean

Particles play an essential role in the global biogeochemical cycle of trace elements in the ocean (Jeandel and Oelkers, 2015). Copper is mainly present in the dissolved fraction with a median of 98.5 % along GEOVIDE. But biologically and lithogenicaly-derived particles were important drivers of copper distribution at the ocean's interfaces (surface, shelves, margins, benthic sediments). Particulate copper distribution along the water column was highly scattered and was not sharing the same inter-basin features as DCu (Figure 2.7). In the mesopelagic layer, the LB had a lower median PCu concentration (15 pM) compared to the IrB and EAB (18 pM for both respective basin). The lack of PCu increase within the deep EAB could indicate the absence of particulate-dissolved exchange at the DCu maximum. But, using the particle composition, interesting features are revealed.

Knowledge of particle composition is essential to understand their origin and fate in the open ocean. Elemental ratios between PCu and other particulate trace elements are interesting proxies to constrain the variation of particles composition within the section. The following section focuses on the study of particulate copper on aluminium ratio (PCu/PAl) and particulate copper on phosphorus ratio (PCu/PP). PCu/PAl ratio is a proxy of lithogenic particles; knowing the Upper Continental Crust ratio of 0.132 mmol mol^{-1} (Taylor and McLennan, 1995), the influence of lithogenic material on PCu cycle can be determined. Figure 2.12a shows the influence of margins and benthic sediments on particles composition. An interesting feature was the low PCu/PAl ratio within the LB (3.23 mmol mol^{-1}) compared to the IrB and EAB (6.58 and 7.89 mmol mol^{-1}, respectively).

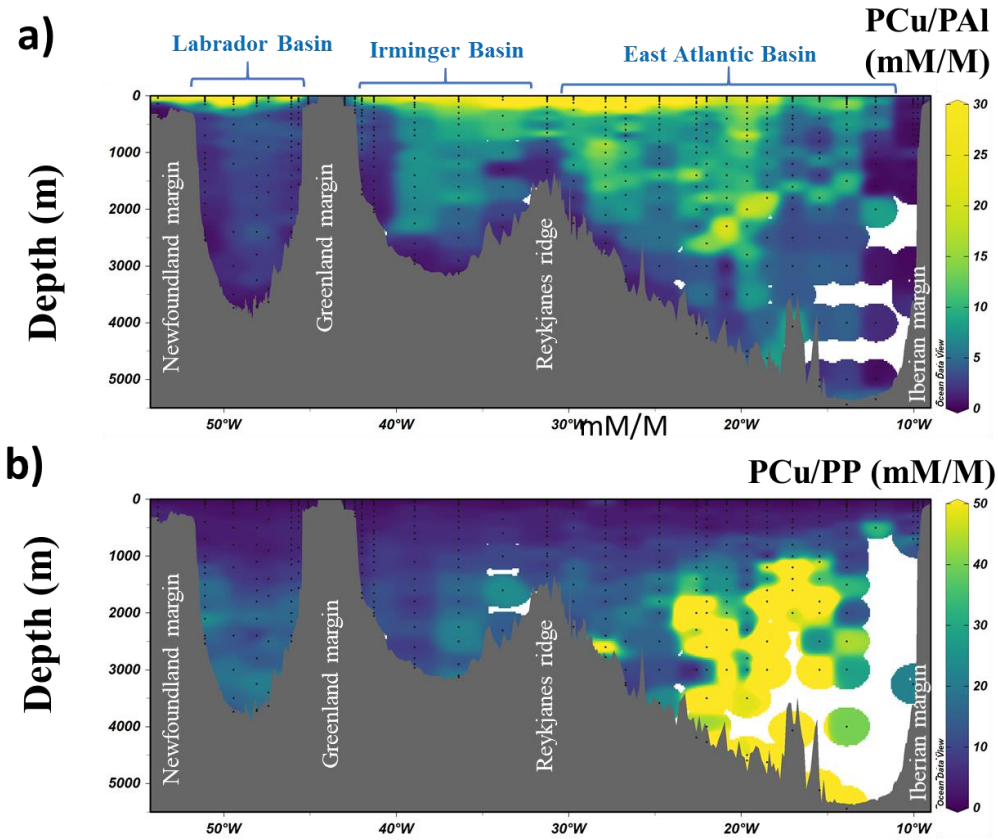

Figure 2.12: Distribution of a) PCu/PAl elemental ratio along GEOVIDE, b) PCu/PP elemental ratio along GEOVIDE. Notice the non-linear scale of the colorbar on the figure 2.12a.

To identify biological particles, the PCu/PP ratio can be compared to the PCu/PP ratio within phytoplankton. According to Twinning and Baines (2013), this ratio varies between 0.4 mmol.mol^{-1} and 2 mmol.mol^{-1} in the open ocean. Using Figure 2.12b, low PCu/PP were observed in surface were the biology is driving the PCu cycle (section 2.4.1). At depth, the ratio increased due to the remineralisation of biogenic particles. In the deep ocean, strong differences were observed between the Arctic basins (LB and IrB) and the EAB. The PCu/PP ratio reached high values below 2000 m (maximum of 337 mmol.mol^{-1}) in the EAB with a median of 40 mmol.mol^{-1} while the median ratios were lower in the Arctic basins (LB and IrB), 16 and 13 mmol.mol^{-1}, respectively. The section of PP and PAl are shown in Figure 2.13.

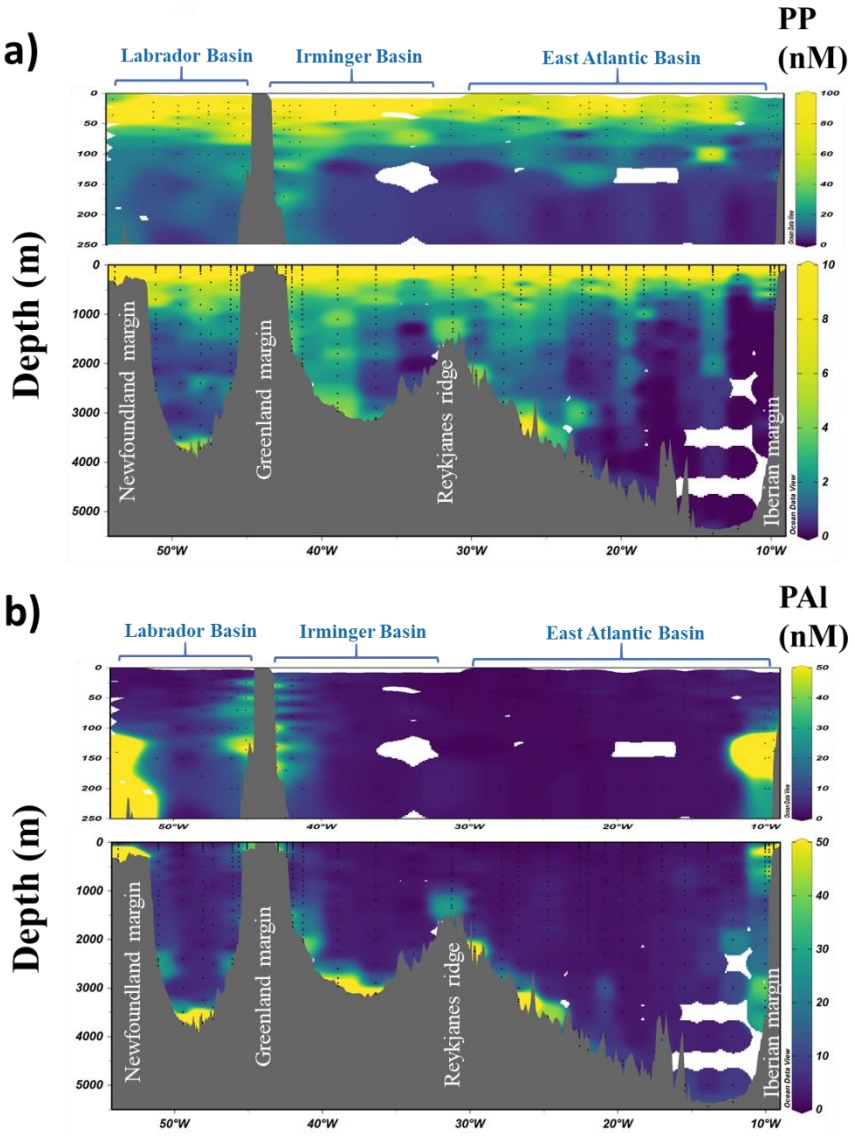

Figure 2.13: Section of a) particulate phosphorus and b) particulate aluminium along GEOVIDE. Please note that the colorbars have been scaled in order to show the interesting features. In consequence, some extreme values higher than 50 nM have the same color as those at 50 nM concentration.

The strong increase in PCu/PP in the EAB reveals an enrichment of particulate copper within particles. This enrichment was not a result of the sinking of biogenic particles, during the remineralisation process, no fractionation between copper and phosphorus is believed to happen. Both elements being present within the same soft tissues of the phytoplankton structures (Twining et al., 2003). Moreover, the PCu/PAl ratio does not suggest an important lithogenic contribution from the sediment of both Iberian margin and benthic sediments (Figure 2.12a). The same feature was observed along other

GEOTRACES sections, GA03 and GP16 (Figure 2.14). Further hypotheses are necessary to understand the origin of the additional PCu at depth of the East Atlantic Basin.

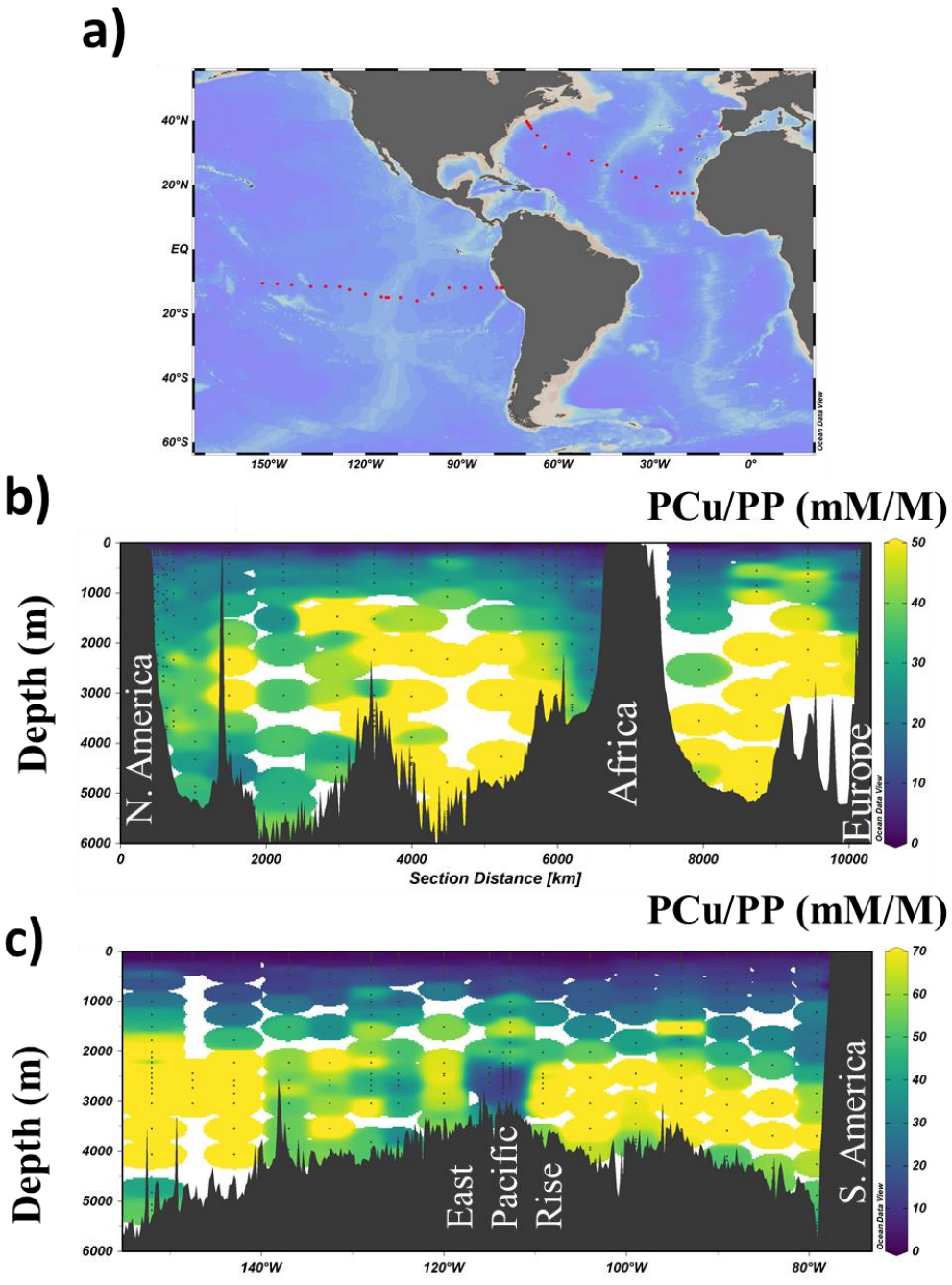

Figure 2.14: a) Map of the GEOTRACES sections GA03 and GP16. Distribution of b) PCu/PP elemental ratio along GA03 (North Atlantic) and c) PCu/PP elemental ratio along GP16 (Equatorial Pacific).

Determination of the lithogenic, biogenic and authigenic fraction of PCu is a useful tool to understand particulate copper cycle. Lithogenic particles were significant in the PCu pool at the sedimentary

interfaces of margin and at the benthic seafloor (Figure 2.15a). Along GEOVIDE, lateral advection from margin were mainly occurring in the vicinity of the Iberian margin (Gourain et al., 2019). These advective features were observed at stations 1 and 11 at 1600 m and 3000 meters depth. In surface and within the water column, lithogenic PCu was non-predominant over the particulate copper cycle. Biogenic PCu was predominant in surface where most of the biological production occurs (Figure 2.15b). The percentage of particulate copper in biogenic particles $\%PCu_{\_Bio}$ was mostly over 95 % in surface due to the biological production. Then, the biogenic percentage decreased to less than 20 % below 2000 m. Disparities between basins were noticed below 2000 m with a median $\%PCu_{\_Bio}$ of 5 % in the EAB while the medians were 16 % and 12 % in the IrB and LB, respectively.

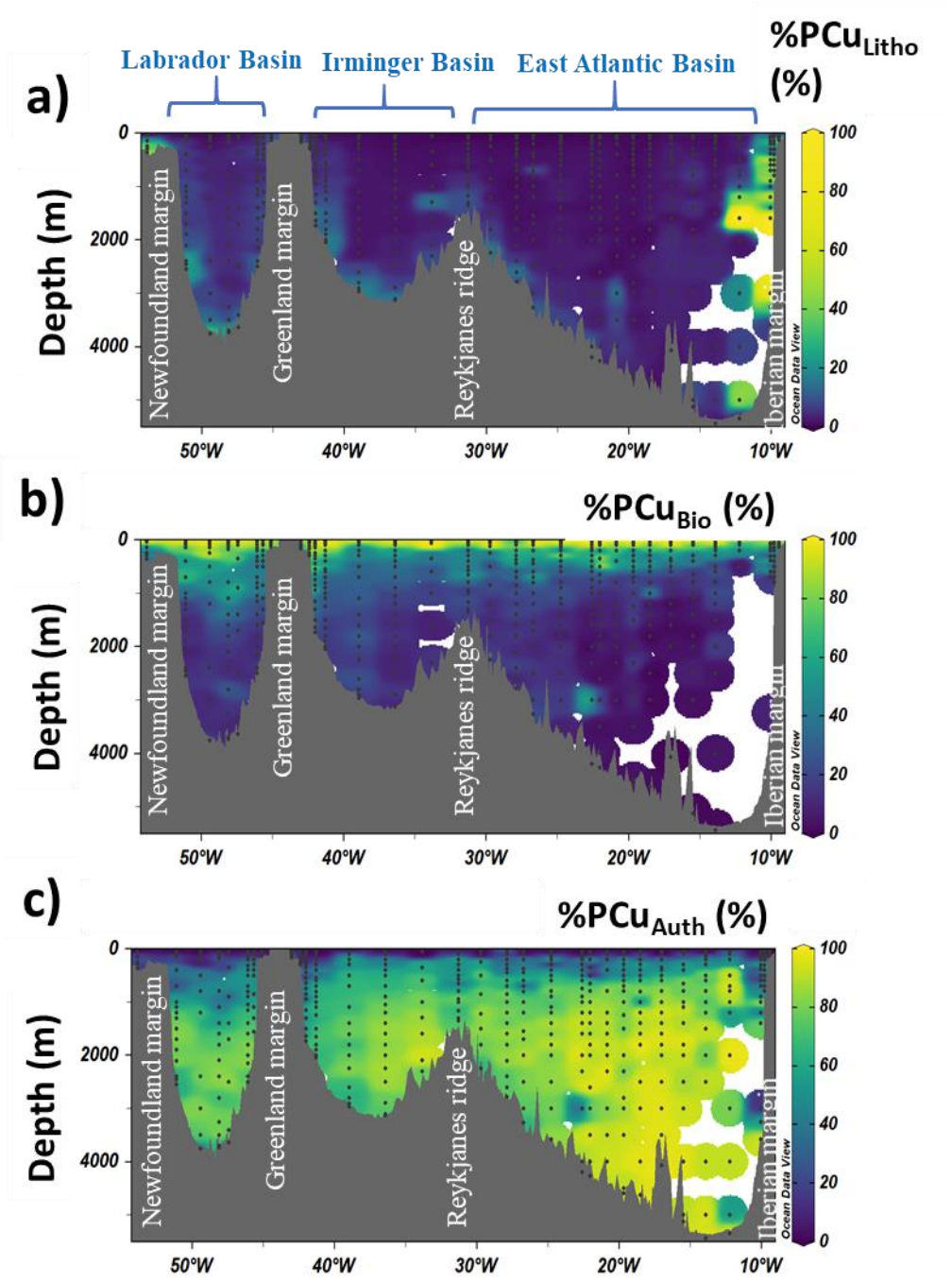

Figure 2.15: Section of a) $\%PCu_{Litho}$, b) $\%PCu_{Bio}$ and c) $\%PCu_{Auth}$ along GEOVIDE. Please note the non-linear colorbar of 14a.

Along GEOVIDE, authigenic particles clearly dominate the PCu cycle below 1000 meters with a median $\%PCu_{\_Aut}$ of 82 %. Strong variations between basins were observed, within the EAB the median $\%PCu_{\_Aut}$ was 89 % while the value was lower in the IrB and LB (77 and 72 %, respectively). Increasing contribution of authigenic PCu at depth of the EAB explains the enrichment in PCu using the PCu/PP ratio (section 4.4.b).

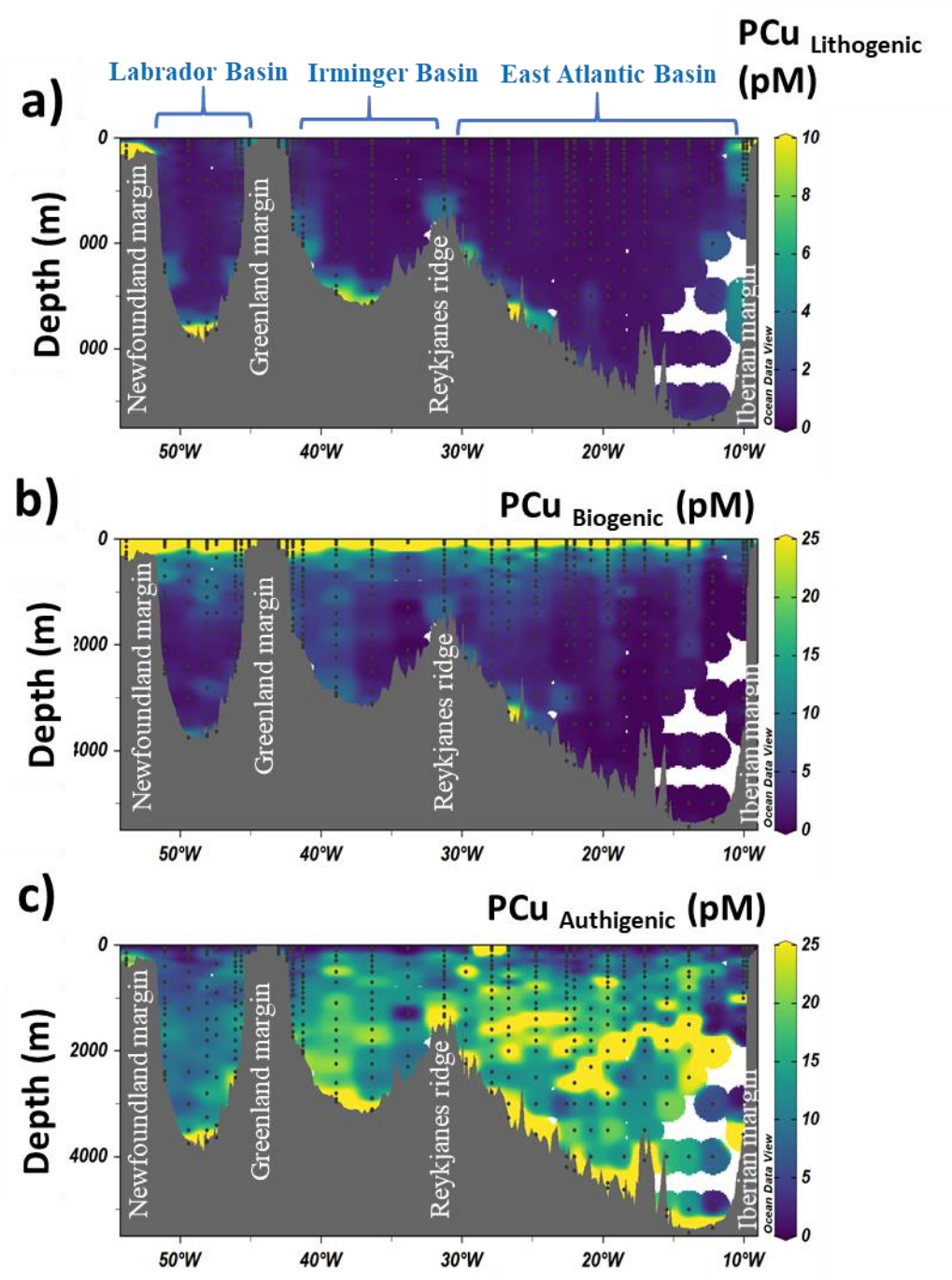

Figure 2.16: Section of a) concentration of lithogenic PCu, b) concentration of biogenic PCu, and c) concentration of authigenic PCu along GEOVIDE.

The enrichment in authigenic PCu associated with the DCu increase at depth of the EAB basin could be linked to two processes. Firstly, the high DCu concentrations could induce an increased scavenging leading to elevated authigenic PCu. The enrichment will be the result of high DCu concentrations. The origin of the DCu is not clear, a possible source could be older water masses (i.e. NEADW) with high

levels of stabilised copper-ligands. But this theory cannot be tested with our current dataset or previous datasets. Secondly, the strong %PCu_$_{Aut}$ concentrations might be reflecting the process of reversible scavenging, leading to higher DCu at depth. To be efficient, reversible scavenging requires fast exchange between particles and the dissolved phase. The authigenic enrichment observed in the EAB might reveal the exchange between dissolved and particulate copper. Indeed, reversible scavenging has recently been point out as the main process driving the copper distribution at a oceanic scale (Richon and Tagliabue, 2019). Moreover, Little et al. (2013) used in their reversible scavenging model, a constant PCu concentration in order to reproduce the linear DCu increase with depth as observed along GEOVIDE. But, copper reversible scavenging has never been directly identified in the ocean; current sampling strategy does not allow to discriminate it from other processes. Specific studies of the exchange dissolved-particles would be necessary to completely understand reversible scavenging.

2.5. Conclusion

This study highlights the role of particles/dissolved interactions for the copper biogeochemical cycle in the North Atlantic. In surface waters, biological uptake was driving the particulate copper cycle through the production of elevated concentration of biogenic particles. Copper ligand distributions were not affected by surface processes in the highly productive regions despite being produced by biological activity. Benthic resuspension was an important source of PCu within the LB and IrB but did not influencing either dissolved copper or their complexing ligands. Along these basins' seafloor, the PCu cycle was dominated by lithogenic particles.

The strong inter-basins feature in DCu distribution between the LB, IrB and the EAB can be explained by the variation in reversible scavenging intensity driven by the ligand's distribution at depth. Within the EAB, elevated concentration of authigenic particles were the consequence of reversible scavenging mediated by elevated ligands concentrations stabilising copper under the dissolved fraction and increasing the desorption from particles. The origin of the elevated ligand concentrations at depth of the EAB still needs more investigation to be resolved; a better characterisation of the ligand pool (e.g. pseudopolarography and LC-ICPMS) is also necessary to better constrain the copper ligands biogeochemical cycle.

In this study, we demonstrated for the first time the evidence of reversible scavenging of copper in the ocean from analysis of seawater samples. It is allowing us to highlight the role of reversible scavenging and ligands availability in driving the copper cycle in the North Atlantic during GEOVIDE.

3. Chapter 3: The lack of hydrothermal signal on copper organic speciation along the Mid-Atlantic ridge, GEOTRACES GA13 section

Abstract:

The influence of hydrothermal activity on copper distribution and its speciation has been studied along the GEOTRACES section GA13, Fridge. An absence of influence from hydrothermal venting sites on dissolved copper and ligand concentration was observed within the hydrothermal plumes encountered. The absence of signal within the plume was due to a combination of dilution with surrounding water masses and removal by coprecipitation with sulphide. The lack of ligand signal is more complex due to both production and degradation of organic matter in the close vicinity of the vents. The absence of obvious source of ligands along the water column is discussed I context of their residence time. Two inter-comparisons have been realised along the section with the GA01 and GA03 GEOTRACES sections. They show the comparability between DCu and ligands profiles; some variability is observed in the (sub-)surface probably mainly driven by local and seasonal events affecting this region.

3.1. Introduction

Hydrothermal activity has recently been described as a major source of trace elements (e.g. iron, manganese, zinc) into the deep ocean (Fitzsimmons et al., 2017; Resing et al., 2015; Tagliabue et al., 2010), but the effect on copper biogeochemical cycle is still not fully constrained. Pure fluids coming from active vents are highly enriched in copper at micromolar levels (Edgcomb et al., 2004; Metz and Trefry, 2000; Sarradin et al., 2009 and reference therein) with concentrations depending on the site: its mineralogy (Metz and Trefry, 2000), the temperature and acidity of the fluids (Charlou et al., 2002; Kleint et al., 2015; Metz and Trefry, 2000). Once out of the vent, the hot hydrothermal fluid rises and mixes with the cold oxygenated surrounding seawater. This drastic change in temperature and redox condition causes numerous physico-chemical reactions (Sarradin et al., 2009) that profoundly affect trace metal speciation within the first few meters away from the vents (Cotte et al., 2018). Hydrothermal fluids are reducing environments and can contain high levels of sulphide (Edgcomb et al., 2004; Styrt

et al., 1981). Sulphide is a strong complexing agent to numerous metals, including copper, and form complexes that are highly insoluble. Copper reaction with sulphide forms an insoluble chalcopyrite complex (CuS) leading to important chalcopyrite deposition in the close vicinity of the vents (Alt et al., 1987; Styrt et al., 1981). However, some studies demonstrated the formation of copper-sulphide nanoparticles (Sander and Koschinsky, 2011) leading to a stabilisation of copper in the colloidal fraction and supposedly allowing its export away from the vents. A recent study has shown that DCu concentrations could decrease within the buoyant plume due to intensive scavenging triggered by elevated particles load (Jacquot and Moffett, 2015). The high complexity of hydrothermal environments is leading to important uncertainties about the biogeochemical cycle of trace elements in their close vicinity.

The role of organic copper ligand complexation on hydrothermal inputs has been studied more intensively over recent decades (Cotte et al., 2018; Kleint et al., 2015; Klevenz et al., 2012; Sarradin et al., 2009). Unlike in the water column, up to 98 % of ligands within the plume are inorganic compounds as complexing inorganic sulphide (Cotte et al., 2018; Klevenz et al., 2012; Sarradin et al., 2009). But the organic fraction is non-negligible; organic ligands are excreted by living organisms (i.e. bacteria and archaea) to complex newly added hydrothermal free copper and reduce its toxicity (Kleint et al., 2015; Klevenz et al., 2012). Moreover, Sander and Koschinsky (2011) theorised the potential stabilisation role of ligands (e.g. thiols) on dissolved copper, preventing its precipitation and allowing its export away from the vents.

This chapter describes the chemical copper speciation along the Fridge section, GEOTRACES GA13. An inter-comparison between stations of the Fridge, GA01 and GA03 has been realised in order to study the comparability between GEOTRACES sections. Along Fridge, we compared copper speciation between known hydrothermal sites and oceanic stations to assess the effect of active vents on organic ligands cycle and the influence on copper biogeochemical cycle. The effect of ligands concentration on DCu concentration is also investigated in order to better constrain the fate of hydrothermal copper in the deep ocean.

3.2. Material and methods

3.2.1. Fridge section overview

The Fridge section took place on board the RSS *James Cook* between December 2017 and February 2018 in the North Atlantic (Figure 3.1) from Southampton (UK) to Pointe-à-Pitre, Guadeloupe. The cruise sailed south-west to the Azores plateau and then southward along the Mid-Atlantic Ridge (MAR), sampling several known hydrothermal sites that were encountered, e.g. Lucky Strike, Rainbow, Lost City, Broken Spur and TAG. Two surveys were carried out around the Rainbow and TAG vents sites to constrain the dispersion of the hydrothermal plumes. Moreover, two rosettes were operated at stations Rainbow and TAG due to the number of proxies sampled leading to 2 station numbers for the same location: stations 16/38 and stations 35/39 respectively.

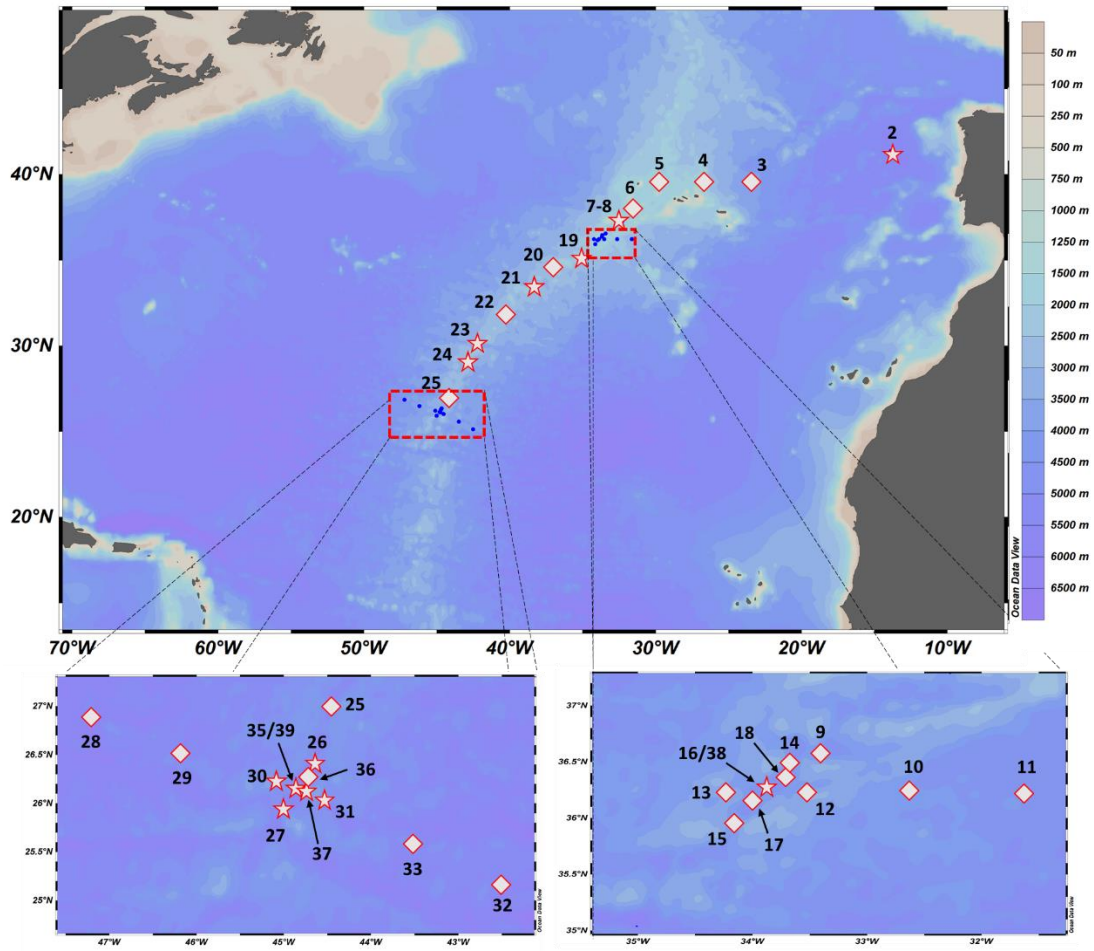

Figure 3.1: Map of the Fridge section (GA13). Red stars represent stations where copper speciation have been sampled while red diamonds show stations where no copper speciation samples were collected. Two zoomed windows are represented around TAG (left panel) and Rainbow (right panel). Station numbers are indicated in black.

3.2.2. On-board sampling

All samples were collected using 10 L OTE bottles mounted on a titanium-frame rosette. After recovery, all bottles were immediately transferred into a clean container for sub-sampling. After sampling the non-filtered samples, bottles were shaken vigorously 3 times and pressurised at 7 psi with 0.2 µm filtered air. Seawater filtration was done either by a Sartobran® 300 (0.2 µm, Sartorius) filter capsule or using 25 mm polyethersulphone filters (0.2 µm, Supor, Pall Gellman) mounted on acid-clean filter holders (Swinnex, Millipore). Filters were later used to determine particulate trace elements. Dissolved trace metals were collected in LDPE bottles after being washed 3 times. Speciation samples were stored in 250 mL bottles (LDPE, ®Nalgene) at -20 °C until analysis at the home laboratory. Dissolved manganese (DMn) samples were collected into 100 mL bottles (LDPE, Bel-Art) acidified at pH ~ 1.7 with ultrapure HCl (Fisher Optima).

3.2.3. Analytical measurements

3.2.3.a. Voltammetric equipment and solution preparation

All analyses took place in the laboratory within a metal-free laminar flow hood using a voltammetric stand. It was constituted of a µAutolab type III connected to a 663-VA stand (Metrohm) equipped with a hanging mercury drop working electrode, a glassy carbon counter electrode and an Ag/AgCl//KCl (3M) reference electrode. Analyses were carried out in a home-designed PTFE voltammetric cell allowing to reduce the volume required from 10 mL to 3 mL of sample. A volume of 5 mL was consistently used for all experiments. A new PTFE steering rod was designed to stir the solution in this small volume cell. The voltammetric analyses were operated using the GPES software (version 4.9, Eco Chem).

All solutions used were either of trace metal grade or were cleaned with manganese oxide (MnO_2) in order to be suitable for trace metal analysis (van den Berg, 1982). To clean solutions, 100 µM MnO_2 was added to the solution, vigorously shaken and left to settle overnight before being filtered through a 0.2 µM filter (Cellulose Nitrate Membrane 47 mm diameter, Whatman®). Solutions of salicylaldoxime acid (SA, Acros Organics) were prepared by diluting 13.7 mg of SA powder in 10 mL of Milli-Q acidified at approximately pH 2 with 10 µL hydrochloric acid (HCl, TraceSELECT® ultra, Fluka). In order to fix the pH of samples around 8.1, a borate buffer solution was elaborated in a 250 mL bottle

with final concentrations of 1 M boric acid (salts, analytical grade, Fisher Scientific) and 0.35 M ammonia solution (TraceMetal grade, Fisher). This buffer solution was UV-digested to destroy any organic matter and cleaned off metals by MnO_2. Copper standard solutions were prepared regularly from a standard 1000 mg L^{-1} Cu^{2+} solution (SpectrosoL®, BDH). A 1 µM copper standard was produced by consecutive dilution in 20 mL Milli-Q acidified at pH 2 with HCl (TraceSELECT® Ultra, Fluka).

3.2.3.b. Dissolved copper analysis

Dissolved copper concentrations (DCu) were determined by cathodic stripping voltammetry (CSV) using SA as a complexing ligand. Samples were defrosted at ambient temperature for few hours under a laminar flow hood. After gentle shaking to dissolve any remaining salts, 10 mL were poured in an acid-clean quartz tube with 10 µL HCl (TraceSELECT® ultra, Fluka) to reach pH ~ 2. After 45 minutes of UV-irradiation in order to destroy all organic matter, tubes were left to cool down until analysis. Inside the voltammetric cell, 5 mL of samples were pipetted with 10 µM of SA and 0.01 M borate buffer (to fix the pH at around 8.1). Before analysis, the sample was purged for 4 min to remove the dissolved oxygen from the solution. Voltammetric scans were made by Differential Pulse CSV (DP-CSV) using a deposition time of 45 s at -0.15 V, 1 s desorption at -1.2 V, 5 s equilibrium before stripping from 0 to -0.5 V with a step potential of 5 mV, a modulation amplitude of 50 mV, a modulation time of 15 ms and an interval time of 0.1 s. Each measurement was done in triplicate. Peak derivative was calculated using the GPES software analysis tool with a manual curve cursor to delimit the peak extent Internal standard additions method has been used in order to determine the DCu concentrations and associated errors. Three Cu additions were accomplished with varying concentrations according to the peak derivative of the first scan (with no addition). Additions were done in order to have a final addition with a peak derivative at least doubled from the initial scan.

3.2.3.c. Organic ligands measurement

Copper speciation was measured at the same time as DCu by competitive-ligand-exchange adsorptive cathodic stripping voltammetry (CLE-AdCSV). From the unfrozen bottle, 75 mL were transfered in a clean 125 mL bottle with 2 µM SA and 0.01 M borate buffer. From this mixture, thirteen 5 mL aliquots were prepared in PTFE cells with increasing Cu^{2+} additions (from no addition up to 15 nM Cu^{2+}). The range of copper addition was done according to the DCu concentration of the sample.

Elevated DCu were leading to elevated addition of free copper. The aliquots were left equilibrating overnight until analysis, starting from the aliquot with no copper added to the highest addition. Measurements were realised by pouring the cell content within the same measurement voltammetric cell. The cell was not rinsed in between aliquots to conserve the conditioning.

The sample was purged prior to analysis with pressurised N_2 for 240 s to remove the oxygen from the sample. After discarding 5 mercury drops, voltammetric measurements were done by DP-CSV using deposition potential of -0.15 V for 300s followed by 5 s of equilibration. The same stripping parameters as for DCu determination were used. A duplicate scan was done to confirm the first obtained peak derivative value obtained. In case of discrepancies, a third scan was done to confirm either one or the others. The peak derivative was measured using the analysis tool of the GPES software using the manual curve cursor to delimit the peak extent. Titrations were treated using the ProMCC software (Omanović et al., 2015) using the Ruzic/Van den Berg linearisation method, but results were compared with other methods (the Langmuir and the Scatchard methods). A one ligand model was found best suited to fit the titration data, similar to previously reported in the North Atlantic (see Chapter 2; Jacquot and Moffet, 2015). The outputs were the ligand concentration (L), the conditional binding strength (log K) and the free copper concentration ($DCu_{\_Free}$). The excess of ligands ($L_{\_Excess}$) was calculated by subtracting DCu from L. All statistical analyses are performed using the software Minitab® 18.

3.2.3.d. Dissolved manganese measurements

Dissolved manganese was measured on-board within 1-10 days after sampling by flow injection analysis with in-line pre-concentration on resin-immobilized 8-hydroxyquinoline followed by colorimetric detection (Aguilar-Islas et al., 2006; Resing and Mottl, 1992) by Dr. Joseph Resing (University of Washington). Daily precision of analysis was ± 0.01 nM with a limit of detection of 0.03 nM.

3.3. Results

3.3.1. Overview of the section, hydrothermal sites

The Fridge section crossed two distinct environments, from the open ocean to the Mid-Atlantic Ridge with active hydrothermal vents. Due to the difficulties of sampling hydrothermal plume, some casts above known active sites did not sampled an identifiable plume (i.e. stations 23, 31 and 37). To follow the plume dispersion, many proxies are available from dissolved/particulate trace elements (e.g.

Mn; Trefry et al., 1985) to redox sensor (Eh, Lough et al., 2019). In this study, dissolved manganese has been used to monitor the influence of hydrothermal inputs (Figure 3.2). Along the section, [DMn] ranged from 0.10 nM to 296.75 nM. Open ocean stations (i.e. 2, 19 and 21) were used as a background reference to identify hydrothermal signals. At depth, DMn concentrations were under 0.35 nM for all open ocean stations (except 0.82 nM at 3250 m of St 21); concentrations higher than this reference were indicative of a hydrothermal plume.

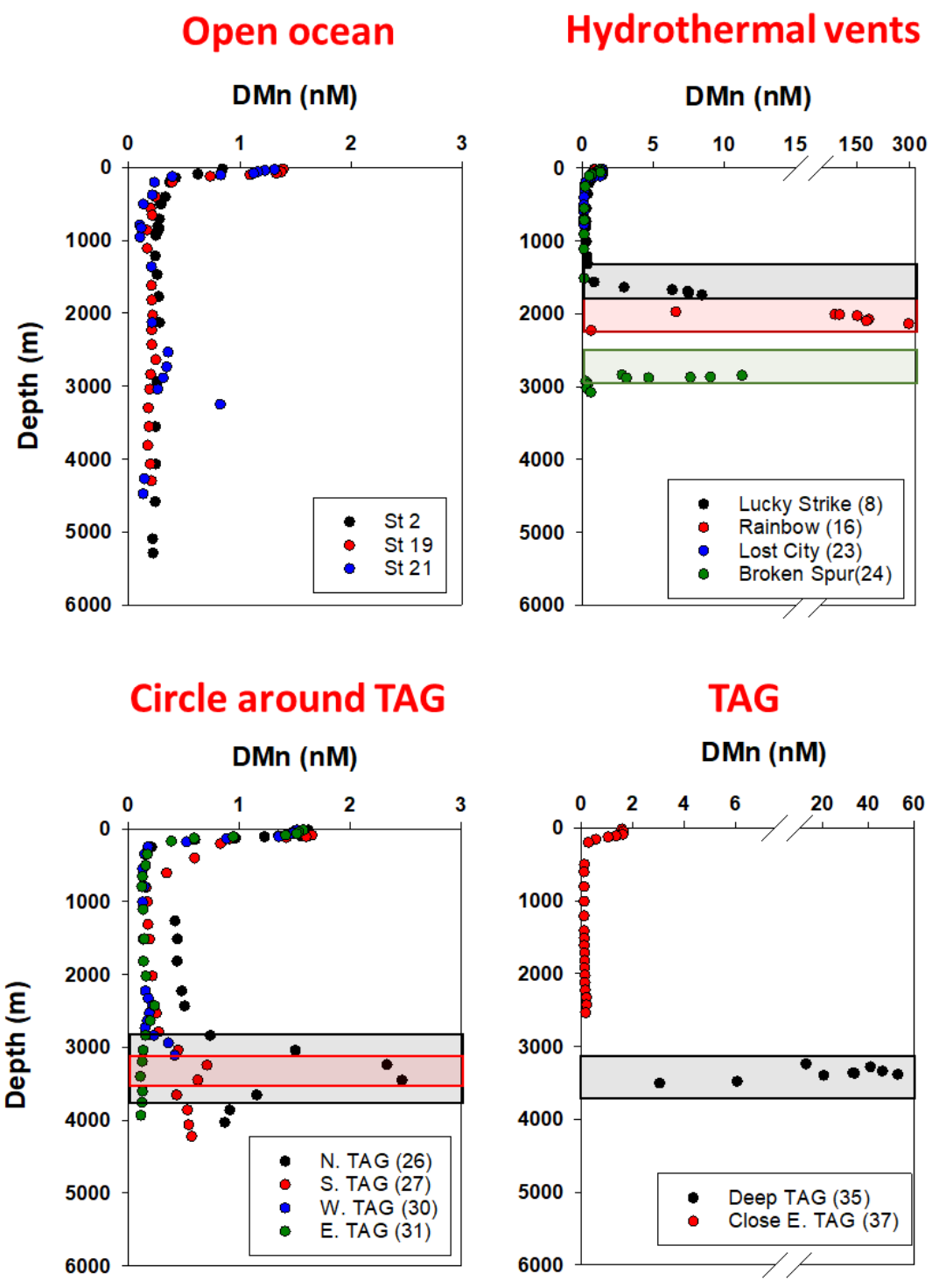

Figure 3.2: Profiles of DMn at every station sampled for copper speciation. Stations have been grouped in four panels (open ocean, hydrothermal sites, circle around TAG and TAG). Notice the change of scale of the x-axis between panels and the axis-break in panel on the top and bottom right. Shaded rectangles are representing the position of plumes where it applies.

During Fridge, several hydrothermal plumes were sampled as observed using DMn (Figure 3.2). Dissolved manganese concentrations varied between the different sites, Lucky Strike's (Station 8) plume showed DMn values up to 8.4 nM while Broken Spur's (Station 24) plume revealed concentrations up to 11.2 nM. The maximum concentration along the section was measured within the Rainbow's plume (Station 16). It is important to notice that Rainbow has been visited twice, at station 16 and 38. Dissolved manganese values showed are originating from station 16 while copper's parameters were collected at station 38. Despite being sampled at 53 hours interval, comparison between both casts can be difficult due to the high volatility of the plume. The TAG site (station 35) revealed elevated DMn concentrations up to 53.0 nM. Only deep samples are shown for TAG in Figure 3.2, no DMn were analysed at the shallow TAG cast (station 39). Around the TAG site, highest DMn concentrations were observed at station 26 with 2.5 nM while other stations had [DMn] close to the background values suggesting a main northward dispersion of the vent. Nevertheless, a small signal (0.7 nM) was also observed southward at station 27 (Figure 3.2).

3.3.2. Dissolved copper along the section

Along the section, dissolved copper concentrations ranged from 0.58 to 4.25 nM with low concentrations in surface followed by an increase with depth (Figure 3.3). No differences were observed between the open ocean stations and the hydrothermal sites; except, around TAG where stations 27 and 30 were presenting elevated concentration (higher than 3 nM, Figure 3.3).

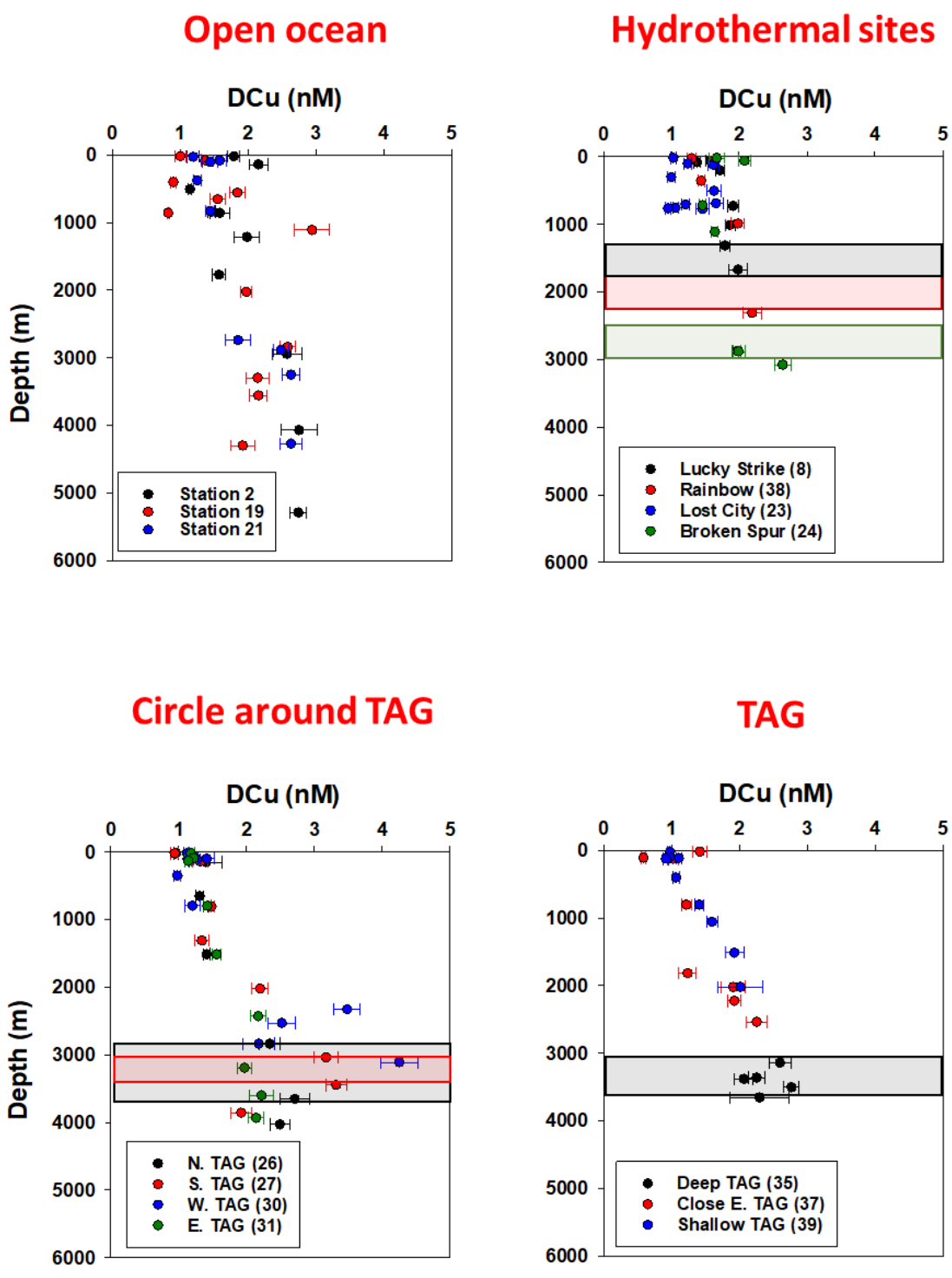

Figure 3.3: Distribution of DCu along the section. Stations have been grouped in four panels (open ocean, hydrothermal sites, circle around TAG and TAG). Shaded rectangles are representing the position of plumes where it applies.

3.3.3. Organic speciation of copper

During Fridge, copper-equivalent ligand concentrations were comprised between 1.09 and 5.35 nM (Figure 3.4). Ligands were constantly in excess compared to the DCu with a median $L_{\_Excess}$ of 1.03 nM (Figure 3.4). The conditional binding strength, log K, was ranging from 12.5 to 14.2 (Figure 3.5) which is within the oceanic range previously reported (See Chapter 2; Jacquot and Moffet, 2015) . Copper complexation was extensive throughout with a median of 99.5%, the lowest being 90%. Distribution of ligands and their binding strength were scattered as previously observed in the ocean (See Chapter 2; Jacquot and Moffet, 2015).

Excess ligands ($L_{\_Excess}$) distribution was scattered along Fridge with concentrations ranging from 0.15 to 2.71 nM (Figure 3.6). Free dissolved copper ($DCu_{\_Free}$) concentrations in surface waters were below 150 fM, except at the station 19 where DCu_Free reached 739 fM at 20 meters depth (Figure 3.7). Concentrations were, then, increasing with depth up to 323 fM. No clear patterns can be identified at the hydrothermal sites; none of the copper speciation proxies (i.e. L, log K, $L_{\_Excess}$ and $DCu_{\_Free}$) showed distinctive signal associated with an identified plume (Figure 3.3-3.5).

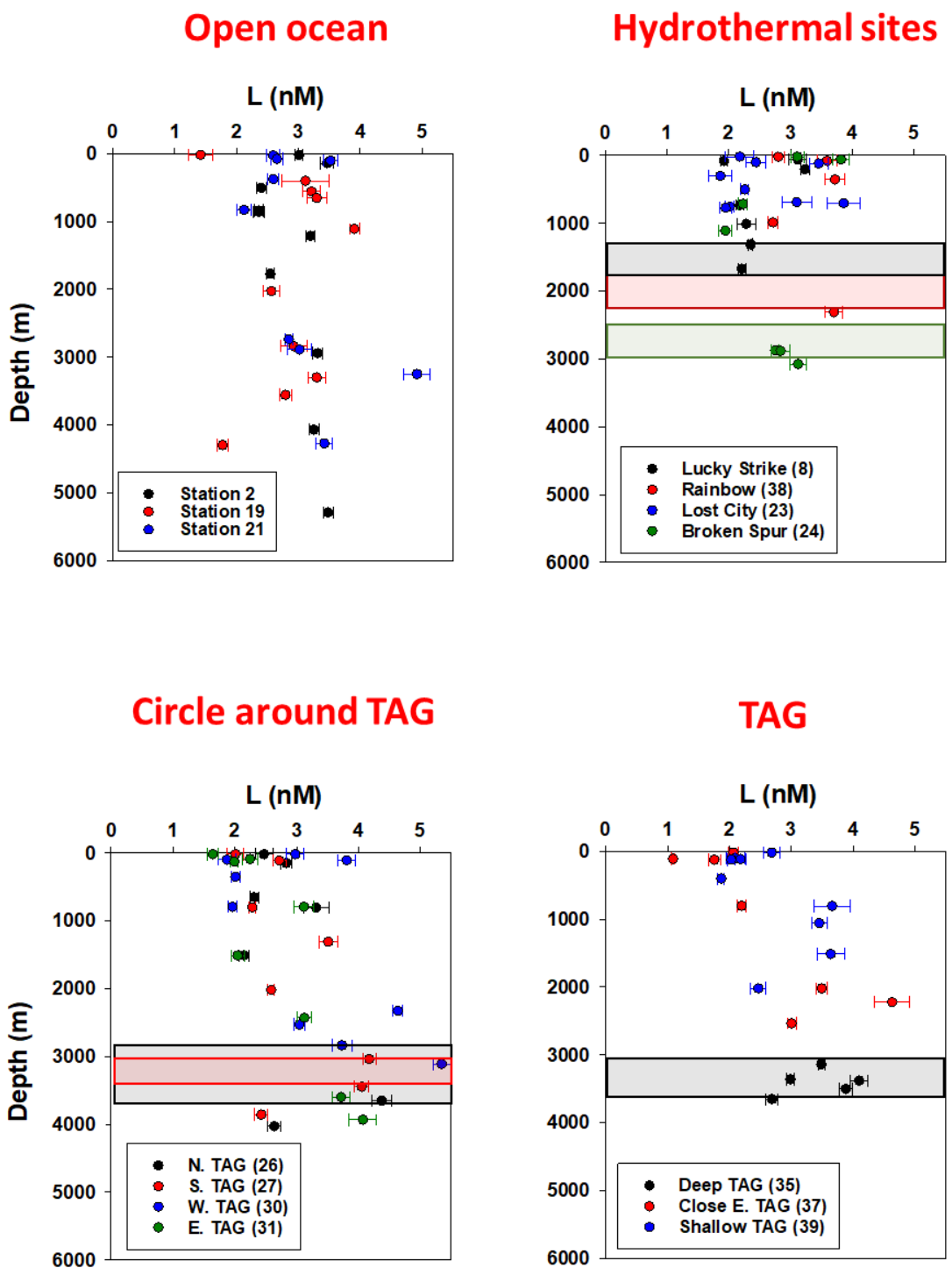

Figure 3.4: Profiles of L along the section. Stations have been grouped in four panels (open ocean, hydrothermal sites, circle around TAG and TAG). Shaded rectangles are representing the position of plumes where it applies.

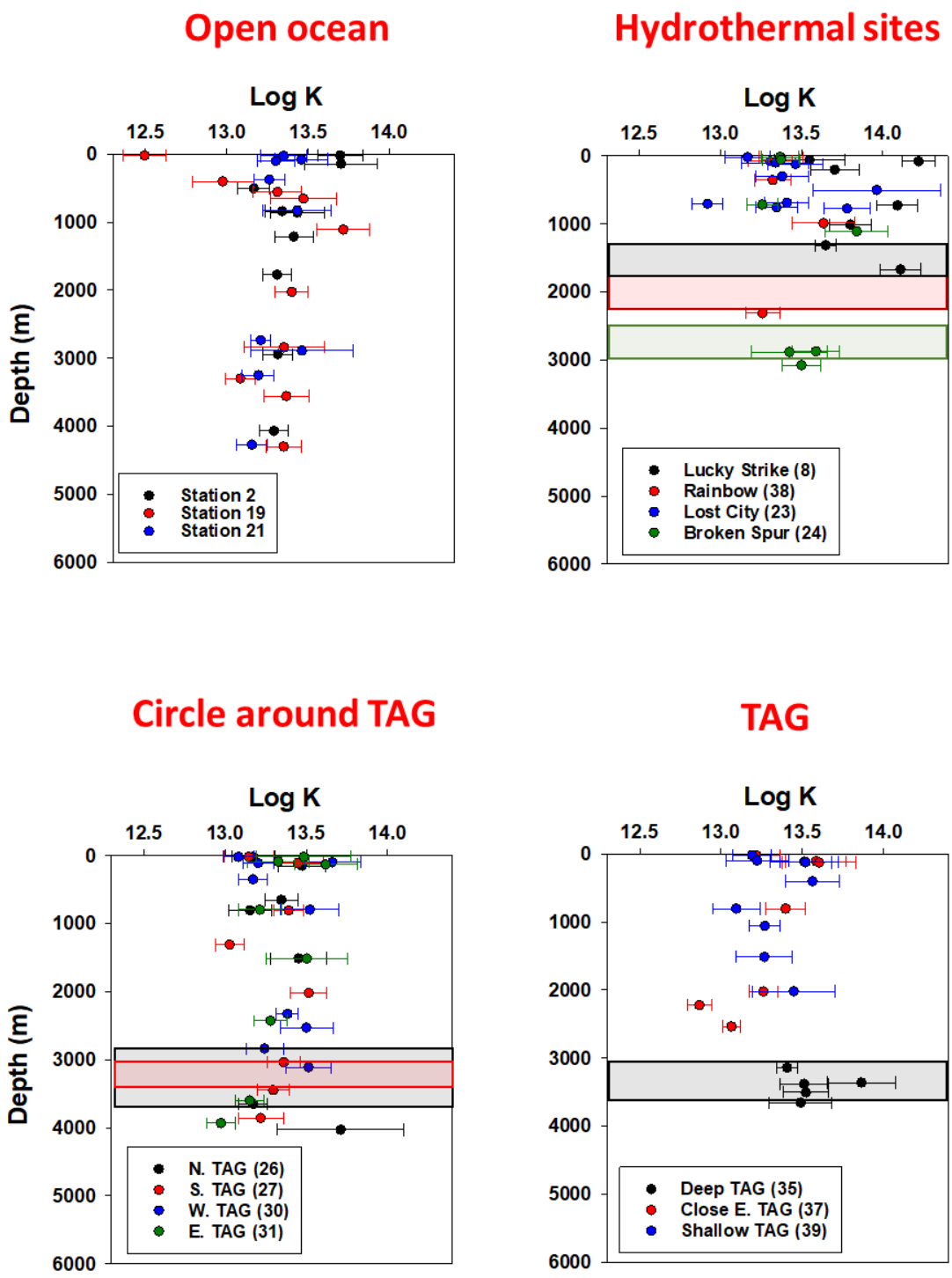

Figure 3.5: Distribution of log K along the section. Stations have been grouped in four panels (open ocean, hydrothermal sites, circle around TAG and TAG). Shaded rectangles are representing the position of plumes where it applies.

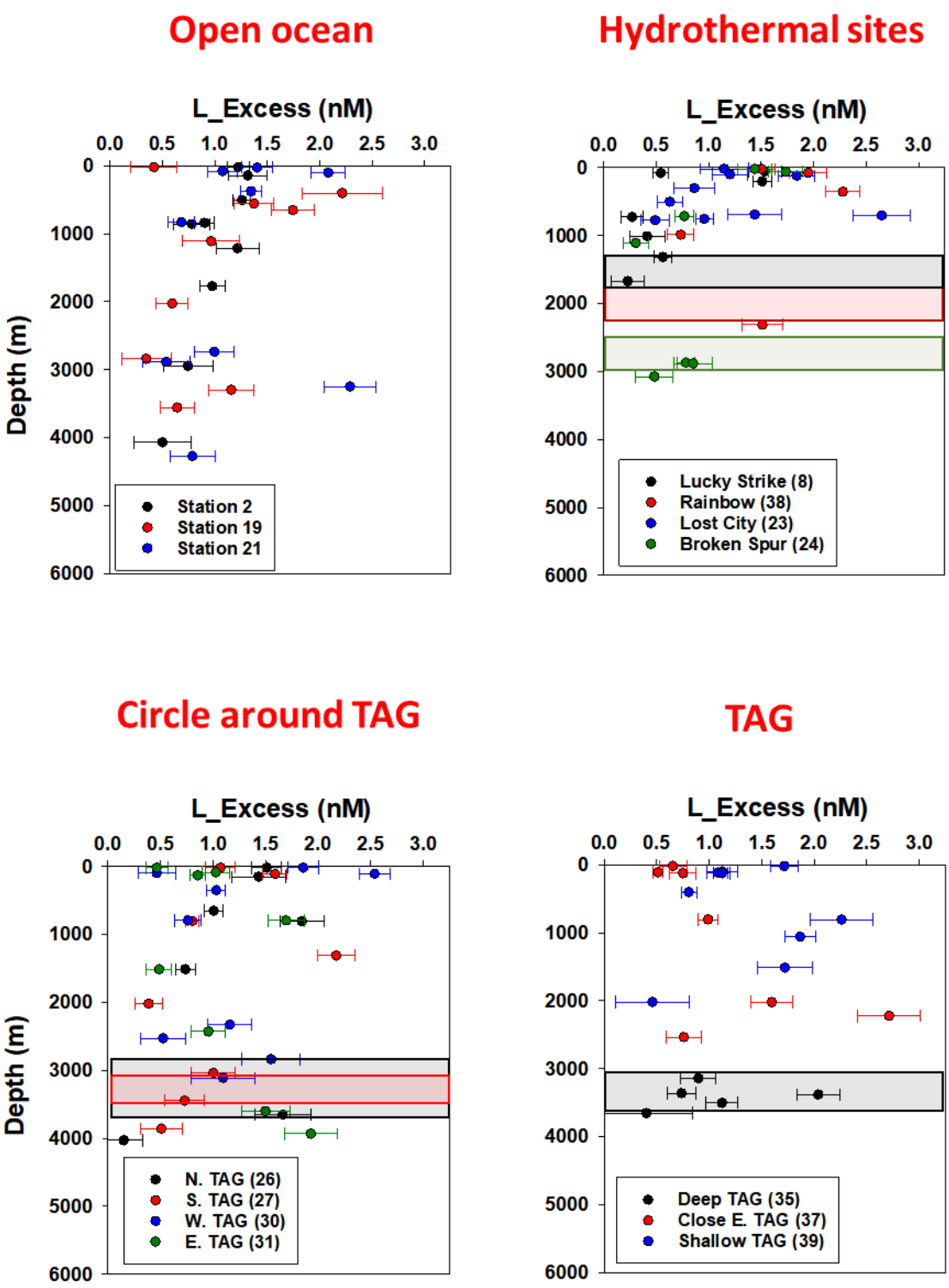

Figure 3.6: Distribution of the excess of ligands along the section. Stations have been grouped in four panels (open ocean, hydrothermal sites, circle around TAG and TAG). Shaded rectangles are representing the position of plumes where it applies.

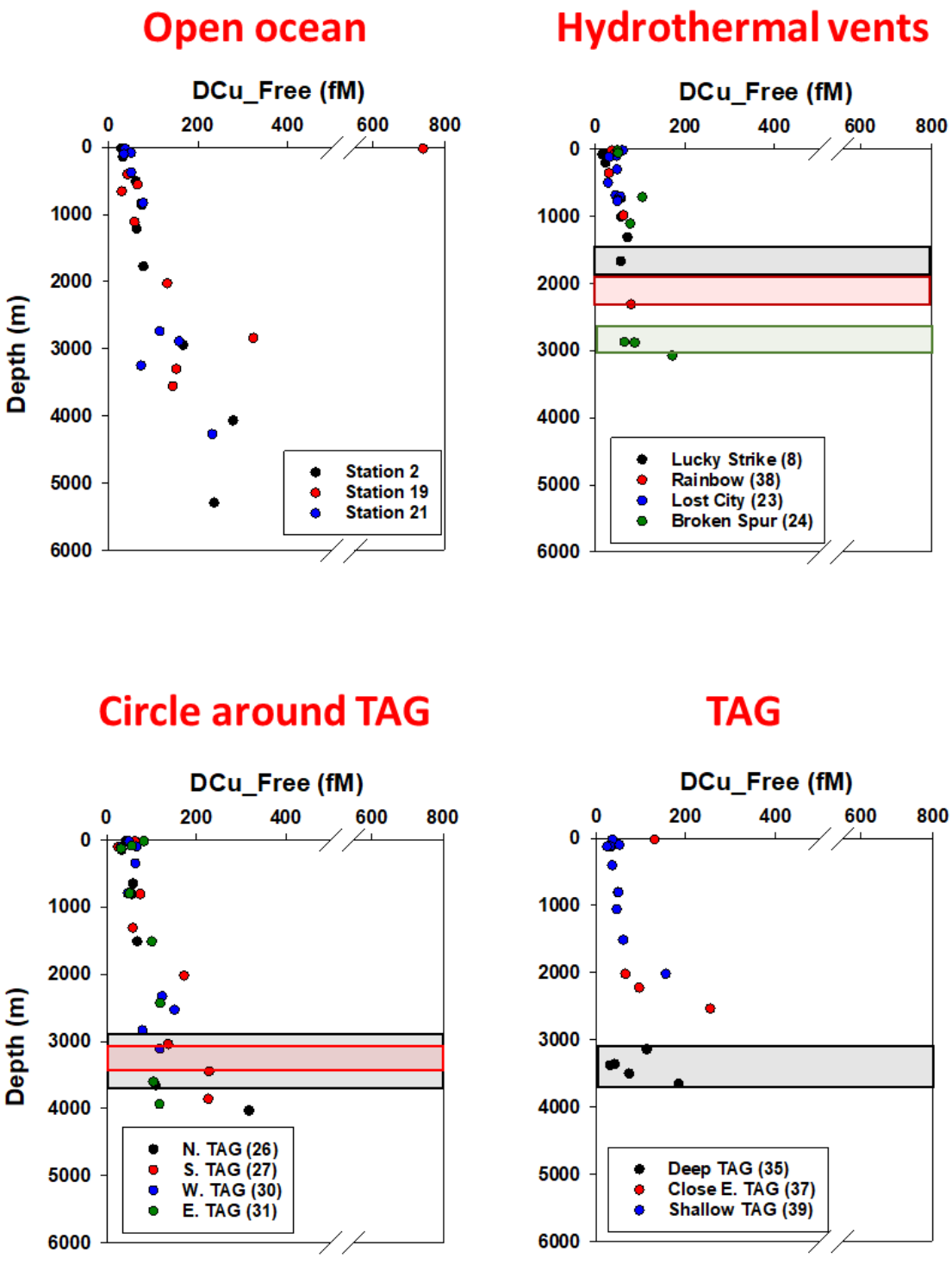

Figure 3.7: Distribution of the free copper along the section. Stations have been grouped in four panels (open ocean, hydrothermal sites, circle around TAG and TAG). Notice the scale break on the x-axis. Shaded rectangles are representing the position of plumes where it applies.

3.4. Discussion

3.4.1. Inter-comparisons with GA01 and GA03

The Fridge cruise sampled two stations previously visited by GEOTRACES sections allowing us to proceed at two inter-comparisons. An inter-comparison study has been previously realised by Buck et al. (2012) using identical samples measured by two laboratories. They showed the comparability of results obtained by two different laboratories. Station 2 of Fridge was selected in order to match the station 13 of GA01 section (GEOVIDE). GA01 samples were collected in May 2014 aboard the R/V *Pourquoi pas?*. Dissolved copper was analysed by ICP-MS at the LEMAR laboratory (France) while copper speciation was analysed by CLE-adCSV at the University of Liverpool by the same operator as the Fridge samples. Dissolved copper concentrations were similar between GA13 and GA01 (Figure 3.8) except in surface where elevated concentration (> 1.7 nM) were observed during GA13. Surface variability between the two cruises could be the result of seasonal and variable surface inputs (e.g. atmospheric deposition, Baker et al., 2016). Copper ligand concentrations and binding strengths were comprised within the same respective range between both sections (Figure 3.8). Two interesting features were observed within the (sub-)surface layer: elevated log K values were observed in surface of GA13 where elevated DCu concentration were identified. Moreover, along GA01 a consistent increase in [L] up to 8.3 nM was observed at 500 meters depth. The nature of this maximum is unknown but the variability in copper speciation between profiles can be explained by the scattered nature of ligands distribution (Figure 3.4) and the expected temporal variability from May 2014 and December 2017. Moreover, comparing physical data (temperature, salinity and oxygen) do not reveal any significant variation in the water masses distribution between the two samplings.

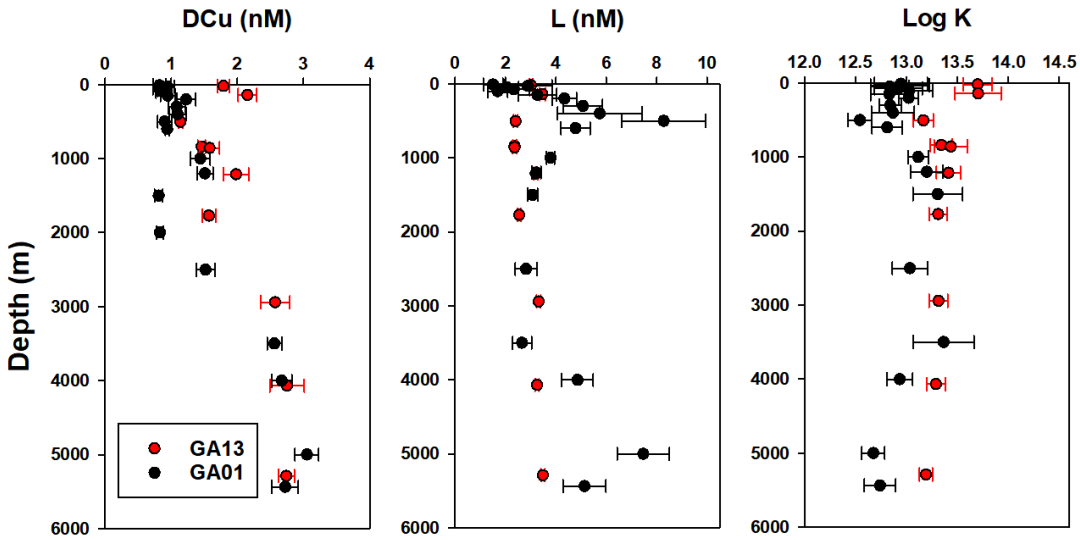

Figure 3.8: Inter-comparison between Fridge (GA13, station 2, red dots) and GEOVIDE (GA01, station 13, black dots)sections. Profiles of DCu, ligands and log K are showed.

The inter-comparison with the GA03 section was at the hydrothermal site TAG. GA03 samples (Station 16) were collected in November 2011 on board R/V *Knorr*. Dissolved copper was measured by ICP-MS while speciation was measured by CLE-AdCSV (Jacquot and Moffett, 2015). Dissolved copper profiles were comparable between both sections while ligands concentrations and binding strength were more disparate (Figure 3.9). High variability above TAG could be explained by the dynamic environment above the ridge with tidal disturbances (Tuerena et al., 2019; Waterhouse et al., 2014). Moreover, samples were measured by two different operators within two different laboratories. Considering these parameters, the divergences between both profiles can be considered as non-significant.

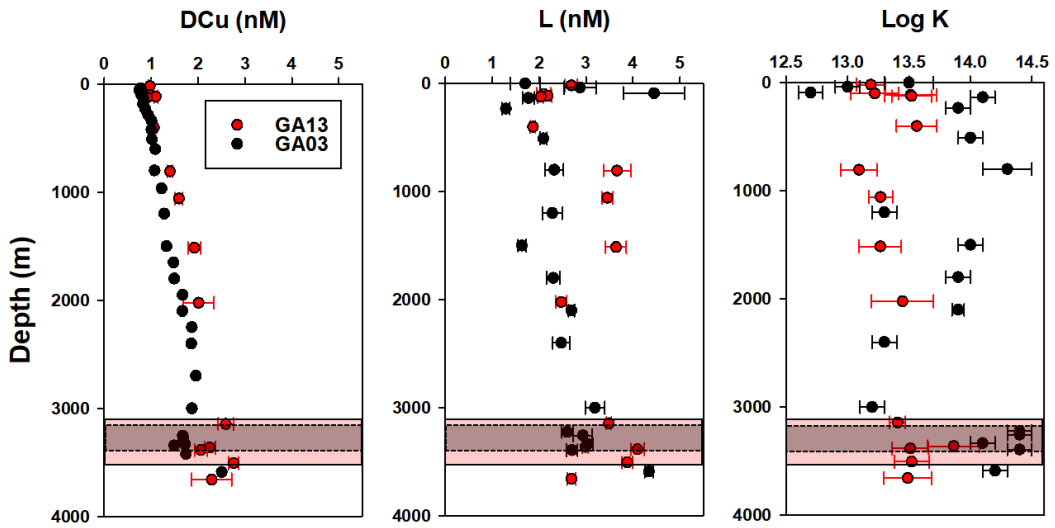

Figure 3.9: Inter-comparison between GA13 Fridge (station 35 and 39, red dots) and GA03 (station 16, black dots) sections. Profiles of DCu, ligands and log K are showed. The red shaded rectangle is representing the position of plumes during the GA13 cruise while the black shaded one represent the plume during the GA03 cruise.

The inter-comparisons demonstrated the comparability between copper speciation datasets from different sections; allowing to discuss Fridge samples using previously published speciation studies.

3.4.2. Correlation between ligands concentration and DCu

Along the Fridge section, copper-ligand concentrations were correlated with the dissolved copper concentrations (Figure 3.10). The Spearman on rank correlation coefficient of determination obtained demonstrated the correlation between the two proxies ($\rho = 0.615$; $p < 0.05$). Despite being in a dynamic environment, high [DCu] were always associated with elevated ligands concentrations along the section. A correlation between ligands and DCu has been observed in a previous study (GEOVIDE, see Chapter 2). This close correlation highlights the role of ligands in driving the DCu distribution through a stabilisation of copper under the dissolved phase. The role of ligands in stabilising dissolved copper has been already documented (Laglera and van den Berg, 2006; Leal and van den Berg, 1998; Sander and Koschinsky, 2011). Extrapolating from this observation, DCu sources need to be associated with ligand sources in order to be significant on an ocean scale. Indeed, without ligands sources, the newly introduced copper would be quickly scavenged and removed from the water column while complexed copper will have the possibility to be exported away from the original source.

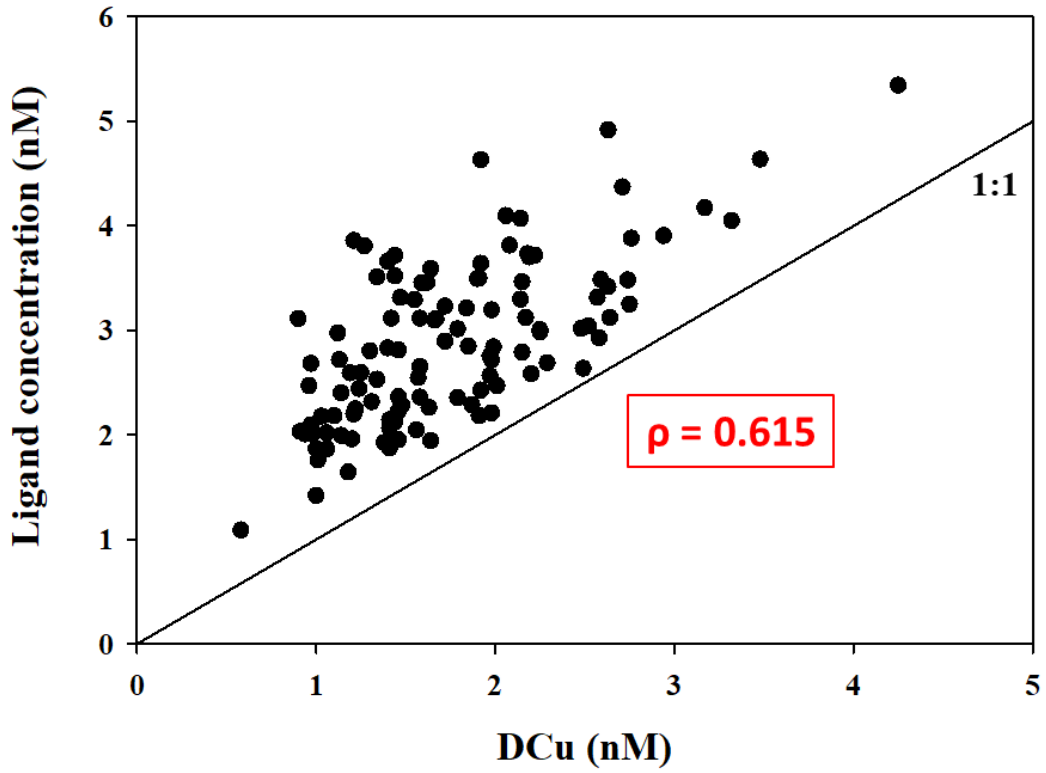

Figure 3.10: Dissolved copper concentration function of the copper equivalent ligands concentrations along Fridge. The linear regression is shown in red with the Spearman on ranks correlation coefficient (ρ with p<0.05). The 1 to 1 relationship is represented by a black line.

3.4.3. Absence of DCu and ligand sources at the hydrothermal vents

The absence of enhanced dissolved copper signal within the plumes (Figure 3.3) despite being highly concentrated in the pure fluid (micromolar concentrations, Edgcomb et al., 2004; Metz and Trefry, 2000; Sarradin et al., 2009), demonstrates the significant dilution and/or removal processes happening during the mixing with surrounding water masses. In order to calculate the influence of each parameter, the dilution factor has been calculated for each identifiable plume. Following Equation 3.1, the dilution factor is estimated from the DMn concentration within the fluid ($DMn_{\_Fluid}$ from Douville et al., 2002), the concentration in the mixing water $DMn_{\_Background}$ and the concentration measured within the plume $DMn_{\_Plume}$.

$$Dilution\ factor = \frac{DMn\_Fluid - DMn\_Background}{DMn\_Plume - DMn\_Background} \qquad (3.1)$$

Equation 3.1 can be transformed to obtain the concentration expected of DCu within the plume as follow:

$$DCu\_Plume = \frac{1}{Dilution\ factor} * DCu\_Fluid + \frac{1}{(1-Dilution\ factor)} * DCu\_Background \qquad (3.2)$$

The $DCu_{\_Plume}$ value is representing the expected concentration of DCu within the plume if dissolved copper was a conservative proxy only affected by dilution. If the actual DCu concentration in the plume is lower, some hydrothermal DCu has been removed; if DCu is similar, dilution is driving copper signal; if DCu is higher, a source of copper else than hydrothermal is significant at depth.

Table 3.1: Table of the calculated DCu_Plume concentration (nM) and the pararameters used to calculate it: Dilution factor, DCu_Fluids and DCu_Background. DCu_Fluids from (a) Charlou et al., 2002, (b) Sarradin et al., 2009 and (c) Trefy et al., 1985.

Hydrothermal sites	Dilution factor	$DCu_{\_Fluids}$ (nM)	$DCu_{\_Background}$ (nM)	$DCu_{\_Plume}$ (nM)
Broken Spur	33867	70000 [a]	2	4.1
Lucky Strike	76013	5150 [b]	2	2.1
TAG	13707	120000 [c]	2.5	11.3
N. TAG	591666	120000 [c]	2.5	2.7
S. TAG	1690476	120000 [c]	3	3.1

Table 3.1 shows two behaviours: for Broken Spur and TAG plume, the $DCu_{\_Plume}$ should be higher than the values observed in the background demonstrating the influence of removal from sulfidic co-precipitation. While the Lucky Strike, N. TAG and S. TAG plumes had $DCu_{\_Plume}$ identical to the background value demonstrating the influence of dilution. Along Fridge, the absence of copper in hydrothermal plumes was due to a combination of mixing and removal. Moreover, it is important to notice that it is not because dilution could explain entirely the absence of hydrothermal copper signal that scavenged removal was not effective. It only means that scavenging is not necessary to explain the DCu concentration observed inside the plume.

No increased of ligand concentrations was observed in the vicinity of the vents or within the buoyant or non-buoyant plumes (Figure 3.4). Previous studies focusing on hydrothermal vents demonstrated a production of organic ligands by the biology present around the vents (Kleint et al., 2015; Klevenz et al., 2012) leading to an increase of [L] up to micro molar level. Despite these studies, ligand production has never been observed on oceanic section (this study; Jacquot and Moffet, 2015). Organic ligands are believed to have a long residence time and their degradation cannot explain the missing signal. Two explanations could explain the discrepancies. Firstly, dilution of the pure fluid with

the surrounding water column could explain the absence of hydrothermal signal. Oceanic sections are sampling hydrothermal site further away than focused study due to different sampling tools (rosette against ROV/submersible). During Fridge, the hydrothermal ligands could have been diluted and mixed with surrounding water masses. In consequence, any hydrothermal signal could be masked by the highly scattered background ligands concentrations (Figure 3.4). Unfortunately, it is not possible to realise the same analysis as for DCu (Equation 3.2) due to the production by biology around the vents. Secondly, some of the ligands identified by CLE-adCSV as organic are now believed to be partially inorganic (Cotte et al., 2018; Sarradin et al., 2009). Sarradin et al., demonstrated that only 2 % of the copper ligands within the fluid was organic while 98 % was inorganic (mainly sulphide compounds). Inorganic copper complexes are believed to have a short residence time (Edgcomb et al., 2004) explaining absence of ligands signal within the plume. It is not possible to test either of the hypotheses with our current dataset and more focussed studies on the production of ligands in the vicinity of the vents will be necessary.

3.4.4. Ligands cycle: the missing sources

The absence of significative ligand production by hydrothermal activity raise more questions on the ligand cycle. Organic ligands are an essential component of trace element biogeochemical cycle in the ocean (Bruland and Lohan, 2004; Morel and Price, 2003), but their composition and chemical structures are still largely unknown. Moreover, no clear surface inputs were observable along Fridge (Figure 3.4 and 3.5) suggesting that neither atmospheric deposition nor the biology are a significant source of ligands. Using the current GEOTRACES copper ligand dataset available: GA01 (see Chapter 2), GA03 (Jacquot and Moffet, 2015) and GA13 (this chapter); no clear ligands source can be identified suggesting a high residence time of copper complexing ligands. The homogenisation leads to a dissimulation of the ligand sources by elevated background concentrations. Due to the absence of characterisation of the ligand pool, no clear residence time study has been accomplished at our current knowledge. Further studies using pseudopolarography (Gibbon-Walsh et al., 2012) and/or LC-ICPMS (Boiteau et al., 2016) on the ligands composition and structure are needed to understand copper ligands cycle.

3.5. Conclusion

This study highlights the absence of influence from hydrothermal vents on copper cycling and its speciation. Hydrothermal plumes along Fridge were characterised by background signal of DCu and ligands (concentration and binding strength). The signal emanating from vents was indistinguishable at any of the sites visited during FRIDGE. The absence of hydrothermal DCu could be explain by the dilution with surrounding water masses at certain stations. But at Broken Spur and TAG, mixing cannot explain by itself the absence of signal; a strong removal of DCu is needed to explain its concentration. The copper ligand concentrations were not sufficient to maintain elevated [DCu] in the water column.

Inter-comparison between our results, GA01 and GA03 demonstrate the comparability of the data obtained. Speciation datasets can be compared and studied together in order to tackle the incertitude on ligands cycle. The ligands cycle was driving the dissolved copper cycle along Fridge as observed by the correlation between both proxies. Elevated ligand concentrations allowed high DCu concentrations to be stabilise in the water column.

The absence of ligand inputs at hydrothermal vent sites could explain the lack of copper signal within plumes, the newly added copper being removed due to the weak organic complexation. This study highlights the necessity to better constrain the cycle of ligands within the open ocean. A clear characterisation (e.g. pseudopolarography and LC-ICPMS) is needed to understand their cycle and impact on trace metals biogeochemistry.

4. Chapter 4: What processes shape the dissolved copper distribution in the ocean interior?

Abstract

Copper profiles have been investigated using a global dataset combining the GEOTRACES IDP 2017 and previously published datasets. Copper shows a linear profile in much of the ocean with a Spearman's rank correlation coefficient higher than 0.8 for 72 % of the stations. The slope of copper profiles varies systematically between ocean basins (low slope in the Atlantic and elevated slope in the Pacific) due to fluctuations in deep ocean concentrations. Applying a diagnostic framework demonstrates that copper distributions can be explained by a combination of regenerated, preformed and reversibly scavenged pools. Regenerated copper mainly represents less than 100 % of the total dissolved copper; a similar behaviour than macronutrient like phosphate while scavenged elements (e.g. iron or manganese) usually have an over-representation of the regenerated component (over 100 %). Analysis of the scavenged components reveals a transition of sign from shallow depth with negative values to greater depth, with positive values. Reversible scavenging switches around 2250 m from a net copper sink to a net source in deeper waters.

4.1. Introduction

The vertical distribution of dissolved elements in the ocean varies from one element to another. Four main types of profiles describing elemental distributions have been identified in the open ocean: nutrient-like, scavenged, hybrid and linear. The nutrient-like profile, as for nitrate and phosphate, is characterised by a minimum in surface waters due to the uptake by biological activity, followed by an increase with depth up to around 1000 m due to remineralisation of sinking particles (Boyd et al., 2017; Buesseler et al., 2007; Dehairs et al., 2008). Deeper in the water column, concentrations of nutrients stays relatively constant due to the absence of additional sources or sinks and accumulates with water age (Bruland and Lohan, 2003; Tagliabue, 2019). The scavenged profile describes those elements highly affected by scavenging on sinking particles like manganese and aluminium (Bruland and Lohan,

2003; Tagliabue, 2019). External surface sources (i.e. atmospheric deposition and riverine inputs) lead to a maximum concentration in surface quickly followed by a sharp decrease in concentration with depth driven by the strong removal of dissolved species by particle scavenging (Menzel Barraqueta et al., 2018; Middag et al., 2011). Some elements such as iron and cobalt are used as nutrients by phytoplankton and are affected by scavenging; in consequence, their distribution is described as hybrid (Bruland and Lohan, 2003; Tagliabue, 2019). The hybrid profile is characterised by low concentration in surface followed by an increase up to the remineralisation layer, below this layer scavenging becomes predominant and affects the vertical profile by decreasing the concentration with depth (Bown et al., 2011; Boyd and Ellwood, 2010; Saito and Moffett, 2002; Tagliabue et al., 2017). Finally, some elements display a linear increase in concentration with depth. Thorium 230 (^{230}Th) is the main example of this distribution (Bacon and Anderson, 1982; Nozaki et al., 1981) and the linear profile of ^{230}Th is caused by the balance between scavenging on particles and the radioactive production of ^{230}Th from its mother element uranium 238 (^{238}U) throughout the water column (Bacon and Anderson, 1982; Nozaki et al., 1981).

Vertical distributions of dissolved copper (DCu) in the open ocean are highly singular for a non-radioactive element with a linear increase with depth in most of the world ocean (see Chapter 2 and IDP 2017; Roshan and Wu, 2015; Schlitzer et al., 2018). A few regions of the world have non-linear profiles including the Labrador Sea, which is discussed in Chapter 2. Distributions of DCu result from the combination of all the sources, sinks and internal processes affecting copper within the ocean. As a consequence, the study of copper (Cu) profiles can help us to better understand the processes affecting the copper cycle in the open ocean. Copper is consumed in surface by phytoplanktonic cells as a micro-nutrient (Peers and Price, 2006). Its unique redox properties are essential for a multitude of enzymatic reaction including denitrification (Moffett et al., 2012; Philippot, 2002) and the iron uptake (Annett et al., 2008; Wells et al., 2005). The main external sources of DCu are atmospheric deposition and riverine inputs (Paytan et al., 2009; Waeles et al., 2015) while benthic inputs (i.e. sediments resuspension and hydrothermalism) can be considered negligible on an ocean scale (Chapter 2, Schlitzer et al., 2018). The unique linear vertical copper profile has always been intriguing since the first study of dissolved copper. Initially most studies (Boyle et al., 1977, 1981) attributed the maximum at depth to a benthic input affecting copper distribution over the entire column. But more recent modeling studies (Little et al., 2013; Richon and Tagliabue, 2019) demonstrated the role of reversible scavenging in shaping the

DCu profile. Reversible scavenging is the extension of the classical scavenging model described previously. While scavenging has been described for a long time as an irreversible process, it appears that it is actually reversible mainly driven by the equilibrium between the particulate and dissolved phases (Honeyman et al., 1988; Trimble et al., 2004). This equilibrium varies according to a few parameters including the particulate load; increase of the particle concentration leads to more adsorption while a decrease in particle load leads to desorption. The balance of adsorption and desorption drives the net effect of scavenging. Within the ocean, reversible scavenging predominantly consists in the adsorption on sinking particles in the surface layer where the particle concentrations are elevated; while deeper in the water column, the particles are scarcer leading to a desorption from these particles at depth (Richon and Tagliabue, 2019).

The observed distribution of trace elements is a snapshot resulting from the multiple sources, sinks and internal processes that affect a given water mass as it is transported through the ocean interior. The study of vertical profiles could inform us of the main processes driving the biogeochemical cycle of trace elements. In order to resolve the biogeochemical transformations affecting trace elements, the physical processes need to be isolated. The main physical process is the transport of trace elements by water masses; the physical component of trace element concentration is called preformed. The preformed component represents the fraction entering abiotically within the ocean by water masses subduction and transport (Duteil et al., 2012; Ito and Follows, 2005). It is estimated using the initial surface concentration prior to the subduction of the water mass and its export. A water mass will have the same preformed concentration through time and transport, the value being set during its formation. Once the physical component is resolved, biogeochemical transformations such as regeneration can be investigated. The regenerated component is the result of the regeneration of biogenic material driven by bacterial activity (Barbeau et al., 2001; Boyd et al., 2010, 2017; Dehairs et al., 2008). It is estimated using the dioxygen (O_2) as a tracer of the bacterial respiration; during regeneration, O_2 is released at the same rate than regenerated elements (Broecker et al., 1985). The Apparent Oxygen Utilisation (AOU) is a proxy of the oxygen cycle showing the consumption (respiration) and the production (photosynthesis) of oxygen using the saturation of oxygen in the seawater according temperature and salinity (Emerson et al., 2004; Ito et al., 2004). In consequence, the AOU can be used to calculate the regenerated fraction produced during regeneration. Analysis of the preformed and regenerated have been developed from the mid-80s to study macro-nutrient cycle like phosphate (PO_4^{3-}) in the open ocean

(Broecker et al., 1985; Duteil et al., 2012; Ito and Follows, 2005). They revealed that around 60 % of the PO_4^{3-} global inventory is preformed while 40 % is produced by regeneration (Duteil et al., 2012). The preformed/regenerated analysis has recently been extended to micro-nutrients such as iron (Fe) in order to better understand the main drivers of their complex biogeochemical cycle (Tagliabue et al., 2014, 2017, 2019). The possibility to apply this framework to study copper cycle will bring a new perspective. The analysis of the regenerated component could allow the estimation of the biological influence on copper distribution over the entire water column.

In this study, we present the analysis of dissolved copper profiles from all over the world's ocean. The linearity of DCu concentration with depth is investigated in the 1st section to understand the processes shaping this linearity. The distribution of DCu is analysed to study which layer of the water column mainly drives the overall linear increase in concentration with depth. In the 2nd section, we deconstruct the DCu concentrations in to several components of regenerated, preformed and scavenged pools. The influence of each component on the DCu concentration is discussed over 3 depth layers to constrain the variability with depth.

4.2. Copper database

The copper dataset has been put together using a combination of the Intermediate Data Product 2017 of the GEOTRACES program (IDP 2017, Schlitzer et al., 2018) and a previous dataset of historical published copper observations compiled by E. Bucciarelli (personal communication). A total of 6563 individual data points distributed over 383 stations constituted the overall dataset (Annexe, Figure 4.1). The observations cover most of the world's oceans (Atlantic Ocean, Indian Ocean, Pacific Ocean and Southern Ocean) and some semi-enclosed seas (Mediterranean Sea and Black Sea). But some regions are not covered as the Arctic Ocean and its seas (e.g. Norwegian); moreover, the coverage of the Southern Ocean is relatively scarce with few stations covering it and no data from deep water mass forming seas such as the Weddell Sea and the Ross Sea.

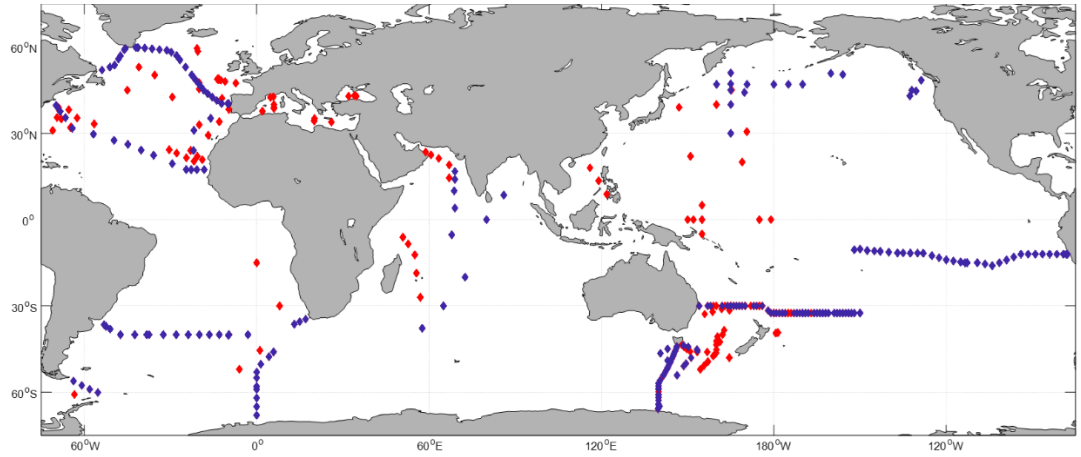

Figure 4.8: Map of the stations constituting the dataset. Red diamonds are representing stations from previously published articles while blue diamonds represent stations extracted from the IDP 2017 where auxiliary parameters (T, S, O_2, PO_4) are also available.

Other parameters as temperature, salinity, oxygen and phosphate concentration (PO_4^{3-}) used through the chapter have been extracted from the IDP 2017 (Schlitzer et al., 2018). These parameters were not available for the historical dataset.

4.3. What is the vertical profile of copper?

The DCu profiles are studied using two statistical tests assessing the linearity of copper distribution with depth. First, a Spearman correlation on ranks is performed (due to the non-parametric nature of the DCu data) in order to obtain the strength of the correlation between DCu and depth, quantified by the Spearman correlation coefficient ρ. This coefficient ranges between -1 and 1; ρ = -1 representing an anticorrelation, ρ =0 the absence of correlation and ρ = 1 a positive correlation.. Secondly, a linear regression is applied on the logarithm of DCu and logarithm of depth in order to access the slope of profile. Both analyses were performed over three depth ranges: the entire water column, the upper 1000m and from 1000 m to the seafloor (Figure 4.2). This approach was used to discriminate which depth layer (shallow or deep) is mainly driving the linearity of the profile.

Copper displays a linear profile over much of the open ocean, which is predominantly driven by deep ocean processes. Over the entire water column, a strong linear correlation is observed in every oceanic basin (Figure 4.2a), 72 % of the stations have a ρ > 0.8 (Figure 4.3a). A few notable exceptions are observed in some semi-enclosed seas as the Mediterranean, Arabian, Black and Labrador Seas. The

Mediterranean and Arabian Sea have a weak linearity due to the surface maximum resulting from dust deposition in this region (Jordi et al., 2012; Saager et al., 1992). The Black Sea is a unique environment where the surface layer is oxygenated but a strong oxycline is observed around 100 m depth with [O_2] dropping below 20 µM (Capet et al., 2016). In the anoxic environment, sulphides dominate the redox chemistry and remove DCu from the water column through the authigenic formation of copper sulphide (CuS). The Black Sea is characterised by elevated DCu concentration in surface waters (> 2 nM) followed by a sharp decrease at the oxycline and constant low values at depth (< 0.5 nM). The lack of linearity found in the Labrador Sea is discussed further in Chapter 2 of this thesis. Turning to the first 1000 m, the correlation is weaker in most basins (Figure 4.2b), only 49 % of the stations have a $\rho > 0.8$ (Figure 4.3b and Table 4.1). When moving to the deeper profiles (below 1000 m depth), the linearity remains very strong compared to the entire water column (Figure 4.2c) with a $\rho > 0.8$ observed in 69 % of stations (Figure 4.3c and Table 4.1). Thus, it appears that the linearity of the DCu profile is mainly driven by processes operating deeper than 1000m.

Table 4.1: Percentage of profiles with a correlation coefficient $\rho > 0.8$ for the entire depth profile, the first 1000 m and from 1000m to the seafloor.

All water column	Shallow profiles	Deep profiles
72%	49%	69%

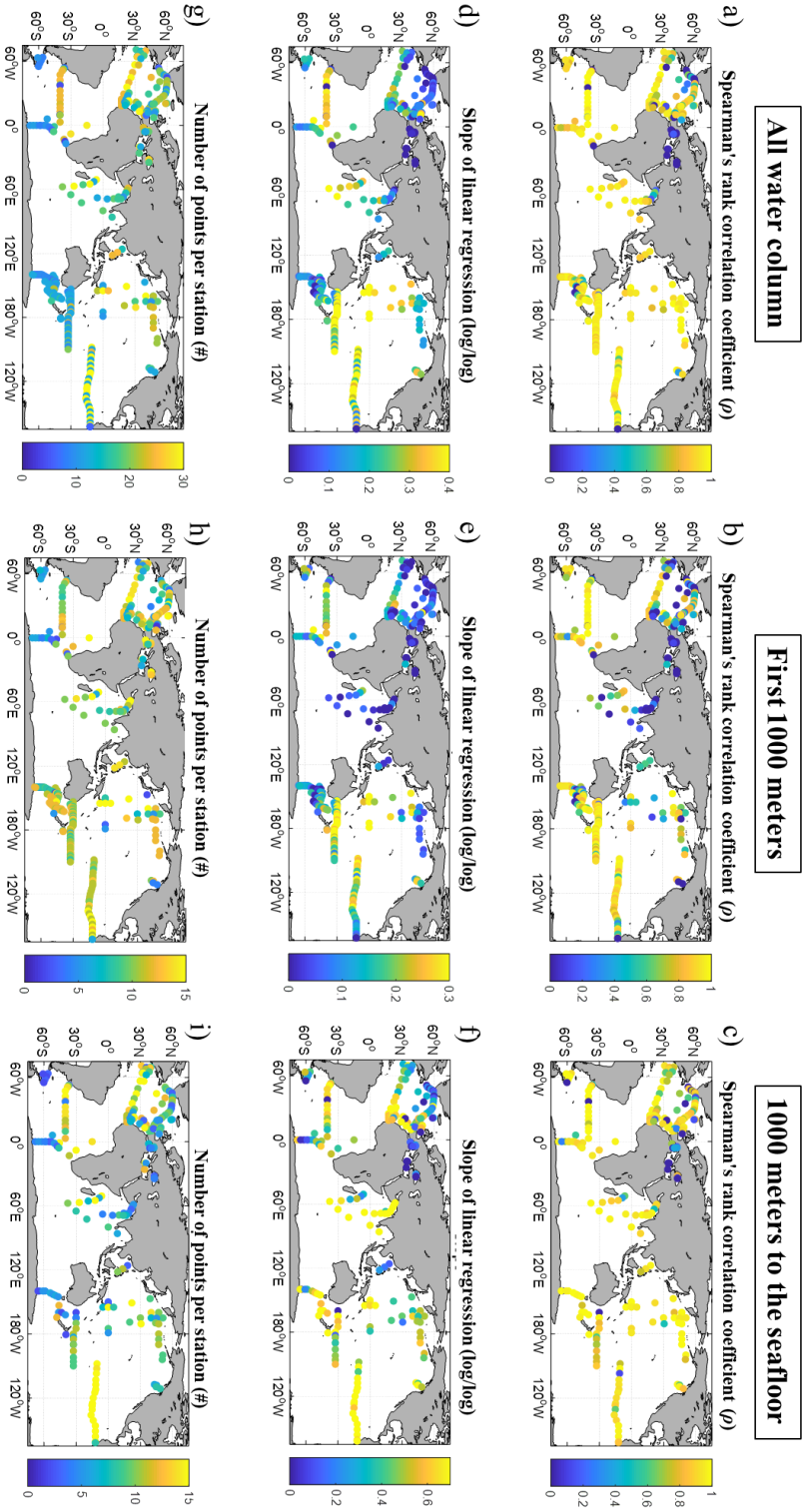

Figure 4.2: Distribution of the spearman's rank correlation of the copper profiles over (a) the entire water column (b) the first 1000 m (c) 1000 meters to the seafloor. Notice the colorbar from 0 to 1. Distribution of the slope of the logarithm copper profiles over (d) the entire water column (e) the first 1000 m (f) 1000 meters to the seafloor. Distribution of the number of datapoints per profiles over (g) the entire water column (h) the first 1000 m (i) 1000 meters to the seafloor.

In order to check the for any bias associated with the number of data points, the number of data used per station has been plotted in Figure 4.2g, 4.2h and 4.2i. Moreover, the number of datapoints per station have been plotted again the spearman correlation coefficient ρ in figure 4.3d, 4.3e and 4.3f. It appears from these figures that the number of data points does not drive any trend in the linearity coefficient. Features observed in the ρ distribution are therefore likely not an artefact derived from our dataset distribution.

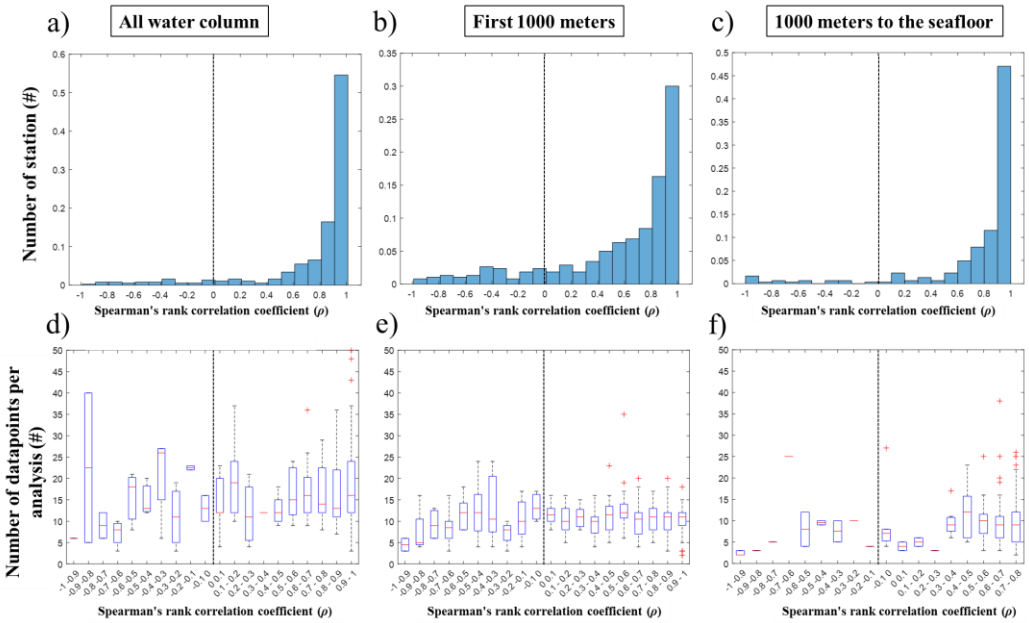

Figure 4.3: Histograms of the number of station function of their Spearman's rank correlation coefficient (a) in the entire water column (b) within the first 1000 meters (c) deeper than a 1000 meters depth. The dashed line is representing the 0 line. And boxplots of the number of datapoints per correlation analysis function of the Spearman's rank correlation coefficient (d) in the entire water column (e) within the first 1000 meters (f) deeper than a 1000 meters depth.

A systematic change in slope of the DCu versus depth concentration change is observed between oceanic basin for the entire water column, the shallow and the deep strata (Figure 4.2d, 4.2e and 4.2f). For the entire water column, the lowest slopes are observed in the North Atlantic with a median of 0.11 nM km^{-1} while the most elevated slopes are found in the Equatorial Pacific with 0.34 nM km^{-1}. The same pattern is also observed in the shallow and deep layers. Variability in the slope can be explained by the dissolved copper distribution. Using four depth layers (0-50 m, 900-1100 m, 2400-2600 m and

3900-4100 m depth), Figure 4.4 shows the variation of DCu concentration with depth. In surface (0-50 m layer), DCu concentrations are relatively homogeneous in every basin (Figure 4.4a), with any surface variations observed in regions affected by atmospheric or riverine inputs as discussed previously. Within the 900-1100 m layer, DCu concentrations are increasing in every basin and concentrations remain relatively similar throughout the ocean. Once we move deeper in the water column (2400-2600m and 3900-4100m), then DCu concentrations increase markedly and the variability between basins is now more apparent (Figure 4.4).

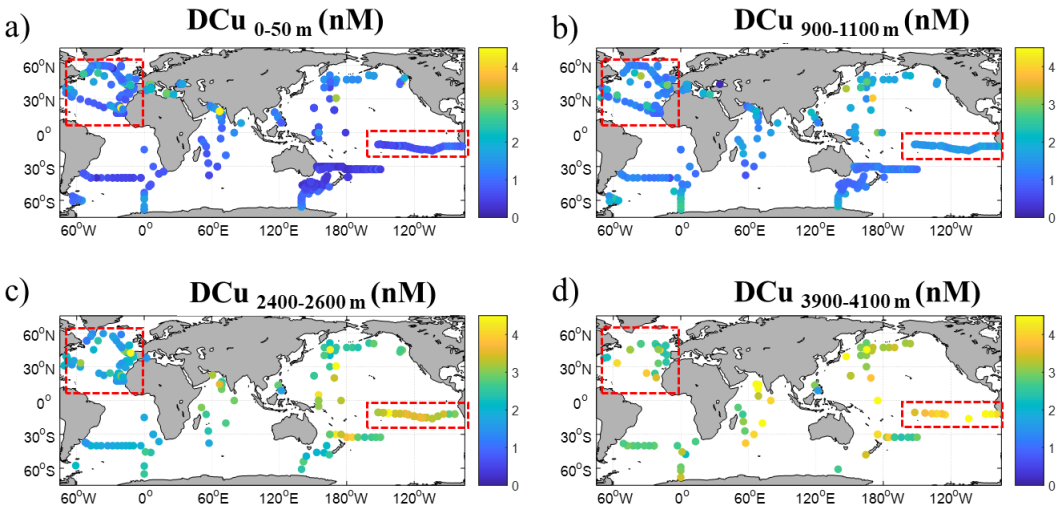

Figure 4.4: Dissolved copper distribution at 4 depth layers: (a) 0-50 meters depth, (b) 900-1100 m, (c) 2400-2600 m and (d) 3900-4100 m. Red dashed square are representing the North Atlantic and the Equatorial Pacific basins.

Focusing on the two regions with the lowest and highest slope (North Atlantic and Equatorial Pacific), Table 4.2 quantises the variation of the median concentration for each the depth layer. In surface, Equatorial Pacific has lower median concentration than the North Atlantic, 0.69 nM versus 1.10 nM, but the interquartile ranges overlap. From the 900-1100 m layer, the trend changes with a more elevated median [DCu] in the Pacific than in the Atlantic (Figure 4.4 and Table 4.2). Deeper in the water column, the difference between the median concentrations is increasing up to 1.55 nM in the 3900-4100 m depth layer (Table 4.2). Variability in the slope of DCu enrichment with depth is indicating a variability in the intensity in the processes shaping the copper profiles between the different oceanic basins at depth.

Table 4.2: Table of the median and interquartile range of DCu concentration in the North Atlantic and Equatorial Pacific at 4 depth layers (0-50 m, 9000-1100 m, 2400-2600 m, 3900-4100 m).

	North Atlantic		Equatorial Pacific	
Layer	Median	Iqr	Median	Iqr
0-50m	1.1	0.41	0.69	0.3
900-1100m	1.21	0.22	1.54	0.11
2400-2600m	1.6	0.27	3.45	0.3
3900-4100m	2.57	0.81	4.12	0.72

Overall, the linearity of the copper profile is mainly driven by its deep component, which implies that deep processes must shape the linearity of DCu distribution. Moreover, the inter-basins variability in DCu concentrations occurs most strongly at depth. Therefore, the following section will be focus on the deep layer and on the processes shaping the copper distribution in the open ocean.

4.4. What processes control the vertical profile of copper?

4.4.1. Identifying the components of the copper distribution

To identify which process mainly control the copper distribution in the ocean, the copper profile is decomposed in several components as shown in Equation 4.1 and Figure 4.5:

$$DCu = DCu_{\_Regenerated} + DCu_{\_Preformed} \pm DCu_{\_Scavenged} \pm DCu_{\_Benthic\_Processes} \qquad (4.1)$$

With DCu being the total dissolved Cu concentration, $DCu_{\_Regenerated}$ being the regenerated Cu concentration and the $DCu_{\_Preformed}$ being the preformed concentration (as for phosphate). Unique for copper is the scavenged concentration ($DCu_{\_Scavenged}$) which can be either positive or negative depending on whether the reversible scavenging equilibrium favours adsorption or desorption.

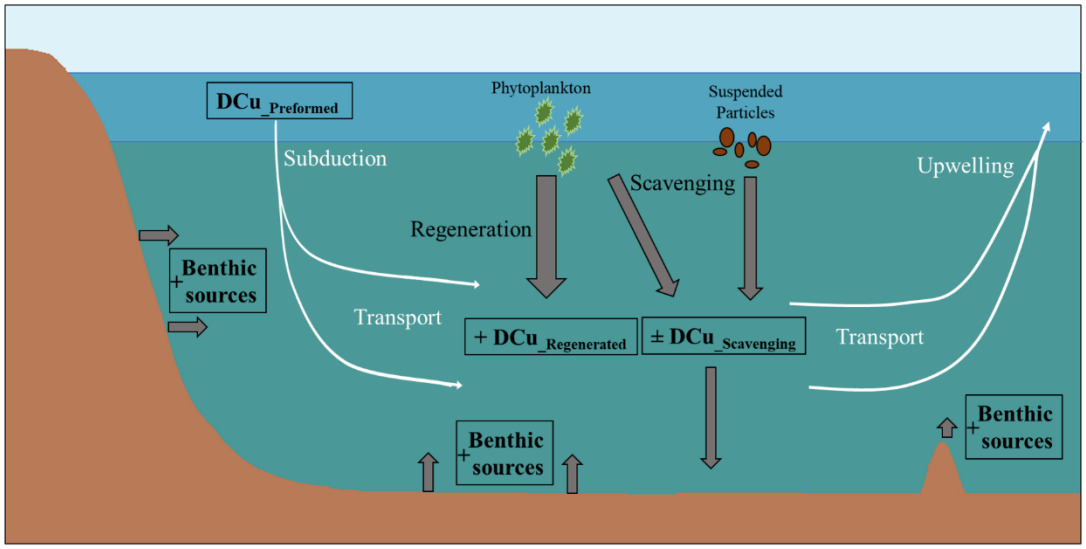

Figure 4.5: Schematic representation of the components analysis on dissolved copper ocean cycle.

The final component $DCu_{\_Benthic\_Processes}$ represents concentrations associated with deep sources from hydrothermal vents and sediments. As hydrothermalism and sediment inputs are non-significant components of the global copper distribution, we simplify Equation 4.1 into Equation 4.2:

$$DCu = DCu_{\_Regenerated} + DCu_{\_Preformed} \pm DCu_{\_Scavenged} \qquad (4.2)$$

4.4.2. Estimation of the regenerated components

The regenerated copper is calculated from Equation 4.3 using the Apparent Oxygen Utilisation (AOU) which can be used as a tracer of remineralisation (Ito et al., 2004). To estimate the amount of copper release during the remineralisation, the Cu/O_2 ratio is needed. In order to access this ratio, the ratio C/O_2 produced during remineralisation is used, an estimated constant derived from the updated Redfield ratio of 117/170 (Anderson and Sarmiento, 1994). The ratio of copper to phosphorus within phytoplanktonic cells is required but this ratio is varying according the phytoplankton species (Ho et al., 2003), its health and the nutrient availability in the medium (Guo et al., 2012a). High variability has previously been observed as reported in the Table 4.3. In order to use the most representative ratio, a ratio Cu/C of 10.9 µmol mol^{-1} will be used (B. Twining pers. comm.). The ratio corresponds to the

geometric mean of 10.9 with a standard error range of 8.2-16.7 μmol mol^{-1} from a global dataset of synchrotron measurements of natural population of phytoplankton.

$$DCu_{\_Regenerated} = AOU * (C/O_2)_{Redfield} * (Cu/C)_{Phytoplankton} \quad (4.3)$$

The Equation 4.4 is used to calculate the percentage of DCu represented by the $DCu_{\_Regenerated}$. If $\%DCu_{\_Regenerated}$ is under 100 %, this means that $DCu_{\_Regenerated}$ is smaller than DCu, while if it is over 100 % it means $DCu_{\_Regenerated}$ is higher than the measured DCu (indicating the need for a $DCu_{\_Scavenged}$ to be negative).

$$\%DCu_{\_Regenerated} = 100 * (DCu_{\_Regenerated} / DCu) \quad (4.4)$$

The same calculations have been applied to phosphate in order to compare the influence of regeneration between both nutrients (Cu and PO_4). The regenerated phosphate component is calculated using the updated P/O_2 Redfield ratio of 1/170 (Eq.. 4.5, Anderson and Sarmiento, 1994). The percentage of regenerated phosphate is calculated with the Equation 4.6.

$$PO_{4\_Regenerated} = AOU * (P/O2)_{Redfield} \quad (4.5)$$

$$\%PO_{4\_Regenerated} = 100 * (PO_{4\_Regenerated} / PO_4) \quad (4.6)$$

Table 4.3: Copper to carbon ratio (μmol mol^{-1}) in phytoplankton in different samples and regions. calculated from the ratio and a C/P ratio of 117 (Anderson and Sarmiento, 1994).*

Source	Sample	Region	Cu/C (μmol mol^{-1})
Ho et al., (2003)*	Cultures		0.34 - 9.49
Sunda and Hunstman (1995) and reference therein	Phytoplankton cells	Pacific	4.6 - 5.1
Tovar-Sanchez et al ., (2006) *	Phytoplankton cells	N. Atlantic	0.9 - 90.4
Twining et al., (2013) *	Particles bulk	All basins	1.1 - 11.3
Twining et al., (2015)	Phytoplankton cells	N. Atlantic	4.2 - 33
Twining et al., (2019)	Phytoplankton cells	Indian	4 to 35

Figure 4.6 shows the regenerated copper concentration for 3 depth layers (1000-1500 m, 2500-3000 and 4000 m to the seafloor) to constrain where the regenerated component is the most affecting DCu. In every layer, $DCu_{\_Regenerated}$ follows AOU by own definition (Figure 4.6a, 4.6b and 4.6c). Low

$DCu_{\_Regenerated}$ is observed in the North Atlantic (median of 1.28 nM) while elevated concentrations are observed in the North Pacific with a median of 3.37 nM. The North Atlantic water masses are relatively young compared to the older North Pacific water masses, which are at the end of the global overturning circulation and tend to accumulate regenerated tracers, such as $DCu_{\_Regenerated,}$ during their transport (Duteil et al., 2012). As expected, the layer 1000-1500 m where most of the remineralisation occurs contains the highest $DCu_{\_Regenerated}$ while going deeper in the water column, the concentrations are lower (Figure 4.6a, 4.6b and 4.6c). In the North Pacific, $DCu_{\_Regenerated}$ drops from 3.37 nM in the 1000-1500 m layer to 2.08 nM in the 4000-bottom layer.

The percentage of regenerated Cu or PO_4^{3-} is a useful metric to understand the behaviour of dissolved copper and how it can be distinct from a major nutrient like phosphate. For instance, regenerated phosphate is always less than the total PO_4^{3-} in our datasets (Figure 4.6g, 4.6h and 4.6i), while scavenged elements like iron are known to display regenerated concentrations that exceed dissolved measurements (by a few hundred percents, Tagliabue et al., 2019). For copper, $\%DCu_{\_Regenerated}$ values are mainly above 100 % in the 1000-1500 m layer (median: 129 %, iqr: 49 %, Figure 4.6d). This indicates the need for a significant internal sink removing the "excess" copper being regenerated and explain the observed total DCu. For iron, the important sink has been identified as scavenging (Tagliabue et al., 2014). At depth, in the 2500-3000m and 4000m-seafloor layers, $\%DCu_{\_Regenerated}$ are mainly under 100% (median: 55 % with iqr: 17 % and median: 43 % with iqr: 18 % respectively, Figure 4.6e and 4.6f). Lower $\%DCu_{\_Regenerated}$ indicates that additional Cu is required to explain the observed total DCu concentration. This implies a role for preformed concentration and/or the presence of an additional deep DCu source.

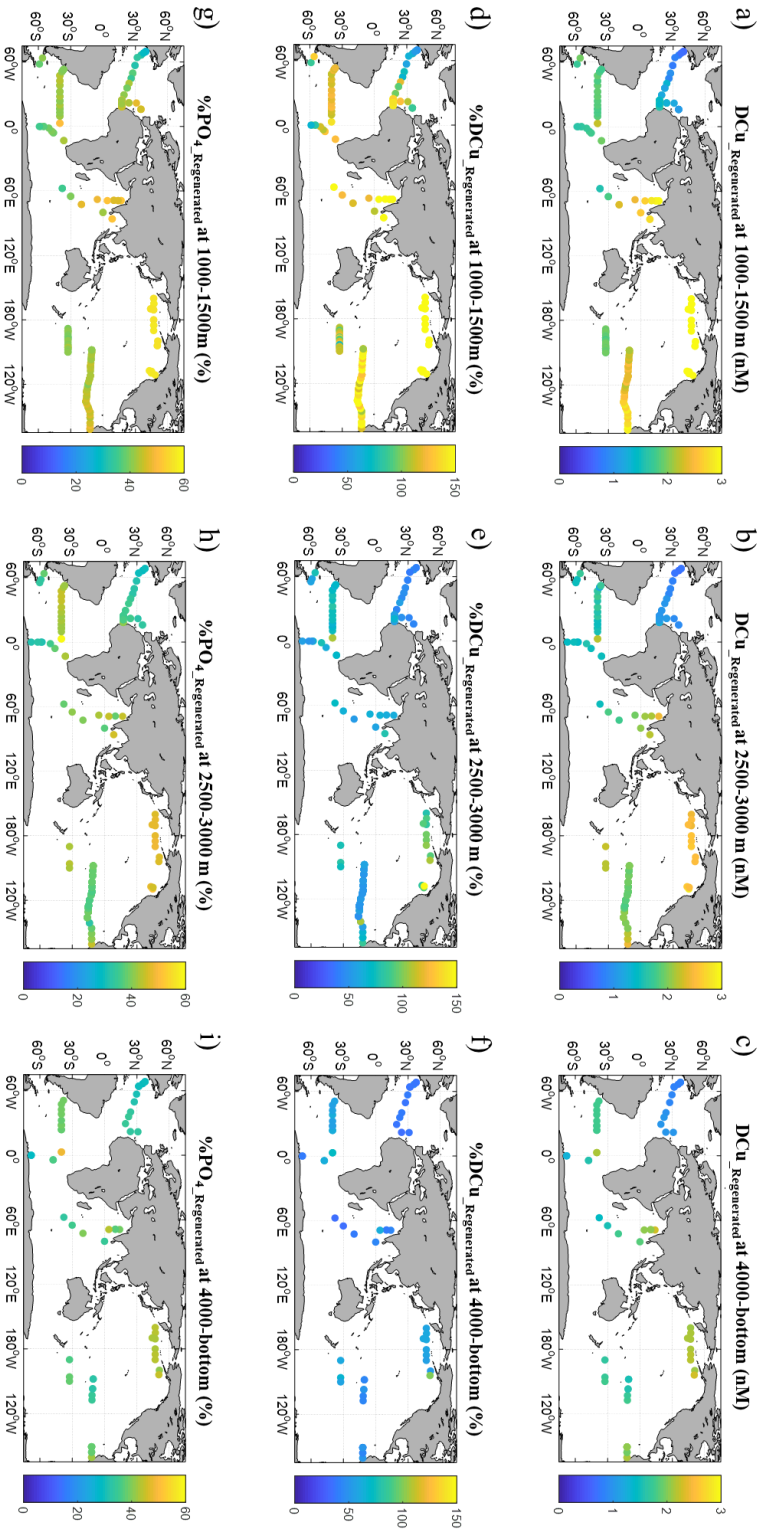

Figure 4.6: Distribution of DCu$_{_Regenerated}$ at the depth layer (a) 1000-1500 m, (b) 2500-3000 m and (c) 4000-bottom. Distribution of the percentage of DCu$_{_Regenerated}$ at the depth layer (d) 1000-1500 m, (e) 2500-3000 m and (f) 4000-bottom. Distribution of the percentage of regenerated phosphorus at the depth layer (g) 1000-1500 m, (h) 2500-3000 m and (i) 4000-bottom.

4.4.3. *Estimation of preformed copper*

The identification of the non-regenerated copper (preformed + scavenged) is essential to resolve the Equation 4.2 which can be rearrange as follow:

$$DCu_{Preformed} + DCu_{Scavenged} = DCu - DCu_{Regenerated} \qquad (4.7)$$

As the preformed Cu concentration is the concentration transported into the ocean interior by physical processes we can use the density of the different deep layers to assess where these waters left the surface ocean. We used the potential density σ_0 at the upper and lower boundary of each depth layer: 1000-1500 m, 2500-3000 m and 4000-bottom and the minimum and maximum σ_0 observed in each layer are identified as represented in Table 4.4. Then, every datapoint where these density potential intervals (minimum σ_0 to maximum σ_0) reach (sub-)surface (< 100 m, from average mixed layer depth from de Boyer Montégut et al., 2004) are identified.

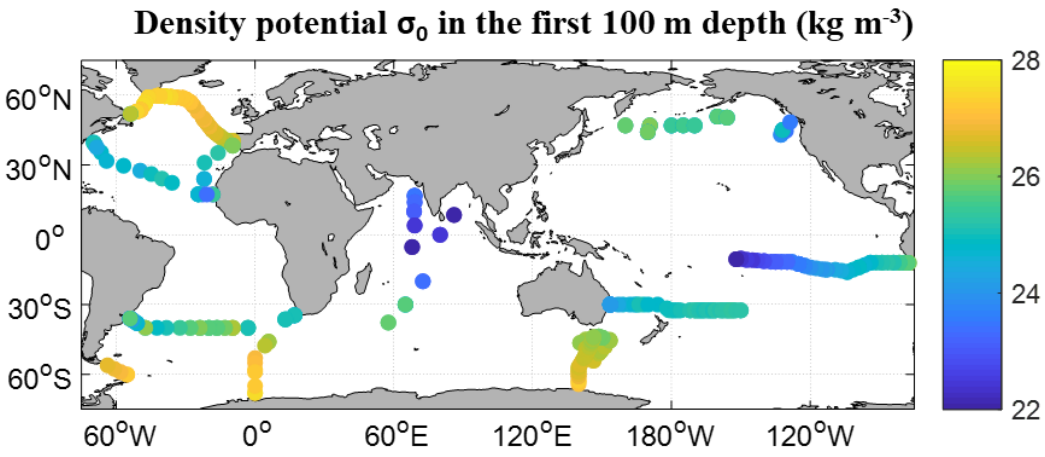

Figure 4.7: Density potential σ_0 observed in Surface (< 100 meters depth) within our dataset.

Figure 4.7 shows the potential density σ_0 in subsurface (< 100 m) over the global ocean. It shows that highest σ_0 in surface are at the poles. The maximum σ_0 value obtained in subsurface using our dataset is 27.5527 kg m^{-3}. As observed in Table 4.4, the minimum σ_0 values in the 2500-3000 m and 4000 m-bottom depth layers are higher than 27.5527 kg m^{-3} leading to the impossibility to estimate the

$DCu_{Preformed}$ within these depth layers. Unfortunately, our dataset is not sampling in region where the potential density reaches elevated values in (sub-)surface. Nevertheless, the $DCu_{Preformed}$ can be calculated for the 1000-1500 m depth layer; a total of 74 datapoints above 100 m are characterised by σ_0 comprised between 27.0990 and 27.7060 kg m^{-3}. The $DCu_{Preformed}$ calculated from this depth layer are extrapolated to the entire dataset due to the impossibility to calculate specific $DCu_{Preformed}$ for each depth layers. In order to be the most representative, the minimum and maximum have been used after removing two outliers (one minimum and one maximum). Values retained for the following analyses are 0.85 and 1.87 nM.

Table 4.4: Minimum and maximum potential density σ_0 observed within the 3 depth layers: 1000-1500 m, 2500-3000 m and 4000 m to the bottom.

	Potential density σ_0 (kg m^{-3})	
Depth layer	Minimum	Maximum
1000-1500 m	27.0990	27.7060
2500-3000 m	27.5650	27.7280
4000 m -bottom	27.6000	27.7290

The $DCu_{Preformed}$ estimation presents caveats mainly linked to the absence of discrimination between water masses. Indeed, every pure water mass has a unique preformed concentration according their region and time of formation. However, in surface waters, DCu concentrations are relatively homogeneous around the globe with a median of 1.3 nM with an interquartile range of 0.4 nM. The low variability in surface [DCu] implies small variation in $DCu_{Preformed}$ between water masses. The assumption of using a range of $DCu_{Preformed}$ from only the 1000-1500 m depth layer can therefore be accepted confidently. Nevertheless, there is no doubt that more copper data are necessary from water masses formation regions in order to obtain better estimates of $DCu_{Preformed}$. The Weddell and Ross seas are known to be the location of formation of intermediate and deep sea flowing in every oceanic basin, but these seas are still under-sampled. To our current knowledge, no study of copper cycle has been undertaken in this area of the globe. The difficulties to sample in the Southern Ocean due to the extreme meteorological conditions are leading to the lack of available data to better constrain the preformed concentrations of copper in our dataset

4.4.4. Scavenged copper, a sink or a source?

All the components have now been identified in order to resolve the Equation 4.2; it is possible to calculate the scavenged fraction following the Equation 4.8. As stated previously, two values of $DCu_{\_Preformed}$ have been selected, a minimum and a maximum. As consequence, for each data points, two $DCu_{\_Scavenged}$ are calculated using both $DCu_{\_Preformed}$ values as described in Equation 4.8.

$$DCu_{\_Scavenged}(min/max) = DCu - DCu_{\_Regenerated} - DCu_{\_Preformed}(min/max) \quad (4.8)$$

In Figure 4.8, both $DCu_{\_Scavenged}$(min) and $DCu_{\_Scavenged}$(max) values are plotted with depth giving an insight on the transition of scavenging from a net sink to a net source of DCu. Assuming the median a Cu/C ratio of 10.9, $DCu_{\_Scavenged}$ are negative in the first 2000 meters indicating a net sink of DCu via the adsorption of DCu on particles where the particles loads are greater. While from 2250m and deeper, 50 % of the $DCu_{\_Scavenged}$ concentrations are positive indicating a net source of DCu from the desorption of DCu from sinking particles. Deeper in the water column, reversible scavenging is responsible for more than 1 nM of DCu (Figure 4.8a). As previously mentioned, the Cu/C ratio within phytoplankton is variable depending on the phytoplanktonic community composition and health. Figure 4.8b and 4.8c show the influence of the Cu/C on $DCu_{\_Scavenged}$ distribution with depth. The two standard deviation values (lower and upper one) of 8.2 and 16.7 μmol mol^{-1} are used (see section 4.2); variable Cu/C in this range is not affecting the overall feature of the $DCu_{\_Scavenged}$ distribution (Figure 4.8). With a Cu/C ratio of 8.2, the transition from negative to positive values of 50% of the $DCu_{\_Scavenged}$ occurs at 2000 m depth while with a ratio of 16.7, this transition happens at 3750 m depth. The particle composition (Cu/C) drives the depth at which reversible scavenging becomes a net source or sink for copper. It is also important to notice that a negative $DCu_{\_Scavenged}$ value does not mean the absence of desorption of DCu from particles, it only indicates that the net budget is going to the adsorption on particles. Moreover, considering the cycle of particles mainly driven by vertical processes in the open ocean, the increase with depth of $DCu_{\_Scavenged}$ from a net negative value to a lower net negative value is showing the dominance of desorption over adsorption from a shallower depth than 2250 m. Using Figure 4.8, $DCu_{\_Scavenged}$ values are increasing below 1000 meters depth demonstrating the shift from adsorption to desorption from this depth.

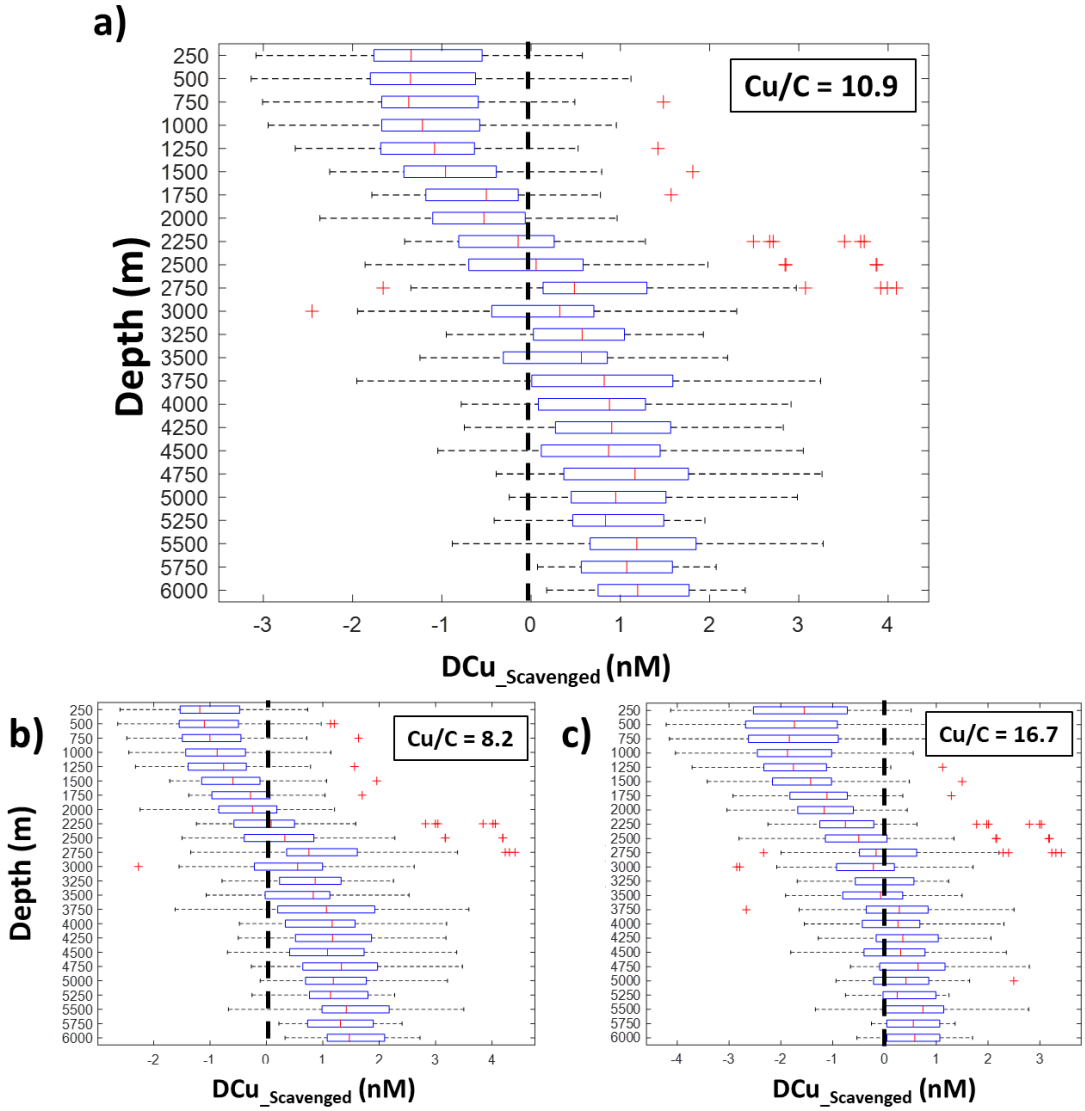

Figure 4.8: Boxplots of the $DCu_{\_Scavenged}$ function of depth with variable Cu/C ratio of a) 1.28, b) 0.96 and c) 1.95 µmol mol^{-1}. The black dashed line is indicating the demarcation between negative to positive values.

The estimation of the $DCu_{\_Regenerated}$ is based on the assumption that only biogenic sinking particles are remineralised and non-biogenic particles are not. The use of a unique Cu/C elemental ratio derived from phytoplanktonic cell quota might also not represent the actual ratio release during regeneration. Indeed, DCu can get scavenged on sinking biogenic particles in (sub-)surface leading to an artificial increase of the Cu/C ratio. This scavenged copper being released during the regeneration of the sinking biogenic particles, the $DCu_{\_Regenerated}$ can be underestimated under certain circumstances. Nevertheless,

Noriki et al. (1985) studied the regeneration rate of chemical elements using particles trap in the Funka Bay, Japan. They measured a Cu/P of regeneration between 1.2 to 1.7 mmol mol^{-1} comparable to the Cu/P ratio used during this study of 1.28 mmol mol^{-1}, from the Cu/C ratio of 10.9 µmol mol^{-1} and a C/P of 1/117 (Anderson and Sarmiento, 1994). The Cu/C ratio used to calculate the $DCu_{\_Regenerated}$ and subsequently the $DCu_{\_Scavenged}$ is the best estimation currently available but further work will be necessary to obtain a more accurate estimate. The impact of copper sinking particles on copper biogeochemical cycle is still unknow, studies focusing on the processes affecting these particles are needed to constrain their fate.

4.5. Conclusion

In this study, we demonstrate the influence of reversible scavenging on copper biogeochemical cycle. Analysis of copper profiles demonstrated that copper shows a linear vertical profile in much of the ocean. But the slope of the enrichment with depth varies systematically between oceanic basins with stronger slope in the Pacific Ocean than in the North Atlantic Ocean. This variability is mainly driven by fluctuations of the DCu concentration in the deep ocean highlighting the role of deep ocean processes in shaping copper vertical distribution.

We applied a diagnostic framework to study the various components explaining the copper distribution. Copper profiles result from a combination of regenerated, preformed and reversibly scavenged pools. Regenerated copper dominates the copper cycle between 1000-1500 m depth layer where it represents more than 100 % of the total DCu concentration. Deeper in the water column, the proportion of regenerated copper decreases to lower values below 50 %. The scavenging component shows a clear switch at 2250 m depth from positive values to negative ones demonstrating the transition of scavenging from a net copper sink to a net copper source in depth. Moreover, the predominance of the desorption from particles over the adsorption on particles is observable from 1000 m where the $DCu_{\_Scavenged}$ proxy is increasing with depth. This study brings new highlight on the copper cycle in the open ocean with a new perspective on the role of reversible scavenging on shaping it. However, additional work need to be accomplished to better constrain the preformed component, future sampling campaigns in water mass forming region will be required to obtain more accurate estimates.

5. Chapter 5: Summary and future work

5.1. Summary of the thesis

In this thesis, we explored the copper biogeochemical cycle in the open ocean with a focus on the North Atlantic. In Chapter 4, the vertical distribution of dissolved copper (DCu) have been studied using a global compilation of data. The DCu profiles were mainly linearly increasing with depth through all the oceanic basins. However, a systematic variation in slope was observable between basins, from low in the North Atlantic to high in the Equatorial Pacific. Variability in slope was driven by variation in DCu concentrations at depth with elevated concentrations in the Equatorial Pacific and low concentrations in the North Atlantic.

The role of organic ligands in controlling the dissolved copper distribution was examined in Chapter 2 and 3. The stabilisation of DCu through complexation with organic ligands has been demonstrated in the North Atlantic. The correlation between ligand and DCu concentrations in the entire column reveals the control of the copper distribution by the ligands.

In Chapter 3, the interaction between DCu and ligands was investigated in the North Atlantic along the Mid-Atlantic ridge. At hydrothermal sites, the absence of enough ligands to complex the newly introduced hydrothermal copper led to the absence of copper signal within the plume. Elevated concentrations of DCu were removed through scavenging on particles and/or authigenic formation of chalcopyrite (CuS). Hydrothermal activity was in consequence not a significant source of DCu and copper-ligands in the deep ocean.

The impact of reversible scavenging on copper vertical distribution was studied in Chapters 2 and 4. Chapter 2 focussed on the North Atlantic studying two contrasted region for DCu distribution. The East Atlantic Basin (EAB) had a classic linear increase of DCu concentrations with depth while the Arctic basins (Labrador and Irminger) showed homogeneous concentrations with depth. The variability between basins was driven by ligand concentrations and particle composition. Increases in DCu at depth in the EAB were associated with elevated ligand concentrations while in the Arctic basins, the ligand concentrations were homogeneous with depth. Moreover, variation in authigenic particle contributions were observed between basins; authigenic particle concentrations were higher in the EAB than in the other basins. Elevated concentrations of authigenic particles resulted from an intense reversible

scavenging in the EAB, while this process was less intense in the Arctic basins. In Chapter 2, the effect of reversible scavenging on copper cycle has been for the first time demonstrated with natural samples. Reversible scavenging has been studied in a global compilation of data in Chapter 4 using a diagnostic framework analysing various components explaining the copper distribution, namely the regenerated, preformed and scavenged components. It shows that regenerated fraction accounted for more than 100 % of the total DCu in the 1000-1500 depth layer. Analysis of the scavenged component showed a switch from negative to positive values at a depth around 2250 m depth. The transition of scavenging from a sink of DCu to a source of DCu highlight the predominant role of reversible scavenging in shaping copper distribution. This confirms the conclusion established for Chapter 2 concerning the source of elevated DCu concentrations in the EAB. Chapters 2 and 4 both demonstrate the effect of reversible scavenging on copper biogeochemical cycle in the ocean.

5.2. Suggestion for future studies

In this thesis, the combination of reversible scavenging and organic speciation has been identified as the main drivers of the copper biogeochemical cycle; nevertheless, many uncertainties remain. Reversible scavenging needs to be better understood, especially the processes triggering the switch from scavenging as a sink to a source of copper. It is essential to comprehend why copper is so different to the other trace elements and the underlying reasons to its sensitivity to reversible scavenging. Copper is not the only trace metal affected by reversible scavenging (e.g. iron) but it is the only non-radioactive to our knowledge having its distribution driven by it. To understand the reversible scavenging, focussed studies on this process are required either designed experiments or using natural samples. The most effective way to study reversible scavenging will be an in-depth understanding of the interactions and exchanges between the dissolved, colloidal and particulate phases. Little is known about the interaction between dissolved on particulate copper; to our knowledge, Chapter 2 of this thesis is one of the first study combining DCu and PCu data. Moreover, colloidal copper data are still scarce for the open ocean. The difficulties in measuring colloidal copper have tampered its study. Indeed, filters usually used for colloid filtrations contains elevated concentrations of copper leading to high blanks. It is necessary to improve our knowledge on the distribution of colloids through the water column in the open ocean. The

understanding of dissolved/colloid/particles interactions will reveal the parameters driving the reversible scavenging.

The copper ligand cycle in the ocean is still widely unknown. A better definition of ligand structures is needed to answer it. Currently, the extreme complexities of ligands characterisation creates a lot of uncertainties. The development of complementary analytical methods such as pseudo-polarography and LC-ICPMS are necessary to comprehend their complexities. A better characterisation of these organic compounds will help to grasp their chemical-physical properties and interaction with trace elements and especially copper. Moreover, the interaction between metals and organic ligands requires more understanding. Some ligands classes are known to bind multiple trace metals, e.g. humic substances or thiols binding iron and copper. But do iron and copper bind the same species or different species? Humic substances and thiols are diverse and complex classes of ligand, some of them could bind one element when others bind another one. The possibility for ligands to bind several trace elements could explain why ligands are always observed in excess compared to DCu.

Concerning the hydrothermal influence on copper cycle in the open ocean, some focussed studies are necessary to understand the fate of copper from the pure fluid to the buoyant plume and non-buoyant plume. The interaction between chemical and physical speciation is currently unknown in the close vicinity of hydrothermal vents.

6. Bibliography

Abadie, C., Lacan, F., Radic, A., Pradoux, C. and Poitrasson, F.: Iron isotopes reveal distinct dissolved iron sources and pathways in the intermediate versus deep Southern Ocean, Proc. Natl. Acad. Sci. U. S. A., 114(5), 858–863, doi:10.1073/pnas.1603107114, 2017.

Abner, B. A., Morel, F. M. M. and Moffett, J. W.: Trace metal control of phytochelatin production in coastal waters, Limnol. Oceanogr., 42(3), 601–608, doi:10.4319/lo.1997.42.3.0601, 1997.

Abualhaija, M. M., Whitby, H. and van den Berg, C. M. G.: Competition between copper and iron for humic ligands in estuarine waters, Mar. Chem., 172, 46–56, doi:10.1016/j.marchem.2015.03.010, 2015.

Aguilar-Islas, A. M., Resing, J. A. and Bruland, K. W.: Catalytically enhanced spectrophotometric determination of manganese in seawater by flow-injection analysis with a commercially available resin for on-line preconcentration, Limnol. Oceanogr. Methods, 4(4), 105–113, doi:10.4319/lom.2006.4.105, 2006.

Ahner, B. a. and Morel, F. M. M.: Phytochelatin production in marine algae. 2. Induction by various metals, Limnol. Oceanogr., 40(4), 658–665, doi:10.4319/lo.1995.40.4.0658, 1995.

Ahner, B. a., Kong, S. and Morel, F. M. M.: Phytochelatin production in marine algae. 1. An interspecies comparison, Limnol. Oceanogr., 40(4), 649–657, doi:10.4319/lo.1995.40.4.0649, 1995.

Alt, J. C., Lonsdale, P., Haymon, R. and Muehlenbachs, K.: Hydrothermal sulfide and oxide deposits on seamounts near 21°N, East Pacific Rise, Geol. Soc. Am. Bull., 98(2), 157, doi:10.1130/0016-7606(1987)98<157:HSAODO>2.0.CO;2, 1987.

Amin, S. a., Moffett, J. W., Martens-Habbena, W., Jacquot, J. E., Han, Y., Devol, A., Ingalls, A. E., Stahl, D. a., Armbrust, E. V. and Virginia Armbrust, E.: Copper requirements of the ammonia-oxidizing archaeon Nitrosopumilus maritimus SCM1 and implications for nitrification in the marine environment, Limnol. Oceanogr., 58(6), 2037–2045, doi:10.4319/lo.2013.58.6.2037, 2013.

Andersen, R. A., Bidigare, R. R., Keller, M. D. and Latasa, M.: A comparison of HPLC pigment signatures and electron microscopic observations for oligotrophic waters of the North Atlantic and Pacific Oceans, Deep. Res. Part II Top. Stud. Oceanogr., 43(2–3), 517–537, doi:10.1016/0967-0645(95)00095-x, 1996.

Anderson, L. a and Sarmiento, J. L.: Redfield ratios of remineralization determined by nutrient data analysis, Global Biogeochem. Cycles, 8(1), 65–80, doi:10.1029/93GB03318, 1994.

Anderson, L. G., Dyrssen, D. and Hall, P. O. J.: On the sulphur chemistry of a super-anoxic fjord, Framvaren, South Norway, Mar. Chem., 23(3–4), 283–293, doi:10.1016/0304-4203(88)90099-0, 1988.

Annett, A. L., Lapi, S., Ruth, T. J. and Maldonado, M. T.: The effects of Cu and Fe availability on the growth and Cu : C ratios of marine diatoms, Limnol. Oceanogr., 53(6), 2451–2461, doi:10.4319/lo.2008.53.6.2451, 2008.

Bacon, M. P. and Anderson, R. F.: Distribution of thorium isotopes between dissolved and particulate forms in the deep sea, J. Geophys. Res., 87(C3), 2045, doi:10.1029/jc087ic03p02045, 1982.

Baker, A. R., Landing, W. M., Bucciarelli, E., Cheize, M., Fietz, S., Hayes, C. T., Kadko, D., Morton, P. L., Rogan, N., Sarthou, G., Shelley, R. U., Shi, Z., Shiller, A. and van Hulten, M. M. P. P.: Trace element and isotope deposition across the air–sea interface: progress and research needs, Philos. Trans. R. Soc. A Math. Phys. Eng. Sci., 374(2081), 20160190, doi:10.1098/rsta.2016.0190, 2016.

Barbeau, K., Kujawinski, E. B. and Moffett, J. W.: Remineralization and recycling of iron, thorium and organic carbon by heterotrophic marine protists in culture, Aquat. Microb. Ecol., 24(1), 69–81, doi:10.3354/ame024069, 2001.

Barón, M., Arellano, J. B., Gorgé, J. L., Baron, M., Arellano, J. B. and Gorge, J. L.: Copper and photosystem II: A controversial relationship, Physiol. Plant., 94(1), 174–180, doi:10.1111/j.1399-3054.1995.tb00799.x, 1995.

Beck, A. J. and Saudo-wilhelmy, S. A.: Impact of Water Temperature and Dissolved Oxygen on Copper Cycling in an Urban Estuary Impact of Water Temperature and Dissolved Oxygen on Copper Cycling in an Urban Estuary, , 41(17), 6103–6108, doi:10.1021/es062719y, 2007.

Behrenfeld, M. J., Bale, A. J., Kolber, Z. S., Aiken, J. and Falkowski, P. G.: Confirmation of iron limitation of phytoplankton photosynthesis in the equatorial Pacific Ocean, Nature, 383(6600), 508–511, doi:10.1038/383508a0, 1996.

Bergquist, B. A., Wu, J. and Boyle, E. A.: Variability in oceanic dissolved iron is dominated by the colloidal fraction>, Geochim. Cosmochim. Acta, 71(12), 2960–2974, doi:10.1016/j.gca.2007.03.013, 2007.

Biswas, H., Bandyopadhyay, D. and Waite, A.: Copper addition helps alleviate iron stress in a coastal diatom: Response of Chaetoceros gracilis from the Bay of Bengal to experimental Cu and Fe addition, Mar. Chem., 157, 224–232, doi:10.1016/j.marchem.2013.10.006, 2013.

Boiteau, R. M., Till, C. P., Ruacho, A., Bundy, R. M., Hawco, N. J., McKenna, A. M., Barbeau, K. A., Bruland, K. W., Saito, M. A. and Repeta, D. J.: Structural characterization of natural nickel and copper binding ligands along the US GEOTRACES eastern Pacific zonal transect, Front. Mar. Sci., 3(NOV), 1–16, doi:10.3389/fmars.2016.00243, 2016.

Bown, J., Boye, M., Baker, A., Duvieilbourg, E., Lacan, F., Le Moigne, F., Planchon, F., Speich, S. and Nelson, D. M.: The biogeochemical cycle of dissolved cobalt in the Atlantic and the Southern Ocean south off the coast of South Africa, Mar. Chem., 126(1–4), 193–206, doi:10.1016/j.marchem.2011.03.008, 2011.

Boyd, P. W. and Ellwood, M. J.: The biogeochemical cycle of iron in the ocean, Nat. Geosci., 3(10), 675–682, doi:10.1038/ngeo964, 2010.

Boyd, P. W., Ibisanmi, E., Sander, S. G., Hunter, K. A. and Jackson, G. A.: Remineralization of upper ocean particles: Implications for iron biogeochemistry, Limnol. Oceanogr., 55(3), 1271–1288, doi:10.4319/lo.2010.55.3.1271, 2010.

Boyd, P. W., Ellwood, M. J., Tagliabue, A. and Twining, B. S.: Biotic and abiotic retention, recycling and remineralization of metals in the ocean, Nat. Geosci., 10(3), 167–173, doi:10.1038/ngeo2876, 2017.

Boyle, E. A., Sclater, F. R. and Edmond, J. M.: The distribution of dissolved copper in the Pacific, Earth Planet. Sci. Lett., 37(1), 38–54, doi:10.1016/0012-821X(77)90144-3, 1977.

Boyle, E. A., Huested, S. S. and Jones, S. P.: On the distribution of copper, nickel, and cadmium in the surface waters of the North Atlantic and North Pacific Ocean, J. Geophys. Res., 86(C9), 8048, doi:10.1029/JC086iC09p08048, 1981.

Brand, L. E., Sunda, W. G. and Guillard, R. R. L.: Reduction of marine phytoplankton reproduction rates by copper and cadmium, J. Exp. Mar. Bio. Ecol., 96(3), 225–250, doi:10.1016/0022-0981(86)90205-4, 1986.

Broecker, W. S., Takahashi, T. and Takahashi, T.: Sources and flow patterns of deep-ocean waters as deduced from potential temperature, salinity, and initial phosphate concentration, J. Geophys. Res., 90(C4), 6925, doi:10.1029/JC090iC04p06925, 1985.

Bruland, K. W.: Oceanographic distributions of cadmium, zinc, nickel, and copper in the North Pacific, Earth Planet. Sci. Lett., 47(2), 176–198, doi:10.1016/0012-821X(80)90035-7, 1980.

Bruland, K. W. and Lohan, M. C.: Controls of Trace Metals in Seawater, in Treatise on Geochemistry, vol. 6, pp. 23–47, Elsevier., 2003.

Buck, C. S., Landing, W. M. and Resing, J. A.: Particle size and aerosol iron solubility: A high-resolution analysis of Atlantic aerosols, Mar. Chem., 120(1–4), 14–24, doi:10.1016/j.marchem.2008.11.002, 2010a.

Buck, C. S., Landing, W. M., Resing, J. A. and Measures, C. I.: The solubility and deposition of aerosol Fe and other trace elements in the North Atlantic Ocean: Observations from the A16N CLIVAR/CO2 repeat hydrography section, Mar. Chem., 120(1–4), 57–70, doi:10.1016/j.marchem.2008.08.003, 2010b.

Buck, K. N. and Bruland, K. W.: Copper speciation in San Francisco Bay: A novel approach using multiple analytical windows, Mar. Chem., 96(1–2), 185–198, doi:10.1016/j.marchem.2005.01.001, 2005.

Buck, K. N., Selph, K. E. and Barbeau, K. A.: Iron-binding ligand production and copper speciation in an incubation experiment of Antarctic Peninsula shelf waters from the Bransfield Strait, Southern Ocean, Mar. Chem., 122(1–4), 148–159, doi:10.1016/j.marchem.2010.06.002, 2010c.

Buck, K. N., Moffett, J., Barbeau, K. a, Bundy, R. M., Kondo, Y. and Wu, J.: The organic complexation of iron and copper : an intercomparison of competitive ligand exchange – adsorptive cathodic stripping voltammetry (CLE-ACSV) techniques, Limnol. Oceanogr. Methods, 10, 496–515, doi:10.4319/lom.2012.10.496, 2012.

Buck, K. N., Sedwick, P. N., Sohst, B. and Carlson, C. A.: Organic complexation of iron in the eastern tropical South Pacific: Results from US GEOTRACES Eastern Pacific Zonal Transect (GEOTRACES cruise GP16), Mar. Chem., 201(June 2017), 229–241, doi:10.1016/j.marchem.2017.11.007, 2018.

Buesseler, K. O., Lamborg, C. H., Boyd, P. W., Lam, P. J., Trull, T. W., Bidigare, R. R., Bishop, J. K. B., Casciotti, K. L., Dehairs, F., Elskens, M., Honda, M., Karl, D. M., Siegel, D. A., Silver, M. W., Steinberg, D. K., Valdes, J., Van Mooy, B. and Wilson, S.: Revisiting Carbon Flux Through the Ocean's Twilight Zone, Science (80-.)., 316(5824), 567–570, doi:10.1126/science.1137959, 2007.

Campbell, A. L., Mangan, S., Ellis, R. P. and Lewis, C.: Ocean acidification increases copper toxicity to the early life history stages of the polychaete arenicola marina in artificial seawater, Environ. Sci. Technol., 48(16), 9745–9753, doi:10.1021/es502739m, 2014.

Campbell, J. W. and Aarup, T.: New production in the North Atlantic derived from seasonal patterns of surface chlorophyll, Deep Sea Res. Part A, Oceanogr. Res. Pap., 39(10), 1669–1694, doi:10.1016/0198-0149(92)90023-M, 1992.

Capet, A., Stanev, E. V., Beckers, J. M., Murray, J. W. and Grégoire, M.: Decline of the Black Sea oxygen inventory, Biogeosciences, 13(4), 1287–1297, doi:10.5194/bg-13-1287-2016, 2016.

Casciotti, K. L. and Ward, B. B.: Dissimilatory Nitrite Reductase Genes from Autotrophic Ammonia-Oxidizing Bacteria Dissimilatory Nitrite Reductase Genes from Autotrophic Ammonia-Oxidizing Bacteria, Appl. Environ. Microbiol., 67(5), 2213–2221, doi:10.1128/AEM.67.5.2213, 2001.

Chadd, H. E., Newman, J., Mann, N. H. and Carr, N. G.: Identification of iron superoxide dismutase and a copper/zinc superoxide dismutase enzyme activity within the marine cyanobacterium Synechococcus sp. WH 7803., FEMS Microbiol. Lett., 138(2–3), 161–165, doi:10.1016/0378-1097(96)00096-1, 1996.

Chapman, C. S., Capodaglio, G., Turetta, C. and Berg, C. M. G. van den: Benthic fluxes of copper, complexing ligands and thiol compounds in shallow lagoon waters, Mar. Environ. Res., 67(1), 17–24, doi:10.1016/j.marenvres.2008.07.010, 2009.

Charlou, J. ., Donval, J. ., Fouquet, Y., Jean-Baptiste, P. and Holm, N.: Geochemistry of high H2 and CH4 vent fluids issuing from ultramafic rocks at the Rainbow hydrothermal field (36°14′N, MAR), Chem. Geol., 191(4), 345–359, doi:10.1016/S0009-2541(02)00134-1, 2002.

Cheize, M., Sarthou, G., Croot, P. L., Bucciarelli, E., Baudoux, A. C. and Baker, A. R.: Iron organic speciation determination in rainwater using cathodic stripping voltammetry, Anal. Chim. Acta, 736, 45–54, doi:10.1016/j.aca.2012.05.011, 2012.

Clegg, S. L. and Whitfield, M.: A generalized model for the scavenging of trace metals in the open ocean—II. Thorium scavenging, Deep Sea Res. Part A. Oceanogr. Res. Pap., 38(1), 91–120, doi:10.1016/0198-0149(91)90056-L, 1991.

Coale, K. H.: Effects of iron, manganese, copper, and zinc enrichments on productivity and biomass in the subarctic Pacific, Limonology Oceanogr., 36(8), 1851–1864, doi:10.4319/lo.1991.36.8.1851, 1991.

Cotte-Krief, M. H., Guieu, C., Thomas, A. J. and Martin, J. M.: Sources of Cd, Cu, Ni and Zn in Portuguese coastal waters, Mar. Chem., 71(3–4), 199–214, doi:Doi 10.1016/S0304-4203(00)00049-9, 2000.

Cotte, L., Omanović, D., Waeles, M., Laës, A., Cathalot, C., Sarradin, P. M. and Riso, R. D.: On the nature of dissolved copper ligands in the early buoyant plume of hydrothermal vents, Environ. Chem., 15(1–2), 58–73, doi:10.1071/EN17150, 2018.

Craig, H.: A scavenging model for trace elements in the deep sea, Earth Planet. Sci. Lett., 23(1), 149–159, doi:10.1016/0012-821X(74)90042-9, 1974.

Croot, P. L.: Seasonal cycle of copper speciation in Gullmar Fjord, Sweden, Limnol. Oceanogr., 48(2), 764–776, doi:10.4319/lo.2003.48.2.0764, 2003.

Croot, P. L., Moffett, J. W. and Brand, L. E.: Production of extracellular Cu complexing ligands by eucaryotic phytoplankton in response to Cu stress, Limnol. Oceanogr., 45(3), 619–627, doi:10.4319/lo.2000.45.3.0619, 2000.

Croot, P. L., Bengt, K., van Elteren, J. T. and Kroon, J. J.: Uptake and efflux of 64 Cu by the marine cyanobacterium Synechococcus (WH7803), Limnol. Oceanogr., 48(1), 179–188, doi:10.4319/lo.2003.48.1.0179, 2003.

Cutter, G. A. and Bruland, K. W.: Rapid and noncontaminating sampling system for trace elements in global ocean surveys, Limnol. Oceanogr. Methods, 10(JUNE), 425–436, doi:10.4319/lom.2012.10.425, 2012.

Danielsson, L.-G., Magnusson, B. and Westerlund, S.: Cadmium, copper, iron, nickel and zinc in the north-east Atlantic Ocean, Mar. Chem., 17(1), 23–41, doi:10.1016/0304-4203(85)90034-9, 1985.

Danielsson, L.-G. L.: Cadmium, cobalt, copper, iron, lead, nickel and zinc in Indian Ocean water, Mar. Chem., 8(3), 199–215, doi:10.1016/0304-4203(80)90010-9, 1980.

de Boyer Montégut, C., Madec, G., Fischer, A. S., Lazar, A. and Iudicone, D.: Mixed layer depth over the global ocean: An examination of profile data and a profile-based climatology, J. Geophys. Res. C Ocean., 109(12), 1–20, doi:10.1029/2004JC002378, 2004.

Dehairs, F., Jacquet, S., Savoye, N., Van Mooy, B. A. S., Buesseler, K. O., Bishop, J. K. B., Lamborg, C. H., Elskens, M., Baeyens, W., Boyd, P. W., Casciotti, K. L. and Monnin, C.: Barium in twilight zone suspended matter as a potential proxy for particulate organic carbon remineralization: Results for the

North Pacific, Deep. Res. Part II Top. Stud. Oceanogr., 55(14–15), 1673–1683, doi:10.1016/j.dsr2.2008.04.020, 2008.

Donat, J. R., Lao, K. A. and Bruland, K. W.: Speciation of dissolved copper and nickel in South San Francisco Bay: a multi-method approach, Anal. Chim. Acta, 284(3), 547–571, doi:10.1016/0003-2670(94)85061-5, 1994.

Doney, S. C., Fabry, V. J., Feely, R. A. and Kleypas, J. A.: Ocean Acidification: The Other CO 2 Problem , Ann. Rev. Mar. Sci., 1(1), 169–192, doi:10.1146/annurev.marine.010908.163834, 2009.

Douville, E., Charlou, J. L., Oelkers, E. H., Bienvenu, P., Jove Colon, C. F., Donval, J. P., Fouquet, Y., Prieur, D. and Appriou, P.: The rainbow vent fluids (36°14′N, MAR): The influence of ultramafic rocks and phase separation on trace metal content in Mid-Atlantic Ridge hydrothermal fluids, Chem. Geol., 184(1–2), 37–48, doi:10.1016/S0009-2541(01)00351-5, 2002.

Dupont, C. L. and Ahner, B. a.: Effects of copper, cadmium, and zinc on the production and exudation of thiols by Emiliania huxleyi, Limnol. Oceanogr., 50(2), 508–515, doi:10.4319/lo.2005.50.2.0508, 2005.

Dupont, C. L., Nelson, R. K., Bashir, S., Moffett, J. W. and Ahner, B. a.: Novel copper-binding and nitrogen-rich thiols produced and exuded by Emiliania huxleyi, Limnol. Oceanogr., 49(5), 1754–1762, doi:10.4319/lo.2004.49.5.1754, 2004.

Dupont, C. L., Moffett, J. W., Bidigare, R. R. and Ahner, B. A.: Distributions of dissolved and particulate biogenic thiols in the subartic Pacific Ocean, Deep. Res. Part I Oceanogr. Res. Pap., 53(12), 1961–1974, doi:10.1016/j.dsr.2006.09.003, 2006.

Dupont, C. L., Butcher, A., Valas, R. E., Bourne, P. E. and Caetano-Anollés, G.: History of biological metal utilization inferred through phylogenomic analysis of protein structures, Proc. Natl. Acad. Sci., 107(23), 10567–10572, doi:10.1073/pnas.0912491107, 2010.

Dutay, J. C., Tagliabue, A., Kriest, I. and van Hulten, M. M. P.: Modelling the role of marine particle on large scale 231Pa, 230Th, Iron and Aluminium distributions, Prog. Oceanogr., 133, 66–72, doi:10.1016/j.pocean.2015.01.010, 2015.

Duteil, O., Koeve, W., Oschlies, A., Aumont, O., Bianchi, D., Bopp, L., Galbraith, E., Matear, R., Moore, J. K., Sarmiento, J. L. and Segschneider, J.: Preformed and regenerated phosphate in ocean general circulation

models: Can right total concentrations be wrong?, Biogeosciences, 9(5), 1797–1807, doi:10.5194/bg-9-1797-2012, 2012.

Edgcomb, V. P., Molyneaux, S. J., Saito, M. A., Lloyd, K., Boer, S., Wirsen, C. O., Atkins, M. S. and Teske, A.: Sulfide Ameliorates Metal Toxicity for Deep-Sea Hydrothermal Vent Archaea, Appl. Environ. Microbiol., 70(4), 2551–2555, doi:10.1128/AEM.70.4.2551-2555.2004, 2004.

Ellwood, M. J., Wilson, P., Vopel, K. and Green, M.: Trace metal cycling in the Whau Estuary, Auckland, New Zealand, Environ. Chem., 5(4), 289, doi:10.1071/EN07077, 2008.

Emerson, S., Watanabe, Y. W., Ono, T. and Mecking, S.: Temporal trends in apparent oxygen utilization in the upper pycnocline of the North Pacific: 1980-2000, J. Oceanogr., 60(3), 139–147, doi:10.1023/B:JOCE.0000038323.62130.a0, 2004.

Fitzsimmons, J. N., Carrasco, G. G., Wu, J., Roshan, S., Hatta, M., Measures, C. I., Conway, T. M., John, S. G. and Boyle, E. A.: Partitioning of dissolved iron and iron isotopes into soluble and colloidal phases along the GA03 GEOTRACES North Atlantic Transect, Deep. Res. Part II Top. Stud. Oceanogr., 116, 130–151, doi:10.1016/j.dsr2.2014.11.014, 2015a.

Fitzsimmons, J. N., Bundy, R. M., Al-Subiai, S. N., Barbeau, K. A. and Boyle, E. A.: The composition of dissolved iron in the dusty surface ocean: An exploration using size-fractionated iron-binding ligands, Mar. Chem., 173, 125–135, doi:10.1016/j.marchem.2014.09.002, 2015b.

Fitzsimmons, J. N., John, S. G., Marsay, C. M., Hoffman, C. L., Nicholas, S. L., Toner, B. M., German, C. R. and Sherrell, R. M.: Iron persistence in a distal hydrothermal plume supported by dissolved-particulate exchange, Nat. Geosci., 10(3), 195–201, doi:10.1038/ngeo2900, 2017.

Florence, T. M. and Stauber, J. L.: Toxicity of copper complexes to the marine diatom Nitzschia closterium, Aquat. Toxicol., 8(1), 11–26, doi:10.1016/0166-445X(86)90069-X, 1986.

La Fontaine, S., Quinn, J. M., Nakamoto, S. S., Dudley Page, M., G??hre, V., Moseley, J. L., Kropat, J. and Merchant, S.: Copper-dependent iron assimilation pathway in the model photosynthetic eukaryote Chlamydomonas reinhardtii, Eukaryot. Cell, 1(5), 736–757, doi:10.1128/EC.1.5.736-757.2002, 2002.

Fragoso, G. M., Poulton, A. J., Yashayaev, I. M., Head, E. J. H., Stinchcombe, M. C. and Purdie, D. A.: Biogeographical patterns and environmental controls of phytoplankton communities from contrasting

hydrographical zones of the Labrador Sea, Prog. Oceanogr., 141, 212–226, doi:10.1016/j.pocean.2015.12.007, 2016.

Francis, C. A., Roberts, K. J., Beman, J. M., Santoro, A. E. and Oakley, B. B.: Ubiquity and diversity of ammonia-oxidizing archaea in water columns and sediments of the ocean, Proc. Natl. Acad. Sci. U. S. A., 102(41), 14683–14688, doi:10.1073/pnas.0506625102, 2005.

Gardner, W. D., Tucholke, B. E., Richardson, M. J. and Biscaye, P. E.: Benthic storms, nepheloid layers, and linkage with upper ocean dynamics in the western North Atlantic, Mar. Geol., 385, 304–327, doi:10.1016/j.margeo.2016.12.012, 2017.

Gardner, W. D., Richardson, M. J. and Mishonov, A. V.: Global assessment of benthic nepheloid layers and linkage with upper ocean dynamics, Earth Planet. Sci. Lett., 482, 126–134, doi:10.1016/j.epsl.2017.11.008, 2018.

Gerringa, L. J. A., Rijstenbil, J. W., Poortvliet, T. C. W., van Drie, J. and Schot, M. C.: Speciation of copper and responses of the marine diatom Ditylum brightwellii upon increasing copper concentrations, Aquat. Toxicol., 31(1), 77–90, doi:10.1016/0166-445X(94)00053-S, 1995.

Gibbon-Walsh, K., Salaün, P. and Van Den Berg, C. M. G.: Pseudopolarography of copper complexes in seawater using a vibrating gold microwire electrode, J. Phys. Chem. A, 116(25), 6609–6620, doi:10.1021/jp3019155, 2012.

Gledhill, M., Achterberg, E. P., Li, K., Mohamed, K. N. and Rijkenberg, M. J. A.: Influence of ocean acidification on the complexation of iron and copper by organic ligands in estuarine waters, Mar. Chem., 177, 421–433, doi:10.1016/j.marchem.2015.03.016, 2015.

Gourain, A., Planquette, H., Cheize, M., Lemaitre, N., Menzel Barraqueta, J. L., Shelley, R., Lherminier, P. and Planquette, H.: Inputs and processes affecting the distribution of particulate iron in the North Atlantic along the GEOVIDE (GEOTRACES GA01) section, Biogeosciences, 16(7), 1563–1582, doi:10.5194/bg-16-1563-2019, 2019.

Guo, C., Yu, J., Ho, T. Y., Wang, L., Song, S., Kong, L. and Liu, H.: Dynamics of phytoplankton community structure in the South China Sea in response to the East Asian aerosol input, Biogeosciences, 9(4), 1519–1536, doi:10.5194/bg-9-1519-2012, 2012a.

Guo, J., Annett, A. L., Taylor, R. L., Lapi, S., Ruth, T. J. and Maldonado, M. T.: Copper-uptake kinetics of coastal and oceanic diatoms, J. Phycol., 46(6), 1218–1228, doi:10.1111/j.1529-8817.2010.00911.x, 2010.

Guo, J., Lapi, S., Ruth, T. J. and Maldonado, M. T.: The effects of iron and copper availability on the copper stoichiometry of marine phytoplankton, J. Phycol., 48(2), 312–325, doi:10.1111/j.1529-8817.2012.01133.x, 2012b.

Guo, J., Green, B. R. and Maldonado, M. T.: Sequence analysis and gene expression of potential components of copper transport and homeostasis in thalassiosira pseudonana, Protist, 166(1), 58–77, doi:10.1016/j.protis.2014.11.006, 2015.

Hansell, D. A., Carlson, C. A. and Schlitzer, R.: Net removal of major marine dissolved organic carbon fractions in the subsurface ocean, Global Biogeochem. Cycles, 26(1), 1–9, doi:10.1029/2011GB004069, 2012.

Hawkes, J. A., Connelly, D. P., Rijkenberg, M. J. A. and Achterberg, E. P.: The importance of shallow hydrothermal island arc systems in ocean biogeochemistry, Geophys. Res. Lett., 41(3), 942–947, doi:10.1002/2013GL058817, 2014.

Heggie, D., Klinkhammer, G. and Cullen, D.: Manganese and copper fluxes from continental margin sediments, Geochim. Cosmochim. Acta, 51(5), 1059–1070, doi:10.1016/0016-7037(87)90200-6, 1987.

Heller, M. I. and Croot, P. L.: Copper speciation and distribution in the Atlantic sector of the Southern Ocean, Mar. Chem., 173(February 2008), 253–268, doi:10.1016/j.marchem.2014.09.017, 2014.

Helmers, E. and Schrems, O.: Wet deposition of metals to the tropical North and the South Atlantic ocean, Atmos. Environ., 29(18), 2475–2484, doi:10.1016/1352-2310(95)00159-V, 1995.

Ho, T.-Y., Quigg, A., Finkel, Z. V., Milligan, A. J., Wyman, K., Falkowski, P. G. and Morel, F. M. M.: The elemental composition of some marine phytoplankton, J. Phycol., 39(6), 1145–1159, doi:10.1111/j.0022-3646.2003.03-090.x, 2003.

Honeyman, B. D., Balistrieri, L. S. and Murray, J. W.: Oceanic trace metal scavenging: the importance of particle concentration, Deep Sea Res. Part A, Oceanogr. Res. Pap., 35(2), 227–246, doi:10.1016/0198-0149(88)90038-6, 1988.

IPCC: Chapter 5: Changing ocean, marine ecosystems, and dependent communities. Intergovernmental Panel of Climate Change, IPCC Spec. Rep. Ocean Cryosph. Chang. Clim., 1–198 [online] Available from: https://report.ipcc.ch/srocc/pdf/SROCC_FinalDraft_Chapter5.pdf, 2019.

Ito, T. and Follows, M. J.: Preformed phosphate, soft tissue pump and atmospheric CO2, J. Mar. Res., 63(4), 813–839, doi:10.1357/0022240054663231, 2005.

Ito, T., Follows, M. J. and Boyle, E. A.: Is AOU a good measure of respiration in the oceans?, Geophys. Res. Lett., 31(17), 1–4, doi:10.1029/2004GL020900, 2004.

Jacquot, J. E. and Moffett, J. W.: Copper distribution and speciation across the International GEOTRACES Section GA03, Deep. Res. Part II Top. Stud. Oceanogr., 116, 187–207, doi:10.1016/j.dsr2.2014.11.013, 2015.

Jacquot, J. E., Kondo, Y., Knapp, A. N. and Moffett, J. W.: The speciation of copper across active gradients in nitrogen-cycle processes in the eastern tropical South Pacific, Limnol. Oceanogr., 58(4), 1387–1394, doi:10.4319/lo.2013.58.4.1387, 2013.

Jacquot, J. E., Horak, R. E. A., Amin, S. A., Devol, A. H., Ingalls, A. E., Armbrust, E. V., Stahl, D. A. and Moffett, J. W.: Assessment of the potential for copper limitation of ammonia oxidation by Archaea in a dynamic estuary, Mar. Chem., 162, 37–49, doi:10.1016/j.marchem.2014.02.002, 2014.

Jeandel, C. and Oelkers, E. H.: The influence of terrigenous particulate material dissolution on ocean chemistry and global element cycles, Chem. Geol., 395, 50–66, doi:10.1016/j.chemgeo.2014.12.001, 2015.

Jickells, T. D., Knap, A. H. and Church, T. M.: Trace metals in Bermuda rainwater., J. Geophys. Res., 89(D1), 1423–1428, doi:10.1029/JD089iD01p01423, 1984.

Jickells, T. D., An, Z. S., Andersen, K. K., Baker, A. R., Bergametti, C., Brooks, N., Cao, J. J., Boyd, P. W., Duce, R. A., Hunter, K. A., Kawahata, H., Kubilay, N., LaRoche, J., Liss, P. S., Mahowald, N., Prospero, J. M., Ridgwell, A. J., Tegen, I. and Torres, R.: Global iron connections between desert dust, ocean biogeochemistry, and climate, Science (80-.)., 308(5718), 67–71, doi:10.1126/science.1105959, 2005.

Johnson, K. S., Michael Gordon, R. and Coale, K. H.: What controls dissolved iron concentrations in the world ocean?, Mar. Chem., 57(3–4), 137–161, doi:10.1016/S0304-4203(97)00043-1, 1997.

Jordi, A., Basterretxea, G., Tovar-Sánchez, A., Alastuey, A. and Querol, X.: Copper aerosols inhibit phytoplankton growth in the Mediterranean Sea., Proc. Natl. Acad. Sci. U. S. A., 109(52), 21246–9, doi:10.1073/pnas.1207567110, 2012.

Kieber, R. J., Williams, K., Willey, J. D., Skrabal, S. and Avery, G. B.: Iron speciation in coastal rainwater: Concentration and deposition to seawater, Mar. Chem., 73(2), 83–95, doi:10.1016/S0304-4203(00)00097-9, 2001.

Kieber, R. J., Skrabal, S. A., Smith, B. J. and Willey, J. D.: Organic complexation of Fe(II) and its impact on the redox cycling of iron in rain, Environ. Sci. Technol., 39(6), 1576–1583, doi:10.1021/es040439h, 2005.

Kleint, C., Kuzmanovski, S., Powell, Z., Bühring, S. I., Sander, S. G., Koschinsky, A., B??hring, S. I., Sander, S. G. and Koschinsky, A.: Organic Cu-complexation at the shallow marine hydrothermal vent fields off the coast of Milos (Greece), Dominica (Lesser Antilles) and the Bay of Plenty (New Zealand), Mar. Chem., 173, 244–252, doi:10.1016/j.marchem.2014.10.012, 2015.

Kleint, C., Hawkes, J. A., Sander, S. G. and Koschinsky, A.: Voltammetric investigation of hydrothermal iron speciation, Front. Mar. Sci., 3(MAY), 1–11, doi:10.3389/fmars.2016.00075, 2016.

Klevenz, V., Sander, S. G., Perner, M. and Koschinsky, A.: Amelioration of free copper by hydrothermal vent microbes as a response to high copper concentrations, Chem. Ecol., 28(5), 405–420, doi:10.1080/02757540.2012.666531, 2012.

Kogut, M. B. and Voelker, B. M.: Strong copper-binding behavior of terrestrial humic substances in seawater, Environ. Sci. Technol., 35(6), 1149–1156, doi:10.1021/es0014584, 2001.

Kondo, Y., Takeda, S., Nishioka, J., Obata, H., Furuya, K., Johnson, W. K. and Wong, C. S.: Organic iron (III) complexing ligands during an iron enrichment experiment in the western subarctic North Pacific, Geophys. Res. Lett., 35(12), 3–7, doi:10.1029/2008GL033354, 2008.

Ksionzek, K. B., Lechtenfeld, O. J., McCallister, S. L., Schmitt-Kopplin, P., Geuer, J. K., Geibert, W. and Koch, B. P.: Dissolved organic sulfur in the ocean: Biogeochemistry of a petagram inventory, Science (80-.)., 354(6311), 456–459, doi:10.1126/science.aaf7796, 2016.

Kuss, J., Kremling, K., Fischer, K., Dymond, J., Lyle, M., Soutar, A., Rau, S., Noriki, S., Shiribiki, T., Yokomizo, H., Harada, K. and Tsunogai, S.: Particulate trace element fluxes in the deep northeast

Atlantic Ocean, Deep. Res. Part I Oceanogr. Res. Pap., 46(1), 149–169, doi:10.1016/S0967-0637(98)00059-4, 1999.

Labatut, M., Lacan, F., Pradoux, C., Chmeleff, J., Radic, A., Murray, J. W., Poitrasson, F., Johansen, A. M. and Thil, F.: Iron sources and dissolved-particulate interactions in the seawater of the Western Equatorial Pacific, iron isotope perspectives, Global Biogeochem. Cycles, 28(10), 1044–1065, doi:10.1002/2014GB004928, 2014.

Laglera, L. M. and van den Berg, C. M. G.: Copper complexation by thiol compounds in estuarine waters, Mar. Chem., 82(1–2), 71–89, doi:10.1016/S0304-4203(03)00053-7, 2003.

Laglera, L. M. and van den Berg, C. M. G.: Photochemical oxidation of thiols and copper complexing ligands in estuarine waters, Mar. Chem., 101(1–2), 130–140, doi:10.1016/j.marchem.2006.01.006, 2006.

Lam, P. J. and Bishop, J. K. B.: The continental margin is a key source of iron to the HNLC North Pacific Ocean, Geophys. Res. Lett., 35(7), 1–5, doi:10.1029/2008GL033294, 2008.

Leal, M. F. C. and Van Den Berg, C. M. G.: Evidence for strong copper(I) complexation by organic ligands in seawater, Aquat. Geochemistry, 4(1), 49–75, doi:10.1023/A:1009653002399, 1998.

Leal, M. F. C., van Vasconcelos M. Teresa S. D., B. den C. M. G., Vasconcelos, M. T. S. D. and van den Berg, C. M. G.: Copper-induced release of complexing ligands similar to thiols by Emiliania huxleyi in seawater cultures, Limnol. Ocean., 44(44 (7)), 1750–1762, doi:10.4319/lo.1999.44.7.1750, 1999.

Lee, J. M., Heller, M. I. and Lam, P. J.: Size distribution of particulate trace elements in the U.S. GEOTRACES Eastern Pacific Zonal Transect (GP16), Mar. Chem., 201(September 2017), 108–123, doi:10.1016/j.marchem.2017.09.006, 2017.

Lelong, a, Bucciarelli, E., Hégaret, H. and Soudant, P.: Iron and copper limitations differently affect growth rates and photosynthetic and physiological parameters of the marine diatom Pseudo-nitzschia delicatissima , Limnol. Oceanogr., 58(2), 613–623, doi:10.4319/lo.2013.58.2.0613, 2013.

Lewis, C., Ellis, R. P., Vernon, E., Elliot, K., Newbatt, S. and Wilson, R. W.: Ocean acidification increases copper toxicity differentially in two key marine invertebrates with distinct acid-base responses, Sci. Rep., 6(September 2015), 1–10, doi:10.1038/srep21554, 2016.

Linder, M. C. and Hazegh-Azam, M.: Copper biochemistry and molecular biology, Am. Soc. Clin. Nutr., 63(5), 797S-811S, doi:10.1093/ajcn/63.5.797, 1996.

Little, S. H., Vance, D., Siddall, M. and Gasson, E.: A modeling assessment of the role of reversible scavenging in controlling oceanic dissolved Cu and Zn distributions, Global Biogeochem. Cycles, 27(3), 780–791, doi:10.1002/gbc.20073, 2013.

Lough, A. J. M., Connelly, D. P., Homoky, W. B., Hawkes, J. A., Chavagnac, V., Castillo, A., Kazemian, M., Nakamura, K., Araki, T., Kaulich, B. and Mills, R. A.: Diffuse Hydrothermal Venting: A Hidden Source of Iron to the Oceans, Front. Mar. Sci., 6(July), 1–14, doi:10.3389/fmars.2019.00329, 2019.

Louis, Y., Garnier, C., Lenoble, V., Omanović, D., Mounier, S. and Pižeta, I.: Characterisation and modelling of marine dissolved organic matter interactions with major and trace cations, Mar. Environ. Res., 67(2), 100–107, doi:10.1016/j.marenvres.2008.12.002, 2009a.

Louis, Y., Garnier, C., Lenoble, V., Mounier, S., Cukrov, N., Omanovic, D. and Pizeta, I.: Kinetic and equilibrium studies of copper-dissolved organic matter complexation in water column of the stratified Krka River estuary (Croatia), Mar. Chem., 114(3–4), 110–119, doi:10.1016/j.marchem.2009.04.006, 2009b.

Lucia, M., Campos, A. M. and van den Berg, C. M. G.: Determination of copper complexation in sea water by cathodic stripping voltammetry and ligand competition with salicylaldoxime, Anal. Chim. Acta, 284(3), 481–496, doi:10.1016/0003-2670(94)85055-0, 1994.

Luther, G. W., Church, T. M. and Powell, D.: Sulfur speciation and sulfide oxidation in the water column of the Black Sea, Deep. Res. Part A, 38(Suppl. 2A), S1121–S1137, doi:10.1016/s0198-0149(10)80027-5, 1991.

Mackey, D. J., O'Sullivan, J. E., Watson, R. J. and Pont, G. D.: Trace metals in the Western Pacific: Temporal and spatial variability in the concentrations of Cd, Cu, Mn and Ni, Deep. Res. Part I Oceanogr. Res. Pap., 49(12), 2241–2259, doi:10.1016/S0967-0637(02)00124-3, 2002.

Mackey, K. R. M., Buck, K. N., Casey, J. R., Cid, A., Lomas, M. W., Sohrin, Y. and Paytan, A.: Phytoplankton responses to atmospheric metal deposition in the coastal and open-ocean Sargasso Sea, Front. Microbiol., 3(OCT), 1–15, doi:10.3389/fmicb.2012.00359, 2012.

Maldonado, M. T., Allen, A. E., Chong, J. S., Lin, K., Leus, D., Karpenko, N. and Harris, S. L.: Copper-dependent iron transport in coastal and oceanic diatoms, Limnol. Oceanogr., 51(4), 1729–1743, doi:10.4319/lo.2006.51.4.1729, 2006.

Mann, E. L., Ahlgren, N., Moffett, J. W., Chisholm, S. W., Hole, W. and Chisholm, S. W.: Copper toxicity and cyanobacteria ecology in the Sargasso Sea, Limnol. Oceanogr., 47(4), 976–988, doi:10.4319/lo.2002.47.4.0976, 2002.

Martin, J. H. and Fitzwater, S. E.: Iron deficiency limits phytoplankton growth in the north-east Pacific subarctic, Nature, 331(6154), 341–343, doi:10.1038/331341a0, 1988.

Martin, J. H., Fitzwater, S. E., Michael Gordon, R., Hunter, C. N. and Tanner, S. J.: Iron, primary production and carbon-nitrogen flux studies during the JGOFS North Atlantic bloom experiment, Deep. Res. Part II, 40(1–2), 115–134, doi:10.1016/0967-0645(93)90009-C, 1993.

Matrai, P. A. and Vetter, R. D.: Particulate thiols in coastal waters: The effect of light and nutrients on their planktonic production, Limnol. Oceanogr., 33(4), 624–631, doi:10.4319/lo.1988.33.4.0624, 1988.

Mcknight, D. M. and Morel, F. M. M.: Release of weak and strong copper-complexing agents by algae, Limnol. Oceanogr., 24(5), 823–837, doi:10.4319/lo.1979.24.5.0823, 1979.

Menzel Barraqueta, J. L., Schlosser, C., Planquette, H., Gourain, A., Cheize, M., Boutorh, J., Shelley, R., Contreira Pereira, L., Gledhill, M., Hopwood, M. J., Lacan, F., Lherminier, P., Sarthou, G. and Achterberg, E. P.: Aluminium in the north atlantic ocean and the Labrador Sea (GEOTRACES GA01 section): Roles of continental inputs and biogenic particle removal, Biogeosciences, 15(16), 5271–5286, doi:10.5194/bg-15-5271-2018, 2018.

Merchant, S. S., Allen, M. D., Kropat, J., Moseley, J. L., Long, J. C., Tottey, S. and Terauchi, A. M.: Between a rock and a hard place: Trace element nutrition in Chlamydomonas, Biochim. Biophys. Acta - Mol. Cell Res., 1763(7), 578–594, doi:10.1016/j.bbamcr.2006.04.007, 2006.

Metz, S. and Trefry, J. H.: Chemical and mineralogical influences on concentrations of trace metals in hydrothermal fluids, Geochim. Cosmochim. Acta, 64(13), 2267–2279, doi:10.1016/S0016-7037(00)00354-9, 2000.

Middag, R., de Baar, H. J. W., Laan, P., Cai, P. H. and van Ooijen, J. C.: Dissolved manganese in the Atlantic sector of the Southern Ocean, Deep. Res. Part II Top. Stud. Oceanogr., 58(25–26), 2661–2677, doi:10.1016/j.dsr2.2010.10.043, 2011.

Millero, F. J., Woosey R., Ditrolio B. and Water J.: Effect of Ocean acidification on the Speciation of Metals in Seawater, Oceanography, 22(4), 72–85 [online] Available from: http://tos.org/oceanography/assets/docs/22-4_millero.pdf, 2009.

Moffett, J. W.: Temporal and spatial variability of copper complexation by strong chelators in the Sargasso Sea, Deep Sea Res. Part I Oceanogr. Res. Pap., 42(8), 1273–1295, doi:10.1016/0967-0637(95)00060-J, 1995.

Moffett, J. W. and Brand, L. E.: Production of strong, extracellular Cu chelators by marine cyanobacteria in response to Cu stress, Limnol. Oceanogr., 41(3), 388–395, doi:10.4319/lo.1996.41.3.0388, 1996.

Moffett, J. W. and Dupont, C.: Cu complexation by organic ligands in the sub-arctic NW Pacific and Bering Sea, Deep. Res. Part I Oceanogr. Res. Pap., 54(4), 586–595, doi:10.1016/j.dsr.2006.12.013, 2007.

Moffett, J. W., Zika, R. G. and Brand, L. E.: Distribution and potential sources and sinks of copper chelators in the Sargasso Sea, Deep Sea Res. Part A, Oceanogr. Res. Pap., 37(1), 27–36, doi:10.1016/0198-0149(90)90027-S, 1990.

Moffett, J. W., Tuit, C. B. and Ward, B. B.: Chelator-induced inhibition of copper metalloenzymes in denitrifying bacteria, Limnol. Oceanogr., 57(1), 272–280, doi:10.4319/lo.2012.57.1.0272, 2012.

Moingt, M., Bressac, M., Bélanger, D. and Amyot, M.: Role of ultra-violet radiation, mercury and copper on the stability of dissolved glutathione in natural and artificial freshwater and saltwater, Chemosphere, 80(11), 1314–1320, doi:10.1016/j.chemosphere.2010.06.041, 2010.

Morel, F. M. M. M. and Price, N. M.: The biogeochemical cycles of trace metals in the oceans, Science (80-.)., 300(5621), 944–947, doi:10.1126/science.1083545, 2003.

Nelson, A. and Mantoura, R. F. C.: Voltammetry of copper species in estuarine waters, J. Electroanal. Chem. Interfacial Electrochem., 164(2), 237–252, doi:10.1016/S0022-0728(84)80209-0, 1984.

Nimmo, M. and Fones, G.: Application of adsorptive cathodic stripping voltammetry for the determination of Cu, Cd, Ni and Co in atmospheric samples, Anal. Chim. Acta, 291(3), 321–328, doi:10.1016/0003-2670(94)80027-8, 1994.

Noriki, S., Ishimori, N. and Tsunogai, S.: Regeneration of chemical elements from settling particles collected by sediment trap in Funka Bay, Japan, J. Oceanogr. Soc. Japan, 41(2), 113–120, doi:10.1007/BF02109181, 1985.

Nozaki, Y., Horibe, Y. and Tsubota, H.: The water column distributions of thorium isotopes in the western North Pacific, Earth Planet. Sci. Lett., 54(2), 203–216, doi:10.1016/0012-821X(81)90004-2, 1981.

Omanović, D., Garnier, C. and Pižeta, I.: ProMCC: An all-in-one tool for trace metal complexation studies, Mar. Chem., 173, 25–39, doi:10.1016/j.marchem.2014.10.011, 2015.

Panzeca, C., Beck, A. J., Leblanc, K., Taylor, G. T., Hutchins, D. A. and Sañudo-Wilhelmy, S. A.: Potential cobalt limitation of vitamin B12 synthesis in the North Atlantic Ocean, Global Biogeochem. Cycles, 22(2), 1–7, doi:10.1029/2007GB003124, 2008.

Paris, R. and Desboeufs, K. V.: Effect of atmospheric organic complexation on iron-bearing dust solubility, Atmos. Chem. Phys., 13(9), 4895–4905, doi:10.5194/acp-13-4895-2013, 2013.

Paris, R., Desboeufs, K. V. and Journet, E.: Variability of dust iron solubility in atmospheric waters: Investigation of the role of oxalate organic complexation, Atmos. Environ., 45(36), 6510–6517, doi:10.1016/j.atmosenv.2011.08.068, 2011.

Paytan, A., Mackey, K. R. M., Chen, Y., Lima, I. D., Doney, S. C., Mahowald, N., Labiosa, R. and Post, A. F.: Toxicity of atmospheric aerosols on marine phytoplankton., Proc. Natl. Acad. Sci. U. S. A., 106(12), 4601–4605, doi:10.1073/pnas.0811486106, 2009.

Peers, G. and Price, N. M.: Copper-containing plastocyanin used for electron transport by an oceanic diatom., Nature, 441(7091), 341–4, doi:10.1038/nature04630, 2006.

Peers, G., Quesnel, S. A. and Price, N. M.: Copper requirements for iron acquisition and growth of coastal and oceanic diatoms, Limnol. Oceanogr., 50(4), 1149–1158, doi:10.4319/lo.2005.50.4.1149, 2005.

Philippot, L.: Denitrifying genes in bacterial and Archaeal genomes, Biochim. Biophys. Acta - Gene Struct. Expr., 1577(3), 355–376, doi:10.1016/S0167-4781(02)00420-7, 2002.

Poorvin, L., Rinta-Kanto, J. M., Hutchins, D. A. and Wilhelm, S. W.: Viral release of iron and its bioavailability to marine plankton, Limnol. Oceanogr., 49(5), 1734–1741, doi:10.4319/lo.2004.49.5.1734, 2004.

Powell, R. T. and Wilson-Finelli, A.: Photochemical degradation of organic iron complexing ligands in seawater, Aquat. Sci., 65(4), 367–374, doi:10.1007/s00027-003-0679-0, 2003.

Pufahl, R., Singer, C., Peariso, K., Lin, S., Schmidt, P., Fahrni, C., Culotta, V., Penner-Hahn, J. and O'Halloran, T.: Metal Ion Chaperone Function of the Soluble Cu(I) Receptor Atx1, Science (80-.)., 278(5339), 853–856, doi:10.1126/science.278.5339.853, 1997.

Quigg, A., Reinfelder, J. R. and Fisher, N. S.: Copper uptake kinetics in diverse marine phytoplankton, Limnol. Oceanogr., 51(2), 893–899, doi:10.4319/lo.2006.51.2.0893, 2006.

Rae, T. D.: Undetectable Intracellular Free Copper: The Requirement of a Copper Chaperone for Superoxide Dismutase, Science (80-.)., 284(5415), 805–808, doi:10.1126/science.284.5415.805, 1999.

Rae, T. D., Schmidt, P. J., Pufahl, R. A., Culotta, V. C., Rae, T. D., Schmidt, P. J., Pufahl, R. A. and Culotta, V. C.: Undetectable Intracellular Free Copper: The Requirement of a Copper Chaperone for Superoxide Dismutase, Science (80-.)., 284(5415), 805–808, doi:10.1126/science.284.5415.805, 1999.

Rasmussen, B., Fletcher, I. R., Brocks, J. J. and Kilburn, M. R.: Reassessing the first appearance of eukaryotes and cyanobacteria., Nature, 455(7216), 1101–1104, doi:10.1038/nature07381, 2008.

Raven, J. A., Evans, M. C. W. and Korb, R. E.: The role of trace metals in photosynthetic electron transport in O-2-evolving organisms, Photosynth. Res., 60(2–3), 111–149, doi:10.1023/a:1006282714942, 1999.

Resing, J. A. and Mottl, M. J.: Determination of Manganese in Seawater Using Flow Injection Analysis with On-Line Preconcentration and Spectrophotometric Detection, Anal. Chem., 64(22), 2682–2687, doi:10.1021/ac00046a006, 1992.

Resing, J. A., Sedwick, P. N., German, C. R., Jenkins, W. J., Moffett, J. W., Sohst, B. M. and Tagliabue, A.: Basin-scale transport of hydrothermal dissolved metals across the South Pacific Ocean, Nature, 523(7559), 200–203, doi:10.1038/nature14577, 2015.

Richards, R., Chaloupka, M., Sano, M. and Tomlinson, R.: Modelling the effects of "coastal" acidification on copper speciation, Ecol. Modell., 222(19), 3559–3567, doi:10.1016/j.ecolmodel.2011.08.017, 2011.

Richon, C. and Tagliabue, A.: Insights into the Major Processes Driving the Global Distribution of Copper in the Ocean from a Global Model, Global Biogeochem. Cycles, doi:10.1029/2019gb006280, 2019.

Robinson, N. J., Procter, C. M., Connolly, E. L. and Guerinot, M. L.: A ferric-chelate reductase for iron uptake from soils., Nature, 397(6721), 694–697, doi:10.1038/17800, 1999.

Roshan, S. and Wu, J.: The distribution of dissolved copper in the tropical-subtropical north Atlantic across the GEOTRACES GA03 transect, Mar. Chem., 176(OCTOBER), 189–198, doi:10.1016/j.marchem.2015.09.006, 2015.

Roshan, S. and Wu, J.: Dissolved and colloidal copper in the tropical South Pacific, Geochim. Cosmochim. Acta, 233(May), 81–94, doi:10.1016/j.gca.2018.05.008, 2018.

Le Roy, E., Sanial, V., Charette, M. A., van Beek, P., Lacan, F., Jacquet, S. H. M., Henderson, P. B., Souhaut, M., García-Ibáñez, M. I., Jeandel, C., Pérez, F. F. and Sarthou, G.: The 226 Ra–Ba relationship in the North Atlantic during GEOTRACES-GA01, Biogeosciences, 15(9), 3027–3048, doi:10.5194/bg-15-3027-2018, 2018.

Rozan, T. F., Lassman, M. E., Ridge, D. P. and Luther, G. W.: Evidence for iron, copper and zinc complexation as multinuclear sulphide clusters in oxic rivers, Nature, 406(6798), 879–882, doi:10.1038/35022561, 2000.

Rue, E. and Bruland, K.: Domoic acid binds iron and copper: A possible role for the toxin produced by the marine diatom Pseudo-nitzschia, Mar. Chem., 76(1–2), 127–134, doi:10.1016/S0304-4203(01)00053-6, 2001.

Ružić, I.: Trace metal complexation at heterogeneous binding sites in aquatic systems, Mar. Chem., 53(1–2), 1–15, doi:10.1016/0304-4203(96)00008-4, 1996.

Saager, P. M., De Baar, H. J. W. W. and Howland, R. J.: Cd, Zn, Ni and Cu in the indian ocean, Deep Sea Res. Part A, Oceanogr. Res. Pap., 39(1), 9–35, doi:10.1016/0198-0149(92)90017-N, 1992.

Saager, P. M., De Baar, K. J. W., De Jong, J. T. M., Nolting, R. F. and Schijf, J.: Hydrography and local sources of dissolved trace metals Mn, Ni, Cu, and Cd in the northeast Atlantic Ocean, Mar. Chem., 57(3–4), 195–216, doi:10.1016/S0304-4203(97)00038-8, 1997.

Saito, M. A. and Moffett, J. W.: Temporal and spatial variability of cobalt in the Atlantic Ocean, Geochim. Cosmochim. Acta, 66(11), 1943–1953, doi:10.1016/S0016-7037(02)00829-3, 2002.

Saito, M. A., Moffett, J. W., Chisholm, S. W. and Waterbury, J. B.: Cobalt limitation and uptake in Prochlorococcus, Limnol. Oceanogr., 47(6), 1629–1636, doi:10.4319/lo.2002.47.6.1629, 2002.

Saito, M. A., Sigman, D. M. and Morel, F. M. M.: The bioinorganic chemistry of the ancient ocean: The co-evolution of cyanobacterial metal requirements and biogeochemical cycles at the Archean-Proterozoic boundary?, Inorganica Chim. Acta, 356, 308–318, doi:10.1016/S0020-1693(03)00442-0, 2003.

Sander, S. G. and Koschinsky, A.: Metal flux from hydrothermal vents increased by organic complexation, Nat. Geosci., 4(3), 145–150, doi:10.1038/ngeo1088, 2011.

Sander, S. G., Koschinsky, A., Hunter, K. a, Massoth, G. and Stott, M.: Evidence for organic complexation of copper in deep-sea hydrothermal vent systems Why are the continents just so ?, Goldschmidt Conf. Abstr., 70(4), 2555, doi:10.1128/AEM.70.4.2551, 2006.

Sanders, R., Brown, L., Henson, S. and Lucas, M.: New production in the Irminger Basin during 2002, J. Mar. Syst., 55(3–4), 291–310, doi:10.1016/j.jmarsys.2004.09.002, 2005.

Sanders, R., Henson, S. A., Koski, M., De La Rocha, C. L., Painter, S. C., Poulton, A. J., Riley, J., Salihoglu, B., Visser, A., Yool, A., Bellerby, R. and Martin, A. P.: The Biological Carbon Pump in the North Atlantic, Prog. Oceanogr., 129(PB), 200–218, doi:10.1016/j.pocean.2014.05.005, 2014.

Sarradin, P.-M., Waeles, M., Bernagout, S., Le Gall, C., Sarrazin, J. and Riso, R.: Speciation of dissolved copper within an active hydrothermal edifice on the Lucky Strike vent field (MAR, 37°N), Sci. Total Environ., 407(2), 869–878, doi:10.1016/j.scitotenv.2008.09.056, 2009.

Sato, M., Takeda, S. and Furuya, K.: Iron regeneration and organic iron(III)-binding ligand production during in situ zooplankton grazing experiment, Mar. Chem., 106(3–4), 471–488, doi:10.1016/j.marchem.2007.05.001, 2007.

Schlitzer, R., Anderson, R. F., Dodas, E. M., Lohan, M., Geibert, W., Tagliabue, A., Bowie, A., Jeandel, C., Maldonado, M. T., Landing, W. M., Cockwell, D., Abadie, C., Abouchami, W., Achterberg, E. P., Agather, A., Aguliar-Islas, A., van Aken, H. M., Andersen, M., Archer, C., Auro, M., de Baar, H. J., Baars, O., Baker, A. R., Bakker, K., Basak, C., Baskaran, M., Bates, N. R., Bauch, D., van Beek, P., Behrens, M. K., Black, E., Bluhm, K., Bopp, L., Bouman, H., Bowman, K., Bown, J., Boyd, P., Boye, M., Boyle, E. A., Branellec, P., Bridgestock, L., Brissebrat, G., Browning, T., Bruland, K. W., Brumsack, H. J., Brzezinski, M., Buck, C. S., Buck, K. N., Buesseler, K., Bull, A., Butler, E., Cai, P., Mor, P. C., Cardinal, D., Carlson, C., Carrasco, G., Casacuberta, N., Casciotti, K. L., Castrillejo, M., Chamizo, E., Chance, R., Charette, M. A., Chaves, J. E., Cheng, H., Chever, F., Christl, M., Church, T. M., Closset, I., Colman, A., Conway, T. M., Cossa, D., Croot, P., Cullen, J. T., Cutter, G. A., Daniels,

C., Dehairs, F., Deng, F., Dieu, H. T., Duggan, B., Dulaquais, G., Dumousseaud, C., Echegoyen-Sanz, Y., Edwards, R. L., Ellwood, M., Fahrbach, E., Fitzsimmons, J. N., Russell Flegal, A., Fleisher, M. Q., van de Flierdt, T., Frank, M., Friedrich, J., Fripiat, F., Fröllje, H., Galer, S. J. G., Gamo, T., Ganeshram, R. S., Garcia-Orellana, J., Garcia-Solsona, E., Gault-Ringold, M., et al.: The GEOTRACES Intermediate Data Product 2017, Chem. Geol., 493(June), 210–223, doi:10.1016/j.chemgeo.2018.05.040, 2018.

Scott, C., Lyons, T. W., Bekker, A., Shen, Y., Poulton, S. W., Chu, X. and Anbar, A. D.: Tracing the stepwise oxygenation of the Proterozoic ocean, Nature, 452(7186), 456–459, doi:10.1038/nature06811, 2008.

Seewald, J. S. and Seyfried, W. E.: The effect of temperature on metal mobility in subseafloor hydrothermal systems: constraints from basalt alteration experiments, Earth Planet. Sci. Lett., 101(2–4), 388–403, doi:10.1016/0012-821X(90)90168-W, 1990.

Semeniuk, D. M., Cullen, J. T., Johnson, W. K., Gagnon, K., Ruth, T. J. and Maldonado, M. T.: Plankton copper requirements and uptake in the subarctic Northeast Pacific Ocean, Deep. Res. Part I Oceanogr. Res. Pap., 56(7), 1130–1142, doi:10.1016/j.dsr.2009.03.003, 2009.

Semeniuk, D. M., Bundy, R. M., Payne, C. D., Barbeau, K. A. and Maldonado, M. T.: Acquisition of organically complexed copper by marine phytoplankton and bacteria in the northeast subarctic Pacific Ocean, Mar. Chem., 173, 222–233, doi:10.1016/j.marchem.2015.01.005, 2015.

Shank, G. C., Skrabal, S. A., Whitehead, R. F. and Kieber, R. J.: Fluxes of strong Cu-complexing ligands from sediments of an organic-rich estuary, Estuar. Coast. Shelf Sci., 60(2), 349–358, doi:10.1016/j.ecss.2004.01.010, 2004a.

Shank, G. C., Skrabal, S. A., Whitehead, R. F. and Kieber, R. J.: Strong copper complexation in an organic-rich estuary: The importance of allochthonous dissolved organic matter, Mar. Chem., 88(1–2), 21–39, doi:10.1016/j.marchem.2004.03.001, 2004b.

Shank, G. C., Whitehead, R. F., Smith, M. L., Skrabal, S. A. and Kieber, R. J.: Photodegradation of strong copper-complexing ligands in organic-rich estuarine waters, Limnol. Oceanogr., 51(2), 884–892, doi:10.4319/lo.2006.51.2.0884, 2006.

Shelley, R. U., Landing, W. M., Ussher, S. J., Planquette, H. and Sarthou, G.: Regional trends in the fractional solubility of Fe and other metals from North Atlantic aerosols (GEOTRACES cruises GA01 and GA03)

following a two-stage leach, Biogeosciences, 155194(1), 2271–2288, doi:10.5194/bg-15-2271-2018, 2018.

Sholkovitz, E. R., Sedwick, P. N. and Church, T. M.: On the fractional solubility of copper in marine aerosols: Toxicity of aeolian copper revisited, Geophys. Res. Lett., 37(20), 2–5, doi:10.1029/2010GL044817, 2010.

Simpson, A. J., Kingery, W. L., Hayes, M. H., Spraul, M., Humpfer, E., Dvortsak, P., Kerssebaum, R., Godejohann, M. and Hofmann, M.: Molecular structures and associations of humic substances in the terrestrial environment, Naturwissenschaften, 89(2), 84–88, doi:10.1007/s00114-001-0293-8, 2002.

Skrabal, S. A., Donat, J. R. and Burdige, D. J.: Fluxes of copper-complexing ligands from estuarine sediments, Limnol. Oceanogr., 42(5 I), 992–996, doi:10.4319/lo.1997.42.5.0992, 1997.

Skrabal, S. A., Lieseke, K. L. and Kieber, R. J.: Dissolved zinc and zinc-complexing ligands in an organic-rich estuary: Benthic fluxes and comparison with copper speciation, Mar. Chem., 100(1–2), 108–123, doi:10.1016/j.marchem.2005.12.004, 2006.

Spokes, L. J. and Jickells, T. D.: Factors controlling the solubility of aerosol trace metals in the atmosphere and on mixing into seawater, Aquat. Geochemistry, 1(4), 355–374, doi:10.1007/BF00702739, 1995.

Spokes, L. J., Campos, M. L. A. M. and Jickells, T. D.: The role of organic matter in controlling copper speciation in precipitation, Atmos. Environ., 30(23), 3959–3966, doi:10.1016/1352-2310(96)00125-2, 1996.

Stauber, J. L. and Florence, T. M.: Mechanism of toxicity of ionic copper and copper complexes to algae, Mar. Biol., 94(4), 511–519, doi:10.1007/BF00431397, 1987.

Stearman, R., Yuan, D. S., Yamaguchi-Iwai, Y., Klausner, R. D. and Dancis, A.: A Permease-Oxidase Complex Involved in High-Affinity Iron Uptake in Yeast, Science (80-.)., 271(5255), 1552–1557, doi:10.1126/science.271.5255.1552, 1996.

Styrt, M. M., Brackmann, A. J., Holland, H. D., Clark, B. C., Pisutha-Arnond, V., Eldridge, C. S. and Ohmoto, H.: The mineralogy and the isotopic composition of sulfur in hydrothermal sulfide/sulfate deposits on the East Pacific Rise, 21°N latitude, Earth Planet. Sci. Lett., 53(3), 382–390, doi:10.1016/0012-821X(81)90042-X, 1981.

Sunda, W.: The relationship between cupric ion activity and the toxicity of copper to phytoplankton, Massachusetts Institute of Technology and Woods Hole Oceanographic Institution, Woods Hole, MA., 1975.

Sunda, W. G. and Huntsman, S. A.: Effect of Competitive Interactions Between Manganese and Copper on Cellular Manganese and Growth in Estuarine and Oceanic Species of the Diatom Thalassiosira, Limnol. Oceanogr., 28(5), 924–934, doi:10.4319/lo.1983.28.5.0924, 1983.

Sunda, W. G. and Huntsman, S. A.: Cobalt and zinc interreplacement in marine phytoplankton: Biological and geochemical implications, Limnol. Oceanogr., 40(8), 1404–1417, doi:10.4319/lo.1995.40.8.1404, 1995a.

Sunda, W. G. and Huntsman, S. A.: Regulation of copper concentration in the oceanic nutricline by phytoplankton uptake and regeneration cycles, Limnol. Oceanogr., 40(1), 132–137, doi:10.4319/lo.1995.40.1.0132, 1995b.

Sunda, W. G., Tester, P. A. and Huntsman, S. A.: Effects of cupric and zinc ion activities on the survival and reproduction of marine copepods, Mar. Biol., 94(2), 203–210, doi:10.1007/BF00392932, 1987.

Sunda, W. G., Tester, P. A. and Huntsman, S. A.: Toxicity of trace metals to Acartia tonsa in the Elizabeth River and southern Chesapeake Bay, Estuar. Coast. Shelf Sci., 30(3), 207–221, doi:10.1016/0272-7714(90)90048-V, 1990.

Tagliabue, A.: Elemental Distribution: Overview, in Encyclopedia of Ocean Sciences, vol. 2010, pp. 122–127, Elsevier., 2019.

Tagliabue, A., Bopp, L., Dutay, J. C., Bowie, A. R., Chever, F., Jean-Baptiste, P., Bucciarelli, E., Lannuzel, D., Remenyi, T., Sarthou, G., Aumont, O., Gehlen, M. and Jeandel, C.: Hydrothermal contribution to the oceanic dissolved iron inventory, Nat. Geosci., 3(4), 252–256, doi:10.1038/ngeo818, 2010.

Tagliabue, A., Williams, R. G., Rogan, N., Achterberg, E. P. and Boyd, P. W.: A ventilation-based framework to explain the regeneration-scavenging balance of iron in the ocean, Geophys. Res. Lett., 41(20), 7227–7236, doi:10.1002/2014GL061066, 2014.

Tagliabue, A., Bowie, A. R., Boyd, P. W., Buck, K. N., Johnson, K. S. and Saito, M. A.: The integral role of iron in ocean biogeochemistry, Nature, 543(7643), 51–59, doi:10.1038/nature21058, 2017.

Tagliabue, A., Bowie, A. R., DeVries, T., Ellwood, M. J., Landing, W. M., Milne, A., Ohnemus, D. C., Twining, B. S. and Boyd, P. W.: The interplay between regeneration and scavenging fluxes drives ocean iron cycling, Nat. Commun., 10(1), 1–8, doi:10.1038/s41467-019-12775-5, 2019.

Takano, S., Tanimizu, M., Hirata, T. and Sohrin, Y.: Isotopic constraints on biogeochemical cycling of copper in the ocean, Nat. Commun., 5(5663), 5663, doi:10.1038/ncomms6663, 2014.

Tang, D., Hung, C.-C., Warnken, K. W. and Santschi, P. H.: The distribution of biogenic thiols in surface waters of Galveston Bay, Limnol. Oceanogr., 45(6), 1289–1297, doi:10.4319/lo.2000.45.6.1289, 2000.

Taylor, S. . and McLennan, S. .: The geochemical evolution of the continental crust, Rev. Geophys., 33(2), 241–265, doi:10.1029/95RG00262, 1995.

Thompson, C. M. M., Ellwood, M. J. J. and Sander, S. G. G.: Dissolved copper speciation in the Tasman Sea, SW Pacific Ocean, Mar. Chem., 164, 84–94, doi:10.1016/j.marchem.2014.06.003, 2014.

Tottey, S., Waldron, K. J., Firbank, S. J., Reale, B., Bessant, C., Sato, K., Cheek, T. R., Gray, J., Banfield, M. J., Dennison, C. and Robinson, N. J.: Protein-folding location can regulate manganese-binding versus copper- or zinc-binding, Nature, 455(7216), 1138–1142, doi:10.1038/nature07340, 2008.

Trefry, J. H., Trocine, R. P., Klinkhammer, G. P. and Rona, P. A.: Iron and copper enrichment of suspended particles in dispersed hydrothermal plumes along the mid-Atlantic Ridge, Geophys. Res. Lett., 12(8), 506–509, doi:10.1029/GL012i008p00506, 1985.

Trimble, S. M., Baskaran, M. and Porcelli, D.: Scavenging of thorium isotopes in the Canada Basin of the Arctic Ocean, Earth Planet. Sci. Lett., 222(3–4), 915–932, doi:10.1016/j.epsl.2004.03.027, 2004.

Tuerena, R. E., Williams, R. G., Mahaffey, C., Vic, C., Green, J. A. M., Naveira-Garabato, A., Forryan, A. and Sharples, J.: Internal Tides Drive Nutrient Fluxes Into the Deep Chlorophyll Maximum Over Mid-ocean Ridges, Global Biogeochem. Cycles, 33(8), 995–1009, doi:10.1029/2019gb006214, 2019.

Twining, B. S. and Baines, S. B.: The Trace Metal Composition of Marine Phytoplankton, Ann. Rev. Mar. Sci., 5(1), 191–215, doi:10.1146/annurev-marine-121211-172322, 2013.

Twining, B. S., Baines, S. B., Fisher, N. S., Maser, J., Vogt, S., Jacobsen, C., Tovar-Sanchez, A. and Sañudo-Wilhelmy, S. A.: Quantifying trace elements in individual aquatic protist cells with a synchrotron X-ray fluorescence microprobe, Anal. Chem., 75(15), 3806–3816, doi:10.1021/ac034227z, 2003.

Twining, B. S., Rauschenberg, S., Morton, P. L. and Vogt, S.: Metal contents of phytoplankton and labile particulate material in the North Atlantic Ocean, Prog. Oceanogr., 137, 261–283, doi:10.1016/j.pocean.2015.07.001, 2015.

Twining, B. S., Rauschenberg, S., Baer, S. E., Lomas, M. W., Martiny, A. C. and Antipova, O.: A nutrient limitation mosaic in the eastern tropical Indian Ocean, Deep. Res. Part II Top. Stud. Oceanogr., 166(May), 125–140, doi:10.1016/j.ds.2019.05.001, 2019.

Valentine, J. S.: BIOCHEMISTRY: Enhanced: Delivering Copper Inside Yeast and Human Cells, Science (80-.)., 278(5339), 817–818, doi:10.1126/science.278.5339.817, 1997.

van den Berg, C. M. G.: Determination of copper complexation with natural organic ligands in seawater by equilibration with MnO2 II. Experimental procedures and application to surface seawater, Mar. Chem., 11(4), 323–342, doi:10.1016/0304-4203(82)90029-9, 1982.

van den Berg, C. M. G., Merks, A. G. A. and Duursma, E. K.: Organic complexation and its control of the dissolved concentrations of copper and zinc in the Scheldt estuary, Estuar. Coast. Shelf Sci., 24(6), 785–797, doi:10.1016/0272-7714(87)90152-1, 1987.

Völker, C. and Tagliabue, A.: Modeling organic iron-binding ligands in a three-dimensional biogeochemical ocean model, Mar. Chem., 173, 67–77, doi:10.1016/j.marchem.2014.11.008, 2015.

Waeles, M., Riso, R. D., Maguer, J. F. and Le Corre, P.: Distribution and chemical speciation of dissolved cadmium and copper in the Loire estuary and North Biscay continental shelf, France, Estuar. Coast. Shelf Sci., 59(1), 49–57, doi:10.1016/j.ecss.2003.07.009, 2004.

Waeles, M., Riso, R. D., Corre, P. Le and Le Corre, P.: Seasonal variations of dissolved and particulate copper species in estuarine waters, Estuar. Coast. Shelf Sci., 62(1–2), 313–323, doi:10.1016/j.ecss.2004.09.019, 2005.

Waeles, M., Riso, R., Pernet-Coudrier, B., Quentel, F., Durrieu, G. and Tissot, C.: Annual cycle of humic substances in a temperate estuarine system affected by agricultural practices, Geochim. Cosmochim. Acta, 106, 231–246, doi:10.1016/j.gca.2012.12.040, 2013.

Waeles, M., Tanguy, V. and Riso, R. D.: On the control of copper colloidal distribution by humic substances in the Penzé estuary, Chemosphere, 119, 1176–1184, doi:10.1016/j.chemosphere.2014.09.107, 2015.

Walker, C. B., de la Torre, J. R., Klotz, M. G., Urakawa, H., Pinel, N., Arp, D. J., Brochier-Armanet, C., Chain, P. S. G. G., Chan, P. P., Gollabgir, A., Hemp, J., Hügler, M., Karr, E. A., Könneke, M., Shin, M., Lawton, T. J., Lowe, T., Martens-Habbena, W., Sayavedra-Soto, L. A., Lang, D., Sievert, S. M., Rosenzweig, A. C., Manning, G. and Stahl, D. A.: Nitrosopumilus maritimus genome reveals unique mechanisms for nitrification and autotrophy in globally distributed marine crenarchaea, Proc. Natl. Acad. Sci. U. S. A., 107(19), 8818–8823, doi:10.1073/pnas.0913533107, 2010.

Waterhouse, A. F., MacKinnon, J. A., Nash, J. D., Alford, M. H., Kunze, E., Simmons, H. L., Polzin, K. L., St. Laurent, L. C., Sun, O. M., Pinkel, R., Talley, L. D., Whalen, C. B., Huussen, T. N., Carter, G. S., Fer, I., Waterman, S., Naveira Garabato, A. C., Sanford, T. B. and Lee, C. M.: Global Patterns of Diapycnal Mixing from Measurements of the Turbulent Dissipation Rate, J. Phys. Oceanogr., 44(7), 1854–1872, doi:10.1175/JPO-D-13-0104.1, 2014.

Wei, L. and Ahner, B. a.: Sources and sinks of dissolved phytochelatin in natural seawater, Limnol. Oceanogr., 50(1), 13–22, doi:10.4319/lo.2005.50.1.0013, 2005.

Wells, M. L., Trick, C. G., Cochlan, W. P., Hughes, M. P. and Trainer, V. L.: Domoic acid: The synergy of iron, copper, and the toxicity of diatoms, Limnol. Oceanogr., 50(6), 1908–1917, doi:10.4319/lo.2005.50.6.1908, 2005.

Whitby, H. and van den Berg, C. M. G. G.: Evidence for copper-binding humic substances in seawater, Mar. Chem., 173, 282–290, doi:10.1016/j.marchem.2014.09.011, 2015.

Whitby, H., Posacka, A. M., Maldonado, M. T. and van den Berg, C. M. G.: Copper-binding ligands in the NE Pacific, Mar. Chem., 204(January), 36–48, doi:10.1016/j.marchem.2018.05.008, 2018.

Willey, J. D., Kieber, R. J., Seaton, P. J. and Miller, C.: Rainwater as a source of Fe(II)-stabilizing ligands to seawater, Limnol. Oceanogr., 53(4), 1678–1684, doi:10.4319/lo.2008.53.4.1678, 2008.

Witter, A. E., Hutchins, D. A., Butler, A. and Luther, G. W.: Determination of conditional stability constants and kinetic constants for strong model Fe-binding ligands in seawater, Mar. Chem., 69(1–2), 1–17, doi:10.1016/S0304-4203(99)00087-0, 2000.

Wozniak, A. S., Shelley, R. U., Sleighter, R. L., Abdulla, H. A. N., Morton, P. L., Landing, W. M. and Hatcher, P. G.: Relationships among aerosol water soluble organic matter, iron and aluminum in European, North

African, and Marine air masses from the 2010 US GEOTRACES cruise, Mar. Chem., 154(July), 24–33, doi:10.1016/j.marchem.2013.04.011, 2013.

Wozniak, A. S., Shelley, R. U., McElhenie, S. D., Landing, W. M. and Hatcher, P. G.: Aerosol water soluble organic matter characteristics over the North Atlantic Ocean: Implications for iron-binding ligands and iron solubility, Mar. Chem., 173, 162–172, doi:10.1016/j.marchem.2014.11.002, 2015.

Yang, R. and van den Berg, C. M. G.: Metal Complexation by Humic Substances in Seawater, Environ. Sci. Technol., 43(19), 7192–7197, doi:10.1021/es900173w, 2009.

Yeats, P. A. and Campbell, J. A.: Nickel, copper, cadmium and zinc in the northwest Atlantic Ocean, Mar. Chem., 12(1), 43–58, doi:10.1016/0304-4203(83)90027-0, 1983.

Zhu, S. H., Guo, J., Maldonado, M. T. and Green, B. R.: Effects of iron and copper deficiency on the expression of members of the light-harvesting family in the diatom Thalassiosira pseudonana (bacillariophyceae), J. Phycol., 46(5), 974–981, doi:10.1111/j.1529-8817.2010.00884.x, 2010.

Appendix

Appendix 1: DCu, PCu, Cu^{2+}, ligands concentrations and stability constant at all stations of GEOVIDE. Errors of DCu and PCu are the standard deviation of measurements. Errors of speciation parameters are the analysis of titrations errors.

Station [#]	LATITUDE [°N]	LONGITUDE [°E]	Pressure [db]	DCu [nM]	error [nM]	L [nM]	error [nM]	Log K	error	Cu^{2+} [fM]	PCu [nM]	error [pM]
1	40.33	-10.04	3578.50	1.97	0.34						66.01	6.41
1	40.33	-10.04	3250.20	2.67	0.37						14.17	2.56
1	40.33	-10.04	3001.30	2.20	0.43						5.88	2.49
1	40.33	-10.04	2500.10	1.44	0.08							
1	40.33	-10.04	2000.60	1.41	0.20	2.85	0.31	13.20	0.13	61.71		
1	40.33	-10.04	1799.90	1.76	0.25	3.24	0.33	13.22	0.12	71.05		
1	40.33	-10.04	1600.20	1.62	0.23	2.16	0.21	13.55	0.18	82.96	6.42	2.25
1	40.33	-10.04	1399.70	1.62	0.23	3.50	0.21	13.25	0.08	47.89		
1	40.33	-10.04	1197.70	1.22	0.17						46.83	4.14
1	40.33	-10.04	1000.20	1.76	0.25	3.85	0.53	12.61	0.16	206.34		
1	40.33	-10.04	898.00	1.49	0.21	3.44	0.14	13.39	0.17	30.95	6.07	3.96
1	40.33	-10.04	799.70	1.35	0.19	1.36	0.22	13.41	0.31	1706.47	12.81	1.65
1	40.33	-10.04	699.60	1.37	0.19							
1	40.33	-10.04	594.70	1.52	0.21	2.37	0.50	13.03	0.24	164.52	13.67	1.88
1	40.33	-10.04	506.00	1.43	0.20	4.25	0.17	13.33	0.13	23.54	28.50	3.29
1	40.33	-10.04	390.00	1.43	0.20						16.37	2.19
1	40.33	-10.04	302.80	0.90	0.13	3.32	0.18	13.14	0.13	27.00	5.80	1.05
1	40.33	-10.04	202.50	0.78	0.11	3.10	0.20	13.14	0.18	24.19		
1	40.33	-10.04	152.20	0.87	0.12	3.22	0.11	13.14	0.08	27.07	8.93	1.03
1	40.33	-10.04	102.50	0.96	0.13						12.33	1.42
1	40.33	-10.04	81.40	0.87	0.12	2.75	0.13	13.18	0.14	30.67		
1	40.33	-10.04	60.40	0.93	0.13	3.33	0.20	13.20	0.16	24.18		
1	40.33	-10.04	21.00	1.10	0.32							
2	40.33	-9.46	138.10	0.62	0.02						220.06	24.65
2	40.33	-9.46	120.30	0.61	0.02						24.43	2.83
2	40.33	-9.46	99.90	0.68	0.03						14.66	1.64
2	40.33	-9.46	75.60	0.69	0.03						25.67	2.53
2	40.33	-9.46	50.60	0.81	0.03						20.93	1.62
2	40.33	-9.46	36.90	0.63	0.03						18.55	2.12
2	40.33	-9.46	19.40	0.77	0.03						35.02	3.71
4	40.33	-9.77	800.00	1.00	0.16						20.26	2.76
4	40.33	-9.77	700.90	1.04	0.02						15.37	1.97
4	40.33	-9.77	601.30	0.98	0.02						17.16	2.22
4	40.33	-9.77	500.10	0.92	0.11						21.28	2.27
4	40.33	-9.77	401.70	0.81	0.03						19.70	2.40
4	40.33	-9.77	302.40	0.90	0.04						19.37	2.58
4	40.33	-9.77	201.30	0.77	0.03						14.43	1.60
4	40.33	-9.77	150.30	0.77	0.03						14.48	1.78
4	40.33	-9.77	72.00	0.81	0.03						9.84	1.21
4	40.33	-9.77	39.70	0.72	0.03						6.83	0.92
4	40.33	-9.77	21.30	1.09	0.04						0.00	0.97
11	40.33	-12.22	5347.90	1.84	0.09						53.46	4.15
11	40.33	-12.22	4999.40	2.66	0.13							
11	40.33	-12.22	4000.70	2.47	0.12						8.61	1.23
11	40.33	-12.22	3500.20	2.28	0.11						0.00	
11	40.33	-12.22	2998.00	0.16	0.23						7.30	1.13
11	40.33	-12.22	2500.10	1.82	0.09							
11	40.33	-12.22	2000.40	1.04	0.05						189.91	17.06
11	40.33	-12.22	1801.00	1.56	0.07							
11	40.33	-12.22	1600.20	1.55	0.07							
11	40.33	-12.22	1200.90	1.30	0.06							
11	40.33	-12.22	1001.10	1.06	0.05						7.03	1.35
11	40.33	-12.22	800.40	1.26	0.06						5.26	0.75
11	40.33	-12.22	701.20	1.15	0.05						7.26	1.20
11	40.33	-12.22	501.10	1.21	0.06						16.59	2.06

11	40.33	-12.22	200.50	1.04	0.05						6.66	0.95
11	40.33	-12.22	101.00	0.96	0.05						9.59	1.01
11	40.33	-12.22	80.40	0.98	0.05						22.40	1.99
11	40.33	-12.22	54.00	0.92	0.04							
11	40.33	-12.22	25.40	0.83	0.12						12.07	1.70
11	40.33	-12.22	14.90	0.11	0.01						17.31	2.02
13	41.38	-13.89	5436.90	2.72	0.20	5.14	0.85	12.74	0.15	204.01	61.44	4.89
13	41.38	-13.89	4999.40	3.05	0.18	7.47	1.04	12.67	0.11	146.06	13.29	5.26
13	41.38	-13.89	4001.20	2.67	0.15	4.86	0.63	12.93	0.13	141.51	16.57	1.94
			3500.00	2.56	0.11	2.66	0.38	13.36	0.30	978.09	18.16	2.30
13	41.38	-13.89	2501.40	1.52	0.14	2.81	0.43	13.03	0.17	108.29	27.03	2.92
13	41.38	-13.89	1999.90	0.83	0.05						22.71	2.61
13	41.38	-13.89	1500.60	0.81	0.06	3.08	0.20	13.31	0.24	17.66	49.52	4.00
13	41.38	-13.89	1201.10	1.51	0.12	3.23	0.18	13.20	0.16	55.63	19.12	2.59
13	41.38	-13.89	1000.60	1.44	0.15	3.79	0.16	13.12	0.10	46.95	16.55	2.19
13	41.38	-13.89	800.30								27.70	2.89
13	41.38	-13.89	601.20	0.94	0.03	4.78	0.58	12.81	0.15		26.01	2.74
13	41.38	-13.89	500.60	0.90	0.11	8.28	1.66	12.54	0.12	34.90	26.97	3.70
13	41.38	-13.89	400.60	1.10	0.13	5.75	1.68	12.87	0.21	32.15		
13	41.38	-13.89	300.60	1.08	0.13	5.08	0.78	12.84	0.11	39.11	16.94	2.55
13	41.38	-13.89	201.00	1.23	0.14	4.33	0.48	13.02	0.09	37.71	21.38	2.42
13	41.38	-13.89	150.80	0.95	0.11	3.27	0.76	12.83	0.18	60.59	25.79	2.59
13	41.38	-13.89	101.00	0.87	0.10	1.69	0.39	13.03	0.23	99.21	45.84	4.06
13	41.38	-13.89	75.40	0.90	0.11	2.34	0.62	12.92	0.24	75.27	31.41	2.78
13	41.38	-13.89	51.20	0.82	0.10	2.06	0.47	12.84	0.19	96.39	25.87	2.51
13	41.38	-13.89	30.70	0.94	0.11	2.89	0.95	12.94	0.29	55.63		
13	41.38	-13.89	11.10	0.82	0.10	1.51	0.38	12.95	0.26	134.06	17.18	2.11
15	42.58	-15.46	5120.80	2.09	0.12						46.30	4.91
15	42.58	-15.46	5000.50	2.54	0.15						11.46	1.77
15	42.58	-15.46	4001.00	2.35	0.14						16.80	2.28
15	42.58	-15.46	3000.60	2.11	0.12						21.50	2.26
15	42.58	-15.46	2500.60	1.97	0.11						13.56	1.48
15	42.58	-15.46	2000.50	1.39	0.08						15.98	1.97
15	42.58	-15.46	1800.50	1.02	0.06						61.73	5.21
15	42.58	-15.46	1600.20	1.49	0.09							
15	42.58	-15.46	1399.60	1.43	0.08						9.76	1.17
15	42.58	-15.46	1100.50	1.24	0.07						33.12	2.87
15	42.58	-15.46	999.60	1.33	0.08						13.81	1.77
15	42.58	-15.46	800.40	1.09	0.06						13.14	2.06
15	42.58	-15.46	650.50	1.33	0.08						18.56	2.15
15	42.58	-15.46	500.80	1.20	0.07							
15	42.58	-15.46	400.30	1.06	0.06						17.48	2.22
15	42.58	-15.46	300.10	1.12	0.06						24.93	2.99
15	42.58	-15.46	100.10	1.01	0.06						24.53	2.97
15	42.58	-15.46	70.50	0.94	0.05						33.96	3.84
15	42.58	-15.46	60.30	1.03	0.06						24.57	3.03
15	42.58	-15.46	49.80	1.01	0.06						24.61	2.73
15	42.58	-15.46	29.90	0.88	0.05						36.67	3.49
15	42.58	-15.46	19.90	1.20	0.07						29.14	2.87
17	43.78	-17.03	4061.70								48.80	4.96
17	43.78	-17.03	3500.50	3.52	0.17						13.51	1.47
17	43.78	-17.03	3000.10	3.63	0.17						12.63	1.53
17	43.78	-17.03	2500.00	2.91	0.14						12.24	1.77
17	43.78	-17.03	2001.10								9.61	1.26
17	43.78	-17.03	1800.50								10.02	1.26
17	43.78	-17.03	1600.30	2.94	0.14						47.26	4.32
17	43.78	-17.03	1400.50	3.25	0.15						8.69	1.12
17	43.78	-17.03	1200.60	2.84	0.14						10.37	1.23
17	43.78	-17.03	1000.30	2.09	0.10						17.23	1.96
17	43.78	-17.03	799.90	2.56	0.12						13.29	2.00
17	43.78	-17.03	600.40	2.94	0.14						18.83	2.25
17	43.78	-17.03	500.30	2.31	0.11						11.88	1.85
17	43.78	-17.03	399.20	1.96	0.09						16.50	1.83
17	43.78	-17.03	351.20	2.22	0.11						13.67	1.61
17	43.78	-17.03	200.30	1.84	0.09						12.81	2.42
17	43.78	-17.03	100.00	2.09	0.10						11.14	1.52
17	43.78	-17.03	69.60	1.92	0.09						16.21	1.56
17	43.78	-17.03	60.80	1.62	0.08						28.30	2.91
17	43.78	-17.03	44.70	2.62	0.12						22.04	2.60
17	43.78	-17.03	30.20	2.21	0.11						29.64	3.58
17	43.78	-17.03	14.80	1.31	0.06						36.25	3.74
19	45.05	-18.51	4625.00	3.66	0.21						47.40	3.16
19	45.05	-18.51	3999.20	3.96	0.24						12.89	1.54
19	45.05	-18.51	3000.80	3.65	0.21						12.42	3.52
19	45.05	-18.51	2500.80	2.99	0.17						7.71	0.90
19	45.05	-18.51	2250.80	2.04	0.12							
19	45.05	-18.51	2000.70	1.96	0.11							

19	45.05	-18.51	1801.30	1.56	0.09						58.99	6.08
19	45.05	-18.51	1601.20	1.96	0.11						11.81	1.56
19	45.05	-18.51	1402.50	1.60	0.09						12.38	1.73
19	45.05	-18.51	1200.90	1.68	0.09						19.71	1.64
19	45.05	-18.51	1001.20	1.69	0.10						16.05	1.78
19	45.05	-18.51	800.80	1.68	0.10						15.57	1.86
19	45.05	-18.51	600.60	1.65	0.10						11.10	1.73
19	45.05	-18.51	500.40	1.54	0.09						14.02	1.55
19	45.05	-18.51	400.80	1.47	0.09						15.67	1.98
19	45.05	-18.51	300.90	1.56	0.09						15.51	2.07
19	45.05	-18.51	201.30	1.39	0.08						15.66	2.00
19	45.05	-18.51	100.30	1.47	0.09						24.72	2.65
19	45.05	-18.51	50.70	1.31	0.08						25.51	2.68
19	45.05	-18.51	40.70	1.29	0.07						23.05	2.61
19	45.05	-18.51	30.40	1.39	0.08						27.55	3.20
19	45.05	-18.51	20.50	1.63	0.09						11.29	1.59
21	46.54	-19.67	4592.00	3.26	0.13	6.43	0.82	12.92	0.13	123.41	42.52	3.66
21	46.54	-19.67	4500.40	4.98	0.20	6.49	0.23	13.53	0.08	96.10	23.68	3.35
21	46.54	-19.67	3499.40	3.36	0.14	5.16	0.55	13.47	0.18	62.58	17.66	2.44
21	46.54	-19.67	3000.40	2.29	0.09	4.43	0.48	13.38	0.14	44.00	16.08	2.57
21	46.54	-19.67	2800.20	1.93	0.08	3.54	0.37	13.46	0.16	41.12	31.32	3.30
21	46.54	-19.67	2300.20	2.05	0.08	5.60	0.77	13.22	0.14	34.88	17.89	2.48
21	46.54	-19.67	2001.60	1.55	0.06	3.36	0.44	13.35	0.16	37.96	42.15	4.03
21	46.54	-19.67	1500.00	1.97	0.08	4.22	0.40	13.35	0.11	38.69	23.30	2.80
21	46.54	-19.67	1250.40	1.70	0.07	3.05	0.27	13.43	0.13	46.32	18.94	2.14
21	46.54	-19.67	999.90	1.67	0.07	3.68	0.44	13.27	0.14	44.07	19.69	2.26
21	46.54	-19.67	799.80	1.77	0.07	3.75	0.41	13.40	0.13	35.11	21.28	2.56
21	46.54	-19.67	700.40	1.29	0.05	2.82	0.28	13.09	0.10	67.95	58.68	6.32
21	46.54	-19.67	599.50	1.25	0.05	2.92	0.35	13.23	0.13	43.61	23.38	2.62
21	46.54	-19.67	500.50	1.43	0.06	4.09	0.35	13.08	0.08	44.72	14.10	1.64
21	46.54	-19.67	400.40	1.27	0.05	2.51	0.28	13.49	0.15	32.69	26.14	2.39
21	46.54	-19.67	299.90	1.26	0.05	3.02	0.41	13.18	0.15	46.95	28.88	2.86
21	46.54	-19.67	200.00	1.56	0.06	3.15	0.41	13.39	0.18	39.46	21.27	2.60
21	46.54	-19.67	99.80	1.17	0.05	3.57	0.54	12.93	0.14	56.58	44.35	3.87
21	46.54	-19.67	79.80	1.26	0.05	3.24	0.48	13.05	0.14	56.09	32.91	3.02
21	46.54	-19.67	49.30	1.30	0.05	2.32	0.31	13.26	0.17	69.34	33.00	3.04
21	46.54	-19.67	29.90	1.14	0.05	2.49	0.44	13.01	0.17	82.22	43.09	3.81
21	46.54	-19.67	19.20	0.91	0.04						37.99	4.09
23	48.04	-20.85	4526.90	2.60	0.11							
23	48.04	-20.85	4000.20	2.76	0.11						14.89	1.84
23	48.04	-20.85	3500.50	2.91	0.12						13.91	1.92
23	48.04	-20.85	3000.00	2.63	0.11						12.58	1.70
23	48.04	-20.85	2300.40	1.50	0.06						49.55	4.53
23	48.04	-20.85	2000.10	0.01	0.00						14.07	2.12
23	48.04	-20.85	1800.80	1.70	0.07						19.32	2.23
23	48.04	-20.85	1601.00	1.93	0.08						16.57	2.14
23	48.04	-20.85	1400.90	1.68	0.07						19.70	2.63
23	48.04	-20.85	1200.70	0.01	0.00						15.78	2.13
23	48.04	-20.85	799.80	1.49	0.06						16.02	2.24
23	48.04	-20.85	600.00	1.51	0.06							
23	48.04	-20.85	400.30	1.49	0.06						12.76	1.46
23	48.04	-20.85	200.30	1.40	0.06						13.10	1.76
23	48.04	-20.85	100.50	1.37	0.06						36.71	5.62
23	48.04	-20.85	70.10	1.31	0.05						32.05	2.87
23	48.04	-20.85	60.10	1.23	0.05						43.79	3.67
23	48.04	-20.85	50.10	1.17	0.05							
23	48.04	-20.85	40.10	1.19	0.05						46.51	4.61
23	48.04	-20.85	29.60	1.27	0.05						75.43	8.99
23	48.04	-20.85	20.10	1.22	0.05						71.62	7.93
25	49.53	-22.02	4269.50	3.27	0.11						57.23	4.79
25	49.53	-22.02	4001.00	3.33	0.11						31.17	3.56
25	49.53	-22.02	3499.80	2.81	0.10						20.76	2.40
25	49.53	-22.02	3001.70	2.14	0.07						15.69	2.19
25	49.53	-22.02	2601.20	1.68	0.06						38.11	3.59
25	49.53	-22.02	2000.80	1.75	0.06						13.32	1.81
25	49.53	-22.02	1800.90	1.40	0.05						38.47	3.35
25	49.53	-22.02	1599.40	1.92	0.07						15.70	2.35
25	49.53	-22.02	1402.30	1.73	0.06						17.23	1.98
25	49.53	-22.02	1200.40	1.56	0.05						18.29	2.46
25	49.53	-22.02	1001.00	1.76	0.06						17.37	2.12
25	49.53	-22.02	800.20	1.56	0.05						15.04	1.83
25	49.53	-22.02	650.00	1.41	0.05						12.63	1.53
25	49.53	-22.02	499.60	1.56	0.05						10.55	1.33
25	49.53	-22.02	349.30	1.26	0.04						0.00	0.61
25	49.53	-22.02	200.10	1.54	0.05						9.74	1.16
25	49.53	-22.02	100.30	1.26	0.04						12.47	2.26
25	49.53	-22.02	74.60	1.34	0.05						34.18	3.17

25	49.53	-22.02	49.30	1.24	0.04						36.61	2.92
25	49.53	-22.02	35.10	0.00	0.00						31.08	3.23
25	49.53	-22.02	25.30	1.16	0.04						55.42	5.34
25	49.53	-22.02	14.20	1.40	0.05						43.69	6.22
26	50.28	-22.60	4192.20	2.28	0.02						117.62	10.19
26	50.28	-22.60	4000.30	2.57	0.02							
26	50.28	-22.60	2999.70	1.74	0.01						11.67	1.30
26	50.28	-22.60	2299.90	1.51	0.01						10.63	1.56
26	50.28	-22.60	2000.30	1.23	0.01						30.79	1.80
26	50.28	-22.60	1599.80	1.26	0.01						15.95	2.29
26	50.28	-22.60	1400.30	1.02	0.01						39.07	3.02
26	50.28	-22.60	1200.10	1.41	0.01						18.99	2.12
26	50.28	-22.60	1000.40	1.28	0.01						15.02	1.75
26	50.28	-22.60	900.70	1.33	0.01						17.29	1.92
26	50.28	-22.60	749.70	1.31	0.01						17.03	2.01
26	50.28	-22.60	600.10	1.25	0.01						15.74	1.67
26	50.28	-22.60	500.50	1.12	0.13						13.06	1.79
26	50.28	-22.60	400.00	1.05	0.12						11.33	1.66
26	50.28	-22.60	300.00	1.16	0.04						9.22	1.10
26	50.28	-22.60	200.70	1.39	0.01						21.52	1.95
26	50.28	-22.60	151.00	1.33	0.01						8.49	1.10
26	50.28	-22.60	98.20	1.31	0.01						14.98	1.23
26	50.28	-22.60	70.00	1.17	0.04							
26	50.28	-22.60	50.20	1.23	0.01						47.43	4.35
26	50.28	-22.60	34.70	1.23	0.01						42.83	3.38
26	50.28	-22.60	20.20	1.28	0.01						54.67	4.78
29	53.02	-24.75	3584.00	2.32	0.01						74.87	7.82
29	53.02	-24.75	3000.10	1.80	0.00						14.05	1.59
29	53.02	-24.75	2501.00	1.53	0.02						14.45	1.81
29	53.02	-24.75	1999.90	1.40	0.03						15.99	1.80
29	53.02	-24.75	1800.00	1.38	0.03						28.54	2.53
29	53.02	-24.75	1601.30	1.43	0.01						19.98	2.19
29	53.02	-24.75	1399.40	1.38	0.04						44.85	3.76
29	53.02	-24.75	1199.10	1.48	0.00						18.45	2.44
29	53.02	-24.75	1099.50	1.40	0.01						17.94	2.00
29	53.02	-24.75	899.70	1.38	0.01						19.01	2.29
29	53.02	-24.75	799.10	1.28	0.01						29.16	3.67
29	53.02	-24.75	599.70								20.44	2.16
29	53.02	-24.75	500.20	1.27	0.01						17.87	2.07
29	53.02	-24.75	401.40	1.26	0.01						17.70	2.00
29	53.02	-24.75	300.80	1.37	0.01						24.86	2.29
29	53.02	-24.75	200.30	1.18	0.01						12.52	1.44
29	53.02	-24.75	150.40	1.19	0.01						22.51	1.86
29	53.02	-24.75	100.10	1.18	0.01						33.16	2.77
29	53.02	-24.75	76.00	1.12	0.01						30.62	2.44
29	53.02	-24.75	50.70	1.12	0.01						41.00	3.14
29	53.02	-24.75	25.10	1.10	0.01						50.87	4.15
29	53.02	-24.75	15.00	1.15	0.01						43.62	3.60
32	55.51	-26.70	3271.60	1.75	0.07	2.80	0.13	13.75	0.08	29.75	117.05	11.59
32	55.51	-26.70	3000.00	1.86	0.07	4.84	0.45	13.13	0.10	45.86	28.12	3.03
32	55.51	-26.70	2801.60	1.59	0.06	4.17	0.43	13.18	0.10	40.51		
32	55.51	-26.70	2500.90	1.61	0.06						14.31	1.77
32	55.51	-26.70	2250.60	1.55	0.06	2.78	0.21	13.39	0.10	51.49	0.00	
32	55.51	-26.70	2001.40	1.59	0.06	3.46	0.22	13.27	0.07	45.15	30.67	3.33
32	55.51	-26.70	1701.80	1.29	0.05	3.81	0.41	13.14	0.10	37.10	23.64	2.59
32	55.51	-26.70	1552.10	1.50	0.06	3.64	0.27	13.42	0.08	26.29	36.96	3.72
32	55.51	-26.70	1400.40	1.45	0.06	2.02	0.08	13.89	0.08	32.88		
32	55.51	-26.70	1200.50	1.42	0.06	2.49	0.29	13.58	0.17	35.14	22.96	3.09
32	55.51	-26.70	1001.40	1.41	0.06						23.07	2.74
32	55.51	-26.70	801.40	1.46	0.06	3.99	0.47	13.38	0.12	23.97	33.74	3.05
32	55.51	-26.70	698.40	1.32	0.05	3.41	0.48	13.04	0.12	57.14		
32	55.51	-26.70	601.90	1.27	0.04	4.37	0.37	12.97	0.07	43.62	37.61	3.53
32	55.51	-26.70	450.60	1.25	0.04	4.22	0.30	13.15	0.07	29.63		
32	55.51	-26.70	379.90	1.39	0.05	3.31	0.27	13.15	0.08	50.80		
32	55.51	-26.70	300.80	1.31	0.05	3.37	0.26	13.24	0.08	36.54	5.30	2.36
32	55.51	-26.70	200.40	1.19	0.04	3.78	0.48	13.17	0.12	30.72	21.17	1.91
32	55.51	-26.70	101.60	1.06	0.03	2.97	0.28	13.26	0.09	30.20	39.09	3.57
32	55.51	-26.70	51.70	0.93	0.03	4.67	0.68	12.95	0.11	27.93	12.94	1.54
32	55.51	-26.70	26.10	1.10	0.04	3.86	0.45	12.96	0.09	43.57	56.89	4.90
32	55.51	-26.70	15.80	1.19	0.05	4.07	0.30	13.04	0.06	37.58	22.28	2.21
34	57.00	-27.88	2776.90	1.86	0.10						45.05	3.99
34	57.00	-27.88	2601.60	1.87	0.10						24.01	2.90
34	57.00	-27.88	2600.70	1.74	0.10						6.52	1.46
34	57.00	-27.88	2400.00	1.28	0.09						14.65	1.67
34	57.00	-27.88	2101.10	1.24	0.09						18.79	2.05

34	57.00	-27.88	1800.80	1.15	0.08						18.54	1.97
34	57.00	-27.88	1600.90	1.41	0.08						35.53	3.12
34	57.00	-27.88	1400.80	1.49	0.08						22.32	2.40
34	57.00	-27.88	1200.60	1.46	0.08						19.90	2.15
34	57.00	-27.88	1000.90								22.01	2.67
34	57.00	-27.88	850.80	1.48	0.13						31.78	3.37
34	57.00	-27.88	700.20	1.41	0.12						20.84	2.79
34	57.00	-27.88	601.00	1.42	0.12						18.22	2.02
34	57.00	-27.88	450.10	1.37	0.12						21.20	2.42
34	57.00	-27.88	380.40	1.30	0.11						17.36	2.08
34	57.00	-27.88	300.80	1.28	0.11						25.70	2.33
34	57.00	-27.88	200.60	1.29	0.11						27.95	2.38
34	57.00	-27.88	101.10	1.36	0.12						24.61	2.45
34	57.00	-27.88	60.90	1.31	0.11						36.12	2.90
34	57.00	-27.88	46.10	0.22	0.02						876.12	89.16
34	57.00	-27.88	29.00	1.22	0.10						60.48	4.92
34	57.00	-27.88	11.10	1.39	0.12						38.57	3.35
36	58.21	-29.72	2244.70	1.30	0.09						47.90	5.40
36	58.21	-29.72	1799.80	1.20	0.09						17.26	2.15
36	58.21	-29.72	1499.70	1.10	0.08						13.10	1.55
36	58.21	-29.72	1218.60	1.18	0.09						16.71	1.90
36	58.21	-29.72	849.00	1.17	0.08						15.46	1.94
36	58.21	-29.72	499.20	1.27	0.09						39.58	4.10
36	58.21	-29.72	249.40	0.90	0.06						23.54	2.87
36	58.21	-29.72	124.70	0.85	0.06						5.94	4.68
36	58.21	-29.72	69.30	0.95	0.07						51.84	4.61
36	58.21	-29.72	39.40	0.85	0.06						44.25	4.15
36	58.21	-29.72	20.60	0.87	0.06						45.21	3.99
38	58.84	-31.27	1353.80	1.23	0.09	2.43	0.15	13.46	0.08	35.23	48.21	5.58
38	58.84	-31.27	1300.70	1.10	0.08	7.72	0.15	12.67	0.12	35.79	37.88	4.59
38	58.84	-31.27	1162.70	0.99	0.07	5.08	0.75	12.96	0.11	26.40	32.42	4.04
38	58.84	-31.27	1001.30	1.11	0.08	3.61	0.29	13.15	0.07	31.21	22.41	2.99
38	58.84	-31.27	950.60	1.03	0.07	3.57	0.29	13.06	0.07	34.98	24.66	5.42
38	58.84	-31.27	800.60	1.17	0.08	3.14	0.23	13.30	0.07	29.57	10.99	4.69
38	58.84	-31.27	650.60	1.01	0.07						8.96	5.66
38	58.84	-31.27	574.70	0.90	0.06	3.53	0.42	12.94	0.10	39.47	16.51	2.07
38	58.84	-31.27	499.90	1.00	0.07	3.14	0.32	13.29	0.10	24.02	14.37	2.47
38	58.84	-31.27	400.90	0.80	0.06	3.95	0.57	12.91	0.11	31.31	19.17	2.67
38	58.84	-31.27	300.40	1.01	0.07	5.65	0.68	12.70	0.08	43.34	25.15	2.96
38	58.84	-31.27	200.50	0.89	0.06	4.38	0.47	12.95	0.08	28.56	31.41	3.50
38	58.84	-31.27	100.60	1.06	0.08	4.88	0.51	12.91	0.08	34.07	37.93	3.75
38	58.84	-31.27	69.60	1.00	0.07	2.59	0.15	13.33	0.06	29.66	40.64	3.99
38	58.84	-31.27	59.90	0.90	0.07	3.60	0.50	13.05	0.11	29.41	37.25	3.00
38	58.84	-31.27	49.20	0.87	0.06	5.15	0.65	12.81	0.09	31.13	32.68	3.19
38	58.84	-31.27	30.10	0.93	0.07	2.49	0.23	13.21	0.09	36.76	40.00	0.00
38	58.84	-31.27	20.30	0.92	0.07	2.10	0.44	13.06	0.20	67.14	17.97	0.00
40	59.10	-33.83	2307.30	1.23	0.04						12.94	1.05
40	59.10	-33.83	2098.70	1.24	0.04						9.29	0.56
40	59.10	-33.83	1598.90								14.21	1.67
40	59.10	-33.83	1298.40	1.07	0.03							
40	59.10	-33.83	999.60	1.13	0.04						15.61	2.02
40	59.10	-33.83	599.30	1.11	0.04						16.49	1.77
40	59.10	-33.83	349.10	1.07	0.03						14.78	1.64
40	59.10	-33.83	150.30	1.06	0.03							
40	59.10	-33.83	68.90	1.06	0.03						92.42	8.02
40	59.10	-33.83	37.50	0.95	0.03							
40	59.10	-33.83	20.30	0.96	0.03						74.42	6.97
42	59.36	-36.40	3130.60	1.38	0.03						84.60	7.87
42	59.36	-36.40	3099.70	1.61	0.04						37.19	4.21
42	59.36	-36.40	2900.40	1.44	0.03						11.81	1.38
42	59.36	-36.40	2500.50	1.56	0.03						11.32	1.50
42	59.36	-36.40	2250.40	1.64	0.04						12.07	1.39
42	59.36	-36.40	2000.70	1.49	0.03						13.02	1.45
42	59.36	-36.40	1801.30	1.30	0.03						27.95	2.23
42	59.36	-36.40	1600.80	1.37	0.03						23.03	2.50
42	59.36	-36.40	1400.60	1.25	0.04						15.46	1.83
42	59.36	-36.40	1200.20	1.12	0.04						14.54	1.67
42	59.36	-36.40	1050.50	1.12	0.04						14.08	1.89
42	59.36	-36.40	900.60	1.22	0.04						15.55	1.74
42	59.36	-36.40	700.50	1.14	0.04						26.91	2.33
42	59.36	-36.40	500.30	1.21	0.04						16.47	1.87
42	59.36	-36.40	401.50	1.12	0.04						18.25	2.16
42	59.36	-36.40	299.80	1.12	0.04						21.49	2.62
42	59.36	-36.40	200.50	1.21	0.04						21.67	2.49
42	59.36	-36.40	100.40	1.12	0.04						35.48	3.43
42	59.36	-36.40	70.40	1.19	0.04						55.36	4.53

42	59.36	-36.40	50.30	1.07	0.03						67.10	6.28
42	59.36	-36.40	35.10	1.09	0.04							
42	59.36	-36.40	20.40	1.15	0.04						116.38	10.20
44	59.62	-38.95	2963.80	1.07	0.13	3.45	0.34	12.98	0.08	46.44	70.21	8.43
44	59.62	-38.95	2901.40	1.28	0.15	3.68	0.44	13.53	0.13	15.76	38.56	7.83
44	59.62	-38.95	2798.60	1.05	0.12	2.49	0.18	13.49	0.08	23.46	37.14	4.63
44	59.62	-38.95	2600.70	1.23	0.14	3.61	0.40	13.23	0.10	30.05	19.40	3.67
44	59.62	-38.95	2250.90	1.19	0.14	3.76	0.39	13.15	0.09	32.40	26.74	2.40
44	59.62	-38.95	2000.60	1.16	0.14	2.25	0.18	13.53	0.11	31.25	23.81	2.30
44	59.62	-38.95	1801.00	0.97	0.11	2.46	0.25	13.41	0.11	25.03	24.88	2.24
44	59.62	-38.95	1601.80	1.11	0.13	2.86	0.18	13.29	0.07	32.18	25.09	2.29
44	59.62	-38.95	1400.20	1.02	0.12	1.98	0.16	13.41	0.10	41.00	23.67	2.31
44	59.62	-38.95	1251.00	1.05	0.12	4.19	0.36	13.05	0.07	29.66		
44	59.62	-38.95	1100.50	1.05	0.12	3.44	0.41	13.31	0.11	21.36	28.22	2.61
44	59.62	-38.95	1001.40	1.09	0.13	2.21	0.20	13.43	0.11	35.94	9.31	2.73
44	59.62	-38.95	901.70	1.05	0.12	1.52	0.10	13.74	0.12	40.60	17.34	1.74
44	59.62	-38.95	700.70	1.26	0.15	1.79	0.10	13.79	0.10	38.24		
44	59.62	-38.95	501.20	1.11	0.13	2.37	0.19	13.39	0.09	35.66	36.11	2.95
44	59.62	-38.95	301.60	0.96	0.11	1.52	0.13	13.61	0.13	41.66	26.22	2.35
44	59.62	-38.95	200.30	0.81	0.09	3.41	0.58	12.95	0.02	34.94	32.26	3.43
44	59.62	-38.95	101.20	1.03	0.12	2.25	0.20	13.50	0.10	26.51	13.36	2.04
44	59.62	-38.95	50.80	0.92	0.11						45.77	3.81
44	59.62	-38.95	40.60	0.98	0.12	2.64	0.29	13.21	0.18	36.37	116.22	9.22
44	59.62	-38.95	31.00	1.01	0.12	2.57	0.12	13.22	0.10	39.08	34.17	2.92
44	59.62	-38.95	20.90	1.09	0.13	2.49	0.16	13.37	0.18	32.90	111.87	11.41
49	59.77	-41.30	2051.50	1.55	0.13						35.95	3.77
49	59.77	-41.30	1999.80	1.67	0.14						27.68	3.04
49	59.77	-41.30	1899.80	1.71	0.15						18.23	2.20
49	59.77	-41.30	1800.60	1.48	0.13						16.00	1.76
49	59.77	-41.30	1650.50	1.68	0.14						21.19	2.44
49	59.77	-41.30	1501.10	1.59	0.14						18.59	2.13
49	59.77	-41.30	1250.20	1.56	0.13						17.63	2.25
49	59.77	-41.30	1101.10	1.61	0.14						17.62	1.97
49	59.77	-41.30	1000.50	1.61	0.14						17.95	1.97
49	59.77	-41.30	901.20	1.48	0.13						19.55	2.07
49	59.77	-41.30	800.90	1.42	0.12						18.25	2.16
49	59.77	-41.30	700.80	1.42	0.12						16.65	1.83
49	59.77	-41.30	599.90	1.43	0.12						16.18	2.20
49	59.77	-41.30	550.20	1.37	0.12						14.81	1.77
49	59.77	-41.30	400.50	1.42	0.12						18.17	2.24
49	59.77	-41.30	300.40								24.65	2.26
49	59.77	-41.30	200.20	1.54	0.13						27.60	2.36
49	59.77	-41.30	101.60	1.20	0.10						55.85	4.73
49	59.77	-41.30	80.30	1.31	0.11						58.02	4.66
49	59.77	-41.30	61.50	1.26	0.11						51.50	4.54
49	59.77	-41.30	40.60	1.16	0.10						41.71	3.79
49	59.77	-41.30	19.50	1.05	0.09						44.31	3.78
53	59.90	-43.00	165.50	1.82	0.13						61.82	5.10
53	59.90	-43.00	130.50	1.77	0.13						40.58	3.87
53	59.90	-43.00	101.20	2.06	0.15						54.68	5.35
53	59.90	-43.00	70.40	2.18	0.16						59.84	5.37
53	59.90	-43.00	55.60	2.10	0.15						96.41	8.08
53	59.90	-43.00	30.50								145.35	13.20
56	59.82	-42.40	298.60								47.02	4.29
56	59.82	-42.40	248.30								49.13	4.62
56	59.82	-42.40	170.10								56.35	4.41
56	59.82	-42.40	120.40	1.19	0.09						56.63	4.04
56	59.82	-42.40	60.90	1.06	0.08						45.78	4.30
56	59.82	-42.40	40.20	1.35	0.10						44.15	3.89
56	59.82	-42.40	20.60								48.29	4.64
60	59.80	-42.00	1737.80	1.40	0.16	4.72	0.45	12.96	0.11	46.21	43.56	4.62
60	59.80	-42.00	1647.40	1.27	0.15	2.37	0.14	13.49	0.33	37.34	21.64	3.33
60	59.80	-42.00	1499.90	1.17	0.14	3.11	0.16	13.11	0.13	46.51	28.03	2.96
60	59.80	-42.00	1300.40	1.20	0.14	3.49	0.17	13.21	0.14	31.98	18.59	2.34
60	59.80	-42.00	1151.10	1.21	0.14	3.47	0.18	13.20	0.15	33.67	16.28	1.89
60	59.80	-42.00	949.30	1.25	0.15	3.44	0.20	13.17	0.16	38.63		
60	59.80	-42.00	850.50								16.41	2.09
60	59.80	-42.00	749.30	1.08	0.13						12.52	1.51
60	59.80	-42.00	649.50	1.19	0.14	4.27	0.19	13.10	0.09	30.54	13.14	1.55
60	59.80	-42.00	548.60	1.23	0.14	4.84	0.26	13.12	0.11	25.79		
60	59.80	-42.00	449.60	1.19	0.14	4.39	0.23	13.05	0.09	33.03	15.13	1.81
60	59.80	-42.00	348.40	1.25	0.15	4.48	0.20	13.12	0.09	29.08	15.85	1.78
60	59.80	-42.00	299.70	1.40	0.05	3.23	0.13	13.28	0.11	39.48	20.29	2.36
60	59.80	-42.00	250.20	1.24	0.04	2.18	0.14	13.70	0.65	26.04	14.56	1.53

60	59.80	-42.00	200.90	1.32	0.05	2.30	0.08	13.60	0.20	33.75	12.10	40.56
60	59.80	-42.00	150.00	1.53	0.06	3.68	0.17	13.47	0.23	23.93	32.64	2.84
60	59.80	-42.00	99.80	1.58	0.06	3.37	0.21	13.25	0.19	49.96	43.38	3.82
60	59.80	-42.00	77.70	1.64	0.07	4.10	0.20	13.20	0.13	42.48	50.04	4.11
60	59.80	-42.00	59.20	1.62	0.07	2.96	0.10	13.56	0.17	33.29	52.11	5.08
60	59.80	-42.00	38.80	1.51	0.06	2.88	0.13	13.53	0.26	32.13	44.46	3.53
60	59.80	-42.00	28.20	1.51	0.06	4.69	0.19	13.02	0.07	45.90		
60	59.80	-42.00	19.00	1.61	0.07	4.41	0.19	13.24	0.12	33.17		
61	59.75	-45.11	138.10	2.87	0.11						62.37	5.51
61	59.75	-45.11	121.20	3.56	0.13						49.95	4.91
61	59.75	-45.11	101.00	3.40	0.12						57.68	4.90
61	59.75	-45.11	70.80								40.99	4.61
61	59.75	-45.11	50.80								42.99	3.80
61	59.75	-45.11	23.60								100.27	9.54
63	59.43	-45.67	1557.40	1.25	0.05						22.19	2.16
63	59.43	-45.67	1300.30	1.19	0.05						19.02	2.26
63	59.43	-45.67	1096.00	1.19	0.05						18.19	2.05
63	59.43	-45.67	850.00	1.25	0.05						15.35	1.61
63	59.43	-45.67	500.50	1.18	0.05						25.90	2.31
63	59.43	-45.67	400.00	1.55	0.07						26.33	2.45
63	59.43	-45.67	300.20	1.40	0.06						32.28	2.93
63	59.43	-45.67	200.30	1.38	0.06						39.17	3.60
63	59.43	-45.67	100.20	1.67	0.07						52.14	4.45
63	59.43	-45.67	71.00								36.37	2.86
63	59.43	-45.67	20.40								55.66	4.62
64	59.07	-46.08	2502.20	1.28	0.18	2.92	0.26	13.17	0.09	52.67	37.29	3.79
64	59.07	-46.08	2401.00	1.17	0.16	2.21	0.21	13.42	0.12	43.41	20.68	2.83
64	59.07	-46.08	2151.10	1.20	0.17	2.20	0.21	13.15	0.11	83.80	9.86	1.04
64	59.07	-46.08	2001.30	1.33	0.19	3.31	0.25	13.18	0.08	43.38	13.90	1.74
64	59.07	-46.08	1800.40	1.21	0.17	1.74	0.17	13.39	0.15	83.32	13.68	1.65
64	59.07	-46.08	1601.20	1.29	0.18	1.67	0.15	13.69	0.19	67.80	14.57	1.54
64	59.07	-46.08	1400.70	1.41	0.20	2.96	0.31	13.54	0.14	25.67	14.92	1.71
64	59.07	-46.08	1150.80	1.31	0.18	1.89	0.14	13.60	0.13	56.58	15.67	2.25
64	59.07	-46.08	1050.70	1.22	0.17	2.86	0.48	13.34	0.18	33.79	0.00	0.64
64	59.07	-46.08	900.40	1.14	0.16	1.78	0.14	13.33	0.10	83.78	13.36	1.49
64	59.07	-46.08	800.90	1.25	0.18	1.78	0.18	13.88	0.26	31.38	13.38	1.61
64	59.07	-46.08	700.60	1.28	0.18						14.57	1.90
64	59.07	-46.08	500.90	1.18	0.16	2.84	0.27	13.05	0.09	62.98	23.61	2.20
64	59.07	-46.08	400.90	1.09	0.15	1.40	0.18	13.51	0.23	107.52	17.18	2.07
64	59.07	-46.08	320.20	1.11	0.16	2.42	0.22	13.01	0.09	83.28	21.31	2.41
64	59.07	-46.08	200.40	1.10	0.15	1.95	0.17	13.14	0.10	94.51	28.60	2.46
64	59.07	-46.08	151.50	1.21	0.17	2.22	0.20	13.48	0.12	39.35	34.36	3.46
64	59.07	-46.08	100.60	1.02	0.14	2.32	0.24	13.21	0.11	48.23	36.23	3.21
64	59.07	-46.08	50.20	1.00	0.14	2.33	0.25	13.48	0.13	18.87	31.49	2.83
64	59.07	-46.08	35.70	0.93	0.13	3.20	0.33	13.04	0.09	36.20	35.89	3.92
64	59.07	-46.08	25.50	1.10	0.15	2.82	0.77	13.40	0.28	25.44	14.19	1.89
64	59.07	-46.08	15.30	2.10	0.29	3.79	0.37	13.34	0.13	55.72		
68	56.91	-47.42	3637.90	1.38	0.04						77.85	8.50
68	56.91	-47.42	3400.10	1.61	0.06						15.39	1.93
68	56.91	-47.42	2500.20	1.55	0.05						14.35	1.82
68	56.91	-47.42	1699.90	1.26	0.04						12.59	1.45
68	56.91	-47.42	1399.70	1.19	0.04						16.15	1.43
68	56.91	-47.42	900.80	1.45	0.05						11.20	2.29
68	56.91	-47.42	348.70	1.23	0.04						13.03	1.76
68	56.91	-47.42	100.70	1.35	0.05						36.08	3.86
68	56.91	-47.42	50.10	1.39	0.05						46.87	6.70
68	56.91	-47.42	35.20	1.47	0.05						39.04	3.82
68	56.91	-47.42	29.50	1.18	0.04						37.34	7.82
68	56.91	-47.42	20.00	1.27	0.04						9.57	1.54
69	55.84	-48.09	3735.70	1.22	0.05	2.28	0.35	13.48	0.19	37.87	84.91	8.96
69	55.84	-48.09	3699.90	1.24	0.05	2.98	0.21	13.03	0.07	66.34	70.96	7.80
69	55.84	-48.09	3500.30	1.18	0.05	3.23	0.23	13.09	0.07	47.04		
69	55.84	-48.09	3250.60	1.48	0.06	2.33	0.17	13.33	0.10	81.16	14.11	1.86
69	55.84	-48.09	2800.60	1.53	0.06	4.25	0.36	13.20	0.08	35.48	12.77	1.68
69	55.84	-48.09	2400.40	1.51	0.06	2.35	0.15	13.37	0.09	76.99	17.78	2.28
69	55.84	-48.09	2100.20	1.21	0.05	2.02	0.16	13.52	0.12	45.05	9.94	1.04
69	55.84	-48.09	1799.90	1.36	0.05	5.22	0.84	13.07	0.15	37.24	12.81	1.38
69	55.84	-48.09	1600.60	1.36	0.05	3.00	0.13	13.31	0.05	40.21	10.60	1.17
69	55.84	-48.09	1397.90	1.29	0.05	3.16	0.20	13.11	0.07	53.68	12.38	1.31
69	55.84	-48.09	1100.00	1.31	0.05	1.41	0.18	13.43	0.23	6474.45	12.31	1.32
69	55.84	-48.09	800.50	1.24	0.05	3.16	0.51	13.23	0.16	66.50	14.89	2.30
69	55.84	-48.09	500.40	1.28	0.05	4.80	0.42	12.97	0.07	58.02	22.19	2.19
69	55.84	-48.09	179.90	1.35	0.05	2.42	0.13	13.10	0.15	101.40	39.71	3.37
69	55.84	-48.09	129.70	1.33	0.05	3.09	0.20	13.31	0.07	36.29	42.85	3.76
69	55.84	-48.09	90.40	1.33	0.05	2.98	0.31	13.31	0.12	38.32	50.74	4.32

69	55.84	-48.09	60.30	1.53	0.06	4.57	0.71	12.92	0.14	59.03	57.16	4.53
69	55.84	-48.09	40.20	1.42	0.06	2.15	0.51	13.84	0.24	27.96	78.88	6.26
69	55.84	-48.09	29.90	1.32	0.05	3.55	0.32	13.21	0.22	36.32		
69	55.84	-48.09	25.80	1.32	0.05	2.09	0.10	13.78	0.44	28.78	76.82	6.16
69	55.84	-48.09	14.50	1.18	0.05	2.91	0.17	13.14	0.16	100.30	96.01	7.79
71	53.69	-49.43	3755.60	1.35	0.03						90.89	10.24
71	53.69	-49.43	3500.00	1.35	0.03						14.10	1.68
71	53.69	-49.43	3000.10	1.25	0.03						8.60	2.06
71	53.69	-49.43	2751.00	1.31	0.03							
71	53.69	-49.43	2400.60	1.13	0.02						8.57	3.56
71	53.69	-49.43	2000.90	1.09	0.02							
71	53.69	-49.43	1700.40	1.09	0.02							
71	53.69	-49.43	1400.40	1.18	0.03							
71	53.69	-49.43	1200.90	1.08	0.02						9.86	1.08
71	53.69	-49.43	800.50	1.17	0.03						9.75	1.37
71	53.69	-49.43	500.70	1.07	0.02						11.19	1.92
71	53.69	-49.43	350.20	1.18	0.03						0.00	0.34
71	53.69	-49.43	250.60	1.16	0.03						8.73	1.01
71	53.69	-49.43	150.60	1.09	0.02						13.15	1.87
71	53.69	-49.43	100.60	1.29	0.03						19.82	1.90
71	53.69	-49.43	60.80	1.12	0.02						42.03	3.73
71	53.69	-49.43	50.00	1.13	0.03						59.36	5.16
71	53.69	-49.43	40.30	1.10	0.02						9.69	1.22
71	53.69	-49.43	30.60	1.05	0.02						46.27	4.32
71	53.69	-49.43	20.30	1.02	0.02						77.47	9.93
77	53.00	-51.10	2543.30	1.16	0.03	2.56	0.22	13.04	0.09	75.34	15.81	1.85
77	53.00	-51.10	2450.70	1.09	0.02	1.19	0.09	13.47	0.14	359.82	16.82	1.90
77	53.00	-51.10	2400.50	1.29	0.03	2.87	0.30	12.89	0.09	81.98	13.71	1.49
77	53.00	-51.10	2100.50	1.12	0.02	1.53	0.18	13.34	0.17	127.49	11.41	1.38
77	53.00	-51.10	1900.30	1.13	0.03	2.77	0.31	12.99	0.10	70.80	13.10	1.42
77	53.00	-51.10	1700.60	1.10	0.02						12.31	1.46
77	53.00	-51.10	1500.20	1.05	0.02						13.02	1.35
77	53.00	-51.10	1300.10	1.02	0.02	1.73	0.22	13.34	0.18	60.15	13.38	1.61
77	53.00	-51.10	1199.90	1.46	0.03	2.14	0.20	13.46	0.15	73.55	13.10	1.52
77	53.00	-51.10	1100.50	1.37	0.03	1.99	0.17	13.39	0.13	89.30	10.25	1.06
77	53.00	-51.10	1000.50	1.50	0.03	2.85	0.20	13.05	0.08	99.60	10.71	1.15
77	53.00	-51.10	700.50	1.46	0.03	1.59	0.15	13.52	0.19	323.97	16.13	1.95
77	53.00	-51.10	400.40	1.35	0.03	2.28	0.24	13.26	0.13	79.18	15.50	1.83
77	53.00	-51.10	150.50	1.36	0.03						28.11	2.58
77	53.00	-51.10	100.50	1.32	0.03						42.08	3.61
77	53.00	-51.10	80.40	1.28	0.03	3.52	0.29	13.20	0.08	35.96	37.27	3.71
77	53.00	-51.10	60.20	1.28	0.03	2.94	0.30	13.11	0.10	58.70	57.96	5.03
77	53.00	-51.10	40.00	1.24	0.03	2.53	0.17	13.31	0.07	46.80	82.18	7.63
77	53.00	-51.10	30.60	1.25	0.03	6.70	0.44	12.10	0.38	182.02	95.53	7.84
77	53.00	-51.10	15.10	1.24	0.03	3.55	0.27	13.20	0.08	33.01	97.14	8.88
78	51.99	-53.82	371.30	1.38	0.03						149.25	16.51
78	51.99	-53.82	290.50	1.46	0.03						71.05	8.17
78	51.99	-53.82	250.80	1.58	0.04						94.75	11.09
78	51.99	-53.82	140.60	2.03	0.05						57.16	5.46
78	51.99	-53.82	36.70	2.60	0.06						50.07	6.00
78	51.99	-53.82	12.00	2.64	0.06						52.21	4.71

Appendix 2: DCu, Cu^{2+}, ligands concentrations and stability constant at all stations of GEOVIDE. Errors of DCu are the standard deviation of measurements. Errors of speciation parameters are the analysis of titrations errors.

Station [#]	Latitude [°N]	Longitude [°E]	Pressure [db]	DCu [nM]	error	L (nM)	error [nM]	Log K	error	Cu^{2+} (fM)
2	41.383	-13.888	20.44	1.79	0.09	3.01	0.06	13.7	0.1	29
2	41.383	-13.888	141.3	2.15	0.14	3.46	0.11	13.7	0.2	32
2	41.383	-13.888	504.77	1.14	0.03	2.40	0.08	13.2	0.1	62
2	41.383	-13.888	838.65	1.46	0.06	2.36	0.07	13.3	0.1	73
2	41.383	-13.888	858.56	1.58	0.15	2.36	0.09	13.4	0.2	74
2	41.383	-13.888	1213.6	1.98	0.19	3.20	0.08	13.4	0.1	63
2	41.383	-13.888	1771.2	1.57	0.10	2.55	0.07	13.3	0.1	78
2	41.383	-13.888	2942.3	2.57	0.22	3.31	0.08	13.3	0.1	167
2	41.383	-13.888	4069.6	2.75	0.26	3.25	0.08	13.3	0.1	279
2	41.383	-13.888	5288.6	2.74	0.12	3.48	0.08	13.2	0.1	236
8	37.292	-32.281	61.366	1.58	0.07	3.12	0.14	13.5	0.2	29
8	37.292	-32.281	79.912	1.38	0.05	1.92	0.05	14.2	0.1	16
8	37.292	-32.281	203.04	1.72	0.06	3.23	0.07	13.7	0.1	22
8	37.292	-32.281	728.97	1.91	0.08	2.18	0.07	14.1	0.1	57
8	37.292	-32.281	1010.7	1.87	0.07	2.28	0.15	13.8	0.1	57
8	37.292	-32.281	1314.1	1.79	0.08	2.36	0.03	13.6	0.1	71
8	37.292	-32.281	1669.8	1.98	0.14	2.21	0.06	14.1	0.1	57
38	36.23	-33.902	22.408	1.30	0.07	2.80	0.10	13.4	0.1	37
38	36.23	-33.902	-999	1.64	0.06	3.59	0.17	13.3	0.1	42
38	36.23	-33.902	356.09	1.44	0.05	3.72	0.15	13.3	0.1	30
38	36.23	-33.902	987.63	1.98	0.10	2.72	0.08	13.6	0.2	62
38	36.23	-33.902	-999	1.46	0.05	2.81	0.06	13.5	0.1	33
38	36.23	-33.902	-999	1.91	0.08	3.50	0.08	13.5	0.1	36
38	36.23	-33.902	-999	1.72	0.10	2.90	0.07	13.5	0.1	43
38	36.23	-33.902	2312.1	2.19	0.14	3.70	0.14	13.3	0.1	80
19	35.04	-35.01	19.711	1.00	0.08	1.42	0.20	12.5	0.1	739
19	35.04	-35.01	80.138	1.36	0.05					
19	35.04	-35.01	402.66	0.90	0.04	3.11	0.38	13.0	0.2	43
19	35.04	-35.01	555.58	1.84	0.11	3.21	0.15	13.3	0.1	65
19	35.04	-35.01	654.48	1.55	0.12	3.29	0.16	13.5	0.2	30
19	35.04	-35.01	857.87	0.82	0.02					
19	35.04	-35.01	1110.6	2.94	0.26	3.91	0.08	13.7	0.2	58
19	35.04	-35.01	2025.5	1.97	0.08	2.56	0.13	13.4	0.1	131
19	35.04	-35.01	2839.2	2.58	0.11	2.93	0.21	13.4	0.2	324
19	35.04	-35.01	3298.5	2.14	0.17	3.30	0.14	13.1	0.1	152
19	35.04	-35.01	3556.1	2.15	0.13	2.79	0.09	13.4	0.1	144
19	35.04	-35.01	4298.4	1.92	0.17	1.78	0.08	13.4	0.1	11601
21	33.608	-38.228	26.381	1.19	0.09	2.59	0.11	13.4	0.1	38
21	33.608	-38.228	79.892	1.58	0.10	2.65	0.10	13.5	0.2	51
21	33.608	-38.228	101.79	1.44	0.11	3.52	0.12	13.3	0.1	34
21	33.608	-38.228	374.42	1.25	0.06	2.60	0.09	13.3	0.1	51
21	33.608	-38.228	829.45	1.44	0.06	2.12	0.11	13.4	0.2	78
21	33.608	-38.228	2736.6	1.85	0.18	2.85	0.06	13.2	0.1	114
21	33.608	-38.228	2888.3	2.48	0.11	3.02	0.19	13.5	0.3	158
21	33.608	-38.228	3248.6	2.63	0.13	4.92	0.21	13.2	0.1	73
21	33.608	-38.228	4270.9	2.63	0.16	3.42	0.14	13.2	0.1	232
23	30.124	-42.12	17.744	1.03	0.04	2.18	0.23	13.2	0.1	61

23	30.124	-42.12	100.28	1.24	0.06	2.44	0.16	13.3	0.2	47
23	30.124	-42.12	121.35	1.62	0.08	3.46	0.15	13.5	0.2	30
23	30.124	-42.12	301.9	1.00	0.06	1.86	0.18	13.4	0.2	48
23	30.124	-42.12	503.67	1.63	0.10	2.26	0.06	14.0	0.4	28
23	30.124	-42.12	689.5	1.66	0.10	3.10	0.24	13.4	0.1	45
23	30.124	-42.12	705.67	1.21	0.06	3.86	0.26	12.9	0.1	55
23	30.124	-42.12	756.57	1.06	0.04	2.02	0.07	13.3	0.1	50
23	30.124	-42.12	762.51	0.95	0.04					
23	30.124	-42.12	773.61	1.46	0.09	1.95	0.10	13.8	0.1	49
24	29.167	-43.174	20.273	1.67	0.12	3.11	0.10	13.4	0.1	50
24	29.167	-43.174	59.295	2.08	0.09	3.82	0.13	13.4	0.1	51
24	29.167	-43.174	715.51	1.46	0.05	2.23	0.07	13.3	0.1	104
24	29.167	-43.174	1110.1	1.64	0.05	1.95	0.11	13.8	0.2	77
24	29.167	-43.174	2872.5	1.97	0.05	2.75	0.06	13.6	0.1	65
24	29.167	-43.174	2881	1.99	0.10	2.84	0.15	13.4	0.2	88
24	29.167	-43.174	3075.6	2.64	0.12	3.12	0.13	13.5	0.1	172
26	26.36	-44.675	19.896	0.96	0.03	2.47	0.14	13.2	0.1	43
26	26.36	-44.675	151.34	1.40	0.24	2.83	0.09	13.5	0.1	33
26	26.36	-44.675	654.53	1.31	0.06	2.32	0.07	13.3	0.1	59
26	26.36	-44.675	806.86	1.47	0.05	3.31	0.20	13.2	0.1	56
26	26.36	-44.675	1514.8	1.41	0.05	2.14	0.08	13.5	0.2	68
26	26.36	-44.675	2837.8	2.34	0.15					
26	26.36	-44.675	3654.5	2.71	0.21	4.37	0.16	13.2	0.1	109
26	26.36	-44.675	4031.5	2.49	0.14	2.64	0.11	13.7	0.4	318
27	25.93	-45.019	19.83	0.94	0.06	2.01	0.13	13.1	0.2	63
27	25.93	-45.019	112.58	1.13	0.04	2.72	0.11	13.4	0.2	25
27	25.93	-45.019	141.24	1.32	0.11					
27	25.93	-45.019	806.65	1.48	0.04	2.28	0.05	13.4	0.1	75
27	25.93	-45.019	1312.1	1.34	0.10	3.51	0.15	13.0	0.1	58
27	25.93	-45.019	2021.8	2.20	0.12	2.59	0.05	13.5	0.1	173
27	25.93	-45.019	3041.1	3.17	0.18	4.17	0.11	13.4	0.1	137
27	25.93	-45.019	3447.5	3.32	0.15	4.05	0.11	13.3	0.1	228
27	25.93	-45.019	3860.1	1.92	0.16	2.43	0.11	13.2	0.1	227
30	26.215	-45.118	20.38	1.12	0.04	2.98	0.14	13.1	0.1	50
30	26.215	-45.118	100.05	1.41	0.12	1.87	0.13	13.7	0.2	67
30	26.215	-45.118	110.33	1.27	0.05	3.81	0.13	13.2	0.1	31
30	26.215	-45.118	351.65	0.98	0.05	2.01	0.07	13.2	0.1	64
30	26.215	-45.118	796.31	1.20	0.11	1.96	0.07	13.5	0.2	47
30	26.215	-45.118	-999	1.34	0.04	2.53	0.10	13.1	0.1	86
30	26.215	-45.118	2328.4	3.48	0.19	4.64	0.08	13.4	0.1	124
30	26.215	-45.118	2531.2	2.52	0.20	3.04	0.09	13.5	0.2	151
30	26.215	-45.118	2837.5	2.18	0.23	3.73	0.16	13.2	0.1	80
30	26.215	-45.118	3112.7	4.25	0.27	5.35	0.14	13.5	0.1	118
31	26.029	-44.553	20.519	1.18	0.05	1.64	0.09	13.5	0.3	83
31	26.029	-44.553	90.792	1.22	0.05	2.25	0.12	13.3	0.2	56
31	26.029	-44.553	130.38	1.14	0.05	1.99	0.06	13.6	0.2	32
31	26.029	-44.553	796.94	1.42	0.06	3.12	0.16	13.2	0.1	51
31	26.029	-44.553	1515.3	1.56	0.06	2.05	0.10	13.5	0.3	101
31	26.029	-44.553	2430.6	2.17	0.12	3.12	0.11	13.3	0.1	119
31	26.029	-44.553	3193.8	1.97	0.10					
31	26.029	-44.553	3602.8	2.22	0.18	3.72	0.14	13.2	0.1	104
31	26.029	-44.553	3934.7	2.14	0.11	4.07	0.22	13.0	0.1	118
35	26.139	-44.826	3143.3	2.59	0.16	3.49	0.05	13.4	0.1	113
35	26.139	-44.826	3362.2	2.25	0.12	2.99	0.06	13.9	0.2	42
35	26.139	-44.826	3382.9	2.06	0.14	4.10	0.15	13.5	0.1	31

35	26.139	-44.826	3504.8	2.76	0.11	3.88	0.11	13.5	0.1	74
35	26.139	-44.826	3656.1	2.29	0.43	2.69	0.10	13.5	0.2	184
39	26.139	-44.826	20.396	0.97	0.03	2.68	0.13	13.2	0.1	36
39	26.139	-44.826	100.25	0.97	0.02	2.09	0.15	13.2	0.2	52
39	26.139	-44.826	116.44	1.10	0.04	2.18	0.09	13.5	0.2	31
39	26.139	-44.826	125.04	0.91	0.04	2.03	0.07	13.5	0.2	24
39	26.139	-44.826	402.89	1.06	0.05	1.87	0.05	13.6	0.2	36
39	26.139	-44.826	807.14	1.40	0.06	3.66	0.29	13.1	0.1	50
39	26.139	-44.826	1059.2	1.59	0.08	3.46	0.12	13.3	0.1	46
39	26.139	-44.826	1515.4	1.92	0.14	3.64	0.22	13.3	0.2	60
39	26.139	-44.826	2022.2	2.01	0.33	2.47	0.12	13.4	0.3	155
37	26.131	-44.77	20.288	1.41	0.10	2.06	0.08	13.2	0.1	131
37	26.131	-44.77	110.1	0.58	0.03	1.09	0.03	13.6	0.2	30
37	26.131	-44.77	126.08	1.01	0.08	1.76	0.10	13.6	0.2	34
37	26.131	-44.77	807.03	1.21	0.07	2.20	0.07	13.4	0.1	49
37	26.131	-44.77	1819.3	1.23	0.13					
37	26.131	-44.77	2022	1.90	0.18	3.49	0.09	13.3	0.1	65
37	26.131	-44.77	2226.1	1.92	0.10	4.63	0.28	12.9	0.1	96
37	26.131	-44.77	2537.4	2.25	0.15	3.01	0.07	13.1	0.1	255